Spring 2010

Chandra News

Published by the Chandra X-ray Center (CXC) Issue Number 17

X-Ray Insights into Star and Planet Formation

Eric D. Feigelson
Scott J. Wolk

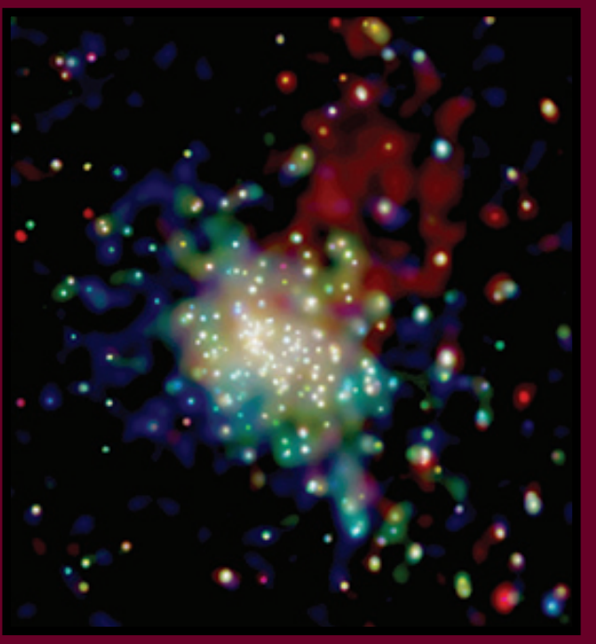

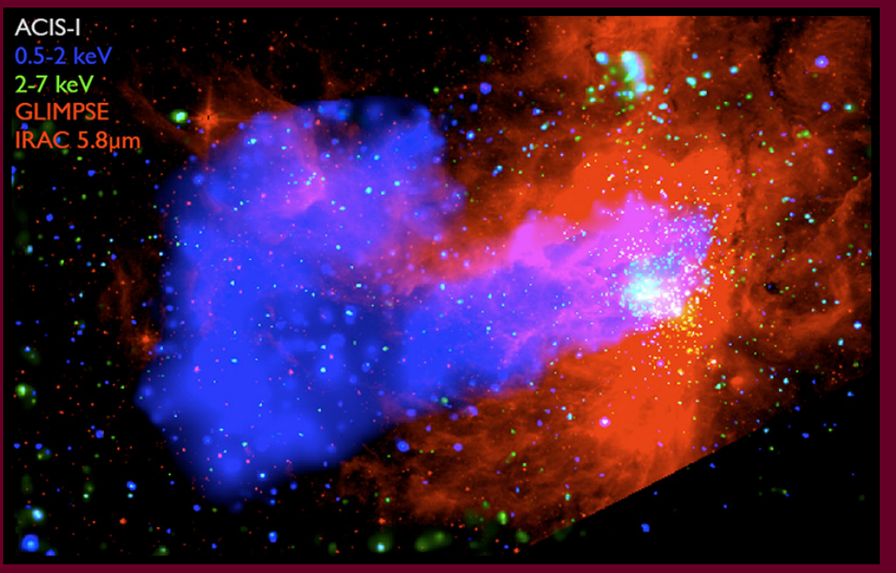

(see page 3 for article)

Table of Contents

X-Ray Insights into Star and Planet Formation

Eric D. Feigelson
Scott J. Wolk

Thermodynamically, X-ray astronomy should have little to say concerning the origin of stars and planets which form in molecular clouds around T ~ 10 K and protoplanetary disks around T ~ 100-1000 K, respectively. It was thus unclear why the Orion Nebula was found to be a spatially resolved source by early X-ray observatories (Bradt & Kelley 1979). The answers began emerging with the focusing optics of the Einstein Observatory: OB stars produce X-rays in their radiatively accelerated winds, and low-mass pre-main sequence (PMS) stars produce powerful magnetic reconnection flares (Pallavicini et al. 1981, Feigelson & DeCampli 1981). Diffuse X-ray emission attributed to past supernova explosions was also seen in the most violent starburst regions (Seward & Chlebowski 1982).

While progress was made in understanding these processes with the *ROSAT* and *ASCA* observatories during the 1990s (Feigelson & Montmerle 1999), the *Chandra X-ray Observatory* provided uniquely spectacular views of star forming regions in X-rays. The subarcsecond imaging of the *Chandra* mirrors is needed to resolve crowded young stellar clusters (YSCs), and the four-dimensions of data (right ascension, declination, energy, and arrival time for each photon) from the Advanced CCD Imaging Spectrometer (ACIS) are needed to characterize the emission processes (Weisskopf et al. 2002, Garmire et al. 2003). Figure 1 shows two ACIS images of nearby star forming regions, one a typical YSC with hundreds of X-ray sources associated with PMS stars, and the other a richer YSC with thousands of X-ray stars and diffuse emission from shocked OB winds outflowing into the Galactic interstellar medium.

But many aspects of star and planet formation are still poorly understood. Consider, for example, the astrophysics of the protoplanetary disk (Armitage 2009). If it were entirely neutral molecular material, as expected from its low temperatures, then there would be no source of viscosity to account for the accretion evident onto protostars. Photoionization by the stellar X-rays could induce turbulence via the magnetorotational instability; a turbulent disk has substantial viscosity and accretion is thereby promoted. But a turbulent disk would greatly affect the physics of planet formation, impeding the collisional growth of solids from dust to planetesimals but reducing inspiralling due to headwinds and torques from protoplanet-disk interaction. Thus, X-ray emission seen by *Chandra* may have substantial effects on the accretional growth of stars and the effects on the physics of planet formation.

FIGURE 1 (cover image): Top: *Chandra* ACIS image of the ~1 Myr old RCW 38 cluster at a distance of 1.7 kpc (Wolk et al. 2006). Bottom: X-ray diffuse emission (blue) channeled by cold molecular cloud (red) produced by the rich ~ 2 Myr old NGC 6618 cluster (white) in the M 17 star forming complex (Broos et al. 2007, Townsley 2009).

X-rays from stellar mass accretion

One of the highlights of the early years of *Chandra* was the discovery of X-ray emission from the process of the accretion of disk material onto the T Tauri star TW Hydrae (Kastner et al 2002). The key evidence was a suppressed forbidden line feature indicating that the X-rays were being emitted by high density plasma. XMM–Newton observations also indicated a suppressed forbidden line in many Classical T-Tauri Stars (Güdel & Telleschi 2007, Robrade & Schmitt 2007). But other explanations, including photoexcitation, were possible.

Brickhouse et al. have recently performed a 500 ks followup observation with the High Energy Transmission Grating (HETG) that resolves three sets of triplets (Brickhouse et al. 2010). They measure the weak forbidden lines of Ne IX, O VII, and Mg XI (Figure 2). All three ions show high densities and appear to be formed at the same temperature around 2.5 MK. These two sets of diagnostics together indicate that we are observing the accretion shock. However, the absorption to the Ne IX emission region is more than twice that of the O VII emission region. The absorber is likely to be cooler portions of the accretion column with nearly neutral gas. In the model developed by Cranmer (2008; see Figure 3), the mass accretion rate depends on the free-fall velocity, the pre-shock density, the area of the stellar surface, and a filling factor. The mass accretion rate is constrained by optical emission line data. Two regions, one representing the shock front and the other representing outflowing post-shock gas, are constrained by the HETG spectrum. The TW Hya results imply filling factors around 1.5% in the shock and 7% in the post-shock gas, in agreement with optical veiling and ultraviolet emission. The post-shock gas occupies a larger volume with 30 times more mass than the shock region.

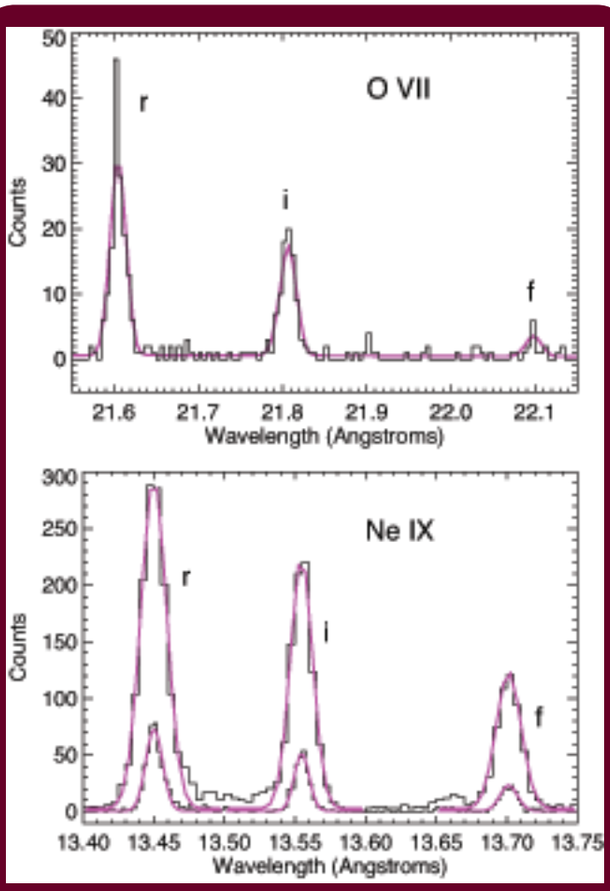

FIGURE 2: Top: Observed MEG spectrum for TW Hya in the O VII spectral region, shown as a histogram, with best-fit model (3 Gaussian lines) overlaid. Bottom: Observed MEG (upper) and HEG (lower) spectra in the Ne IX region, shown as histograms, with best-fit model overlaid. Resonance (r), intercombination (i) and forbidden (f) lines are identified. (Brickhouse et al. 2010)

X-rays from protostellar outflow shocks

Surveys of molecular and atomic line emission across star forming regions reveal high-velocity (v ~ 100-700 km/s) bipolar outflows produced by the youngest Class 0 and Class I protostars (Reipurth & Bally 2001). These are understood as disk material accelerated outward by magneto-centrifugal forces from the inner regions of protoplanetary disks. Collisions with the surrounding interstellar cloud produce shocks which are revealed by a variety of excited atomic and molecular lines; these emission line structures are known as Herbig-Haro (HH) objects. The jets are seen on scales <100 AU to several parsecs, and they sweep up ambient material to produce the bipolar outflows commonly seen in CO maps of active star formation regions. The cumulative kinetic energy of these outflows may be an important source of turbulent energy in molecular clouds, helping retard the rate of star formation to its observed low levels.

Soft X-ray emission from shock-heated plasma due to jets was discovered early in the *Chandra* mission from a knot of HH 2 far from the host protostar in the Orion molecular cloud (Pravdo et al. 2001). X-ray emission was later found from several knots of HH 80-81 in a distant cloud, HH 168 in Cepheus, and a 'finger' of the HH 210 outflow from massive protostars in Orion's OMC-1. Soft X-rays have also been found near the base of several HH outflows (Güdel & Telleschi 2007). The X-ray knot near the base of HH 154 ejected from IRS 5 the Taurus L1551 cloud (the host of the first molecular bipolar flow known) exhibited a v ~ 500 km/s expansion between *Chandra* observations in 2001 and 2005 (Favata et al. 2006). The 'Beehive' in the Orion nebula and other systems show constant soft excess emission which is spectrally, but not spatially, resolved from the hard flaring emission of the host star. The Class II PMS star DG Tau in Taurus exhibits two X-ray jets; the counterjet shows absorption attributable to gas in the intervening protoplanetary disk as illustrated in Figure 4.

Structure of young stellar clusters

While *Chandra* studies of individual PMS stars have provided insights into the astrophysics of pre-main sequence systems, *Chandra* studies of rich young stellar clusters have led to improved understanding of star formation on larger scales. *Chandra* maps typically have ~ 10% contamination by field stars in comparison to >10-fold contamination in many *JHK* or *Spitzer* mid-infrared maps. The reason is that magnetic activity in solar-type stars responsi-

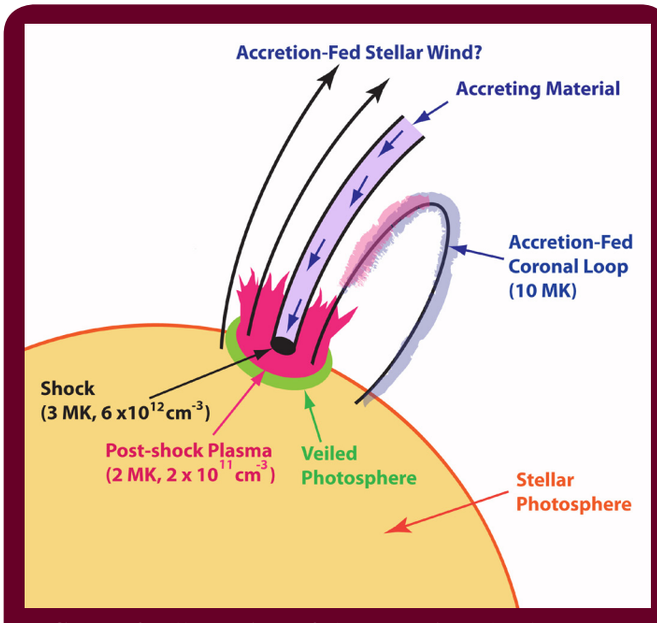

FIGURE 3: Illustration of the accretion shock onto TW Hydrae and its surrounding environment (Brickhouse et al. 2010).

ble for the X-ray flaring is high throughout the PMS stages, but declines ~10^2-fold during the first billion years on the main sequence (Preibisch & Feigelson 2005).

A benefit of the selectivity of *Chandra* X-ray samples for PMS stars is the opportunity to study the spatial distribution of young stars and star formation under a variety of star forming conditions. As expected from infrared studies (Lada & Lada 2003), many PMS populations are dominated by the rich YSCs which ionize HII regions. These clusters have hundreds or thousands of members with roughly spherical distributions. Figure 1 shows two examples, RCW 38 and central NGC 6618 cluster in M 17 (Wolk et al. 2006, Broos et al. 2007). Less populous YSCs are often seen still embedded in molecular clouds adjacent to HII regions. They can have clumpy structures, as seen in the obscured regions of the M 17 cloud. The W 3 complex has three HII complexes with different morphologies: W 3 Main is a rich spherical cluster, W 3(OH) is less rich with clumpy substructure, and W 3 North is an isolated O star without associated PMS stars (Feigelson & Townsley 2008).

A major result of both infrared and X-ray studies of rich YSCs is the presence of triggered star formation on the peripheries of their expanding HII regions. The nearby giant HII region IC 1396 ionized by the Trumpler 37 cluster is an excellent laboratory for small-scale triggered star formation in bright-rimmed cloudlets. The IC 1396N cloudlet has produced about 30 stars with ages spanning Class I to III; a clear spatial gradient in star ages is seen consistent with the ablation of the cloud over several million years (Getman 2006). The Cepheus B molecular cloud core on the edge of the Cep OB3b YSC has produced a richer triggered cluster, again spread over several million years (Getman et al. 2009). The Rosette Nebula's NGC 2244 has triggered substantial satellite clusters, both in the past and today (Wang et al. 2009).

An important aspect of YSC studies concerns mass segregation, the concentration of massive OB stars in the central regions of rich YSCs. This is a correlation between spatial structure and the stellar Initial Mass Function (IMF). The causes of mass segregation are not well-understood: Do massive stars form in regions of high gas density from rapid accretion, or in regions of high protostar density from stellar collisions? Since X-ray images more effectively trace the distribution of lower mass stars, new findings on mass segregation are emerging. Most rich clusters show mass segregation, but the NGC 2244 cluster illuminating the Rosette Nebula has dispersed O stars. Both of its ~ 40 $M_\odot$ stars are off-center, one isolated and the other with a dense subcluster (Wang et al. 2008). The obscured W3 Main cluster has a rich older population of PMS stars distributed over several parsecs, and a dense concentration of younger OB stars at the center (Feigelson & Townsley 2008). This is an unusual case where the youth of the OB stars can be established by the small size of their HII regions.

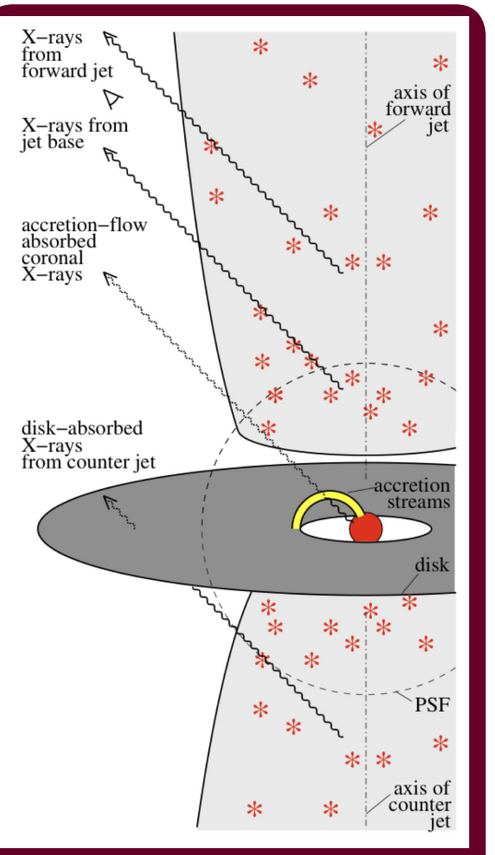

FIGURE 4: Sketch of the proposed model of DG Tau X-ray structures including: magnetosphere producing hard X-ray flares absorbed by infalling accretion streams; spatially unresolved but spectrally identified soft X-rays from the base of the jet; forward jet producing soft unabsorbed resolved emission from the forward jet; and counter jet producing soft moderately-absorbed resolved emission. (Güdel et al. 2008)

Stellar Initial Mass Function

Despite the diversity and complications of star formation processes, the distribution of stellar masses appears to be nearly universal across star formation regions, open and globular clusters, and the Galactic field population. It follows a powerlaw relation at high masses (the Salpeter law), peaks around 0.3 $M_\odot$, and declines towards brown dwarfs. The physical causes underlying this distribution are widely discussed and probably involve the interplay between gravity, turbulence, thermal and magnetic pressures, fragmentation, disk accretion, and star cluster dynamics (Bonnell et al. 2007).

X-ray samples of PMS stars provide a new opportunity to measure IMF shapes and spatial distributions, particularly the lower mass regime (typically $0.5 < M < 5\ M_{\odot}$) which are difficult to sample from infrared studies of rich YSCs. IMFs can be estimated from X-ray luminosity functions due to a strong, though poorly understood, statistical correlation between X-ray luminosity and mass; $\log L_x = 30.4 + 1.9 \log M$ erg/s over the range $28 < \log L_x < 31$ erg/s and $0.3 < M < 3M_{\odot}$ (Telleschi et al. 2007). Masses of X-ray selected PMS stars can be estimated either directly from X-ray luminosities (hard band luminosities are more reliable to reduce obscuration effects), or from the *JHK* color-magnitude diagram. The results for several rich young clusters show general consistency with the standard Galactic IMF, though small differences in the lower mass distributions are sometimes present (Damiani et al. 2006, Wang et al. 2008).

Fate of OB stellar winds

The radiatively accelerated winds of massive OB stars have been known for several decades, but only close to the star where their broad emission and absorption lines can be studied in the ultraviolet and X-ray bands. At greater distances, their emission disappears from any band although the collective effects of their winds on large-scales are important for energizing and enriching the Galactic interstellar medium. The long-standing prediction of powerful hard X-ray emission from the terminal shocks of winds from young massive stars colliding with surrounding molecular clouds (Weaver et al. 1977) was not validated by early X-ray observations.

Chandra has now clearly discovered the large-scale shocked OB winds in a few YSCs. The most dramatic case is M 17, where 10 million K plasma fills the HII regions and streams outward into the Galaxy through a broad channel in the cold molecular cloud shown as the blue plume in Figure 1 (Townsley et al. 2003). As the emission appears center-filled rather than edge-brightened, it likely arises from the low-density shocks of the winds from several dozen OB stars rather than from terminal shocks where they interact with the molecular cloud. The absence of strong terminal shock emission, particularly in embedded ultra-compact HII regions, requires explanations such as entrainment of the winds by colder gas and/or dispersal of wind plasma through the fractal structure of the surrounding cloud gas.

X-ray irradiation of protoplanetary disks

There is increasing recognition that the circumstellar disks around PMS stars where planetary systems form are irradiated by light from the host stars. A considerable body of theoretical calculations have been made of the effects of PMS X-rays on disk thermodynamics, structure, dynamics, and chemistry — see reviews Glassgold et al. 2000, Alexander 2007, Armitage 2009, Balbus 2010, Bergin 2010. Calculations indicate that X-rays will be the dominant source of ionization in the outer disk layers, stimulating ion-molecular chemical reactions, desorbing molecules from grain surfaces, heating the gas (but not dust) to several thousand degrees, and photoevaporating the disk gases towards the end of the disk lifetime. One of the most important implications of X-ray ionization is the induction of the magneto-rotational instability. While the outer layers of a disk will always be partially ionized by PMS X-rays, the effect on planet formation processes depends on whether this ionization penetrates towards the midplane. This, in turn, depends on the spectrum of the incident X-rays; in cases where the PMS flaring is unusually luminous, the plasma temperature can exceed ~ 200 million K (Getman et al. 2008). In such cases, the turbulent region may reach the midplane over much of the disk, while in cases with less penetrating X-rays, a substantial 'dead zone' of non-turbulent gas is expected.

Chandra studies provide observational evidence that the stellar X-rays do efficiently irradiate protoplanetary disks. First, the 6.4 keV fluorescent line of neutral iron is seen in a small fraction of PMS X-ray sources, particularly the very young Class I protostars with heavy disks. The best example of this fluorescent line emission is shown in Figure 5 (Imanishi et al. 2001). The measured soft X-ray absorption requires that fluorescing material does not line up along the line-of-sight, so a disk-like geometry is favored. A mid-infrared Ne II emission line is also seen in some protoplanetary disks and can be attributed to X-ray irradiation (Pascucci et al. 2007).

X-ray flares and ancient meteorites

A fascinating approach to the challenges of planet formation is the study of ancient meteorites which recently impacted Earth from disturbances in their long-lived orbits in the Asteroid Belt. The meteorites are remnants of the protoplanetary disk and thereby reveal stages in the growth of planetesimals during the PMS stages of the Sun's protoplanetary disk starting 4.567 billion years ago (Lauretta & McSween 2006). Two characteristics of stony meteorites have been particularly puzzling for decades, and may have explanations linked to the X-ray flares seen in *Chandra* observations of PMS stars.

First, a large fraction of the mass of stony meteorites are in the form of chondrules, millimeter-sized globules of flash-melted rock. Simple models of protoplanetary disks cannot explain the sudden melting of these solids and a variety of explanations have been invoked: protoplanet-induced spiral shocks; supersonic bow shocks around gravitationally accelerated planetesimals; lightening; and magnetic reconnection events (Krot et al 2005). The prevalence of X-ray flares seen in PMS systems provides an empirical basis for this last possibility.

Second, the most ancient melted rock components – the calcium-aluminum-rich inclusions in carbonaceous chondrites – have very strange isotopic compositions with excess nuclei that are decay product of short-lived radionuclides like ^{10}Be, ^{26}Al, ^{41}Ca, and ^{53}Mn and (controversially) ^{60}Fe (Chaussidon & Gounelle 2006). Some of these parent nuclei, for example ^{10}Be and the possible presence of ^{7}Be, require a spallogenic origin where a proton or helium nucleus with MeV energy impacts a normal nucleus and produces a rare unstable nucleus in a disk solid particle (Gounelle et al. 2006). Solar energetic particles from flares which produce X-rays are known to produce spallogenic isotopes on lunar rocks; however, the abundances of anomalous isotopes in ancient meteoritic inclusions requires orders of magnitude excess of energetic particles over contemporary solar levels. Measurement of the flaring intensity and frequency in PMS stars from the *Chandra* Orion Ultradeep Project (Wolk et al. 2005) gives an estimated 10^5 enhancement in MeV proton production, sufficient to explain some of the important isotopic anomalies (Feigelson et al. 2002).

Exoplanets

Over the last decade, the discovery of exoplanets has fundamentally changed our perception of humanity's place in the universe. The role of X-rays in the study of exoplanets is subtle, but recent work indicates that exoplanets, and especially Jupiter mass planets at a distance < 0.1 AU from their parent stars (so called *hot Jupiters*), are subject to strong high-energy stellar radiation. The X-rays have been cited as a cause of excess heating of the planet which can induce mass loss. Further, it has been argued that the magnetic fields of the two bodies can interact. Recent statistical analysis of X-ray activity of stars possessing hot-Jupiters indicates that stars with close orbiting planets have enhanced X-ray emission (Kashyap et al. 2008). Inclusion of stellar X-ray and UV flux in irradiance calculations leads to enhanced expansion and escape of the planetary atmosphere, and the radiation plays a crucial role in photo-chemistry of the upper atmosphere (Burrows et al. 2008). The photo-chemical products can act, in turn, as high-altitude absorbers, create thermal inversions, and otherwise alter the observable properties of the planet's upper atmosphere.

Conclusions

From an astronomical viewpoint, there is no doubt that *Chandra* studies of star formation regions provide vivid, often unexpected results. These studies are propelled both by the subarcsecond resolution of the *Chandra* mirrors, and the sensitivity to harder X-rays that can penetrate extinction up to hundreds of visual magnitudes. A rich phenomenology is present in all four dimensions provided by the ACIS detector so that full visualization of the data requires a color movie (CXC 2005). *Chandra* has devoted several percent of its observing time to studies of PMS and young OB stars, including seven Large Projects and one Very Large Projects. In recent years, about 50 refereed papers appear annually reporting *Chandra* results or studying their implications for star and planet formation astrophysics.

There is little doubt that the X-ray selected samples of young stars are beginning to be enormously useful in studies that do not directly relate to the X-ray emission itself. For young stellar populations that are difficult to study in the infrared band due to field star or nebula contamination, or that are sufficiently old that many members have lost their infrared-emitting disks, the X-ray sources can give the best cluster membership lists. These censuses are needed to study the stellar Initial Mass Function, cluster structure, triggering processes, protoplanetary disk longevities, and star formation histories of molecular cloud complexes. A particularly valuable synergism between NASA's *Chandra* and *Spitzer* Great Observatories is emerging. Together they

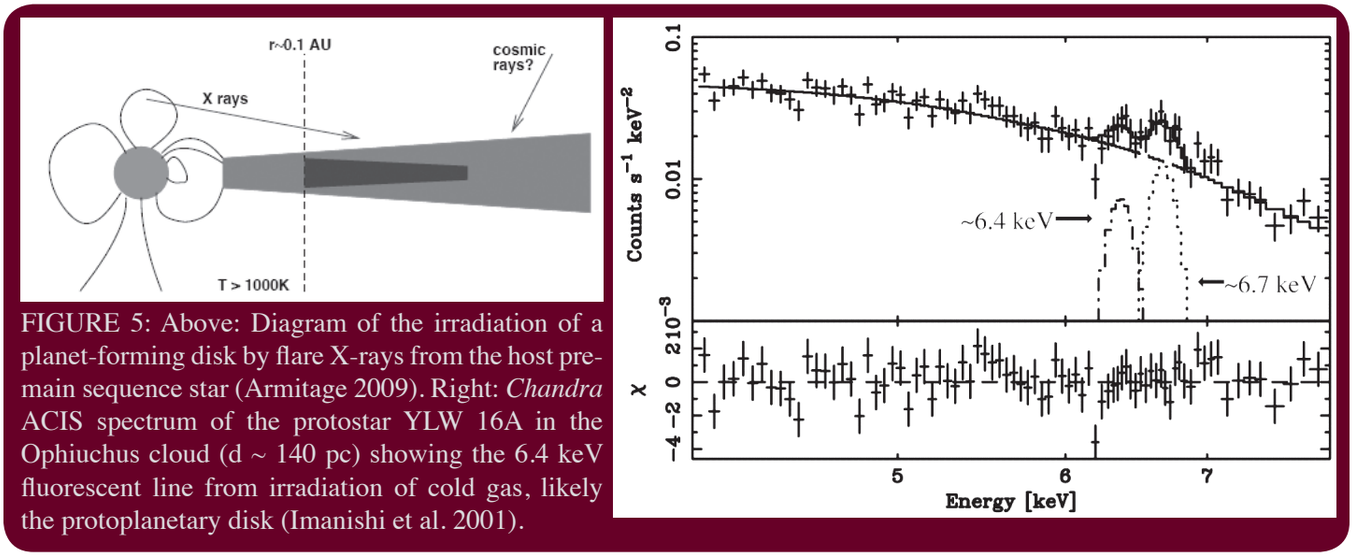

FIGURE 5: Above: Diagram of the irradiation of a planet-forming disk by flare X-rays from the host pre-main sequence star (Armitage 2009). Right: *Chandra* ACIS spectrum of the protostar YLW 16A in the Ophiuchus cloud (d ~ 140 pc) showing the 6.4 keV fluorescent line from irradiation of cold gas, likely the protoplanetary disk (Imanishi et al. 2001).

are giving new censuses of PMS stars in a wider variety of star forming regions (Dahm & Hillenbrand 2007, Tsujimoto et al. 2007, Winston et al. 2007, Caramazza et al. 2008, Wang et al. 2008, Wolk et al. 2008, Mercer et al. 2009, Pravdo et al. 2009, Skinner et al. 2009, Stelzer & Scholz 2009) and elucidating the evolution of protoplanetary disks and triggered star formation (Getman et al. 2007, Getman et al. 2008, Jensen et al. 2009).

From an astrophysical viewpoint, it is not yet clear how important X-ray findings will be to our understanding of star and planet formation. X-ray results are only now beginning to be incorporated into our empirical knowledge and theoretical understanding of star formation processes (Elmegreen 2009, Lada 2009). The discovery and elucidation of diffuse X-ray emitting plasma from shocked OB winds is astrophysically important. It not only reveals the supply of energy and gases to the Galactic interstellar medium at levels comparable to that of supernova remnants, but changes our view of HII regions as bubbles filled with 10^7K rather than 10^4K gas. For planet formation, it is very likely that X-rays irradiate protoplanetary disks and that the consequent heating and ionization will have a variety of important effects on disk physics and chemistry. It is possible, though far from established today, that X-ray emission plays a critical role in establishing disk turbulence and thereby regulating the formation and early dynamical processes of planet formation. These issues are being studied intensively in theoretical models of turbulent disks and their possible role in planet formation. The magnetic reconnection flares we see with *Chandra* today may also be responsible for the energetic melting and nucleosynthetic processes on our Sun's protoplanetary disk as revealed by structures in ancient meteorites.

Acknowledgments: Acknowledgements: E.D.F. acknowledges support for this work from SAO (SV4-74018), NASA (NNX09AC74G) and NSF (AST-0908038). He is affiliated with The Center for Exoplanets and Habitable Worlds is supported by the Pennsylvania State University, Eberly College of Science, and Pennsylvania Space Grant Consortium. S.J.W. was supported by NASA contract NAS8-03060. A more detailed review of these matters can be found in E.D.F.'s chapter in the proceedings of the *Chandra's First Decade of Discovery* symposium as well as the chapter by Swartz, Wolk & Fruscione (PNAS Press, forthcoming). ✯

REFERENCES

Alexander, R. (2007) *New Astron. Rev.*, 52, 60-77.
Armitage, P. (2009) Cambridge Univ. Press
Balbus, S. A. (2010) *Physical Processes in Circumstellar Disks Around Young Stars* (P. Garcia, ed.), Univ. Chicago Press.
Bergin, E. A. (2010) *Physical Processes in Circumstellar Disks Around Young Stars* (P. Garcia, ed.), Univ. Chicago Press.
Bonnell, I. A., Larson, R. B. and Zinnecker, H. (2007) *Protostars and Planets*. (B. Reipurth, et al., eds.), Univ. Arizona Press, 149-164.
Bradt, H. V. and Kelley, R. L. (1979) *Astrophys. J.*, 228, L33-L36.
Broos, P. S. et al. (2007) *Astrophys. J. Suppl.*, 169, 353-385.
Brickhouse, N.H. et al. (2010),.*Astrophys. J.* Accepted
Burrows, A. Budaj, J.,. Hubeny, I. 2008, *Astrophys. J.*. 678, 1436
Caramazza, M. et al. (2008), *Astron. Astrophys.*, 488, 211-218.
Chaussidon, M. and Gounelle, M. (2006) *Meteorites and the Early Solar System II* (D. S. Lauretta and H. Y. McSween, eds.), Univ. Arizona Press, 323-339.
Cranmer SR (2008) *Astrophysical Journal* 689, 316-334
Chandra X-ray Center (2005) Time-Lapse Movie of *Chandra* Observations (*Chandra* Orion Ultradeep Project), *http://chandra.harvard.edu/photo/2005/orion/animations.html*.
Dahm, S. E. and Hillenbrand, L. A. (2007) *Astron. J.*, 133, 2072-2086.
Damiani, F. et al. *Astron. Astrophys.*, 460, 133-144.
Elmegreen, B. G. (2009) *The Evolving ISM in the Milky Way and Nearby Galaxies* (K. Sheth, et al., eds.), *http://ssc.spitzer.caltech.edu/mtgs/ismevol/*
Favata, F. et al. (2006) *Astron. Astrophys.*, 450, L17-L20.
Feigelson, E. D. and DeCampli, W. M. (1981) *Astrophys. J.*, 243, L89.
Feigelson, E. D. and Montmerle, T. (1999) *Ann. Rev. Astron. Astrophys.*, 37, 363.
Feigelson, E. D., Garmire, G. P., Pravdo, S. H. (2002) *Astrophys. J.*, 572, 335.
Feigelson, E. D., Townsley, L. K. (2008) *Astrophys. J.* 673, 354.
Garmire, G. P. et al. (2003) *Proc. SPIE*, 4851, 28-44
Getman, K. V. et al. (2006) *Astrophys. J.*, 654, 316-337.
Getman, K. V. et al. (2008) *Astrophys. J.*, 688, 418-436.
Getman, K. V. et al. (2009) *Astrophys. J.*, 699, 1454-1472.
Glassgold, A. E., Feigelson, E. D. and Montmerle, T. (2000) *Protostars and Planets III*, Univ. Arizona Press, 429-456.
Gounelle, M. et al. (2006) *Astrophys. J.*, 640, 1163-1170.
Güdel, M. et al. (2007) *Astron. Astrophys.*, 468, 515-528.
Güdel, M.,. Telleschi, A. (2007), *Astron. Astrophys.*, 474, L25-32
Güdel, M. et al. (2008) *Astron. Astrophys.*, 478, 797-807.
Imanishi, K., Koyama, K., Tsuboi, Y. (2001) *Astrophys. J.*, 557, 747-760.
Jensen, E. L. N., Cohen, D. H. and Gagn'e, M. (2009) *Astrophys. J.*, 703, 252-269.
Kastner, J.H. et al. (2002) *Astrophys. J.* 567, 434-440.
Kashyap, V. L., Drake, J. J.,. Saar, S. H. 2008, *Astrophys. J.*. 687, 1339
Krot, A. N., Scott, E. R. D., Reipurth, B. eds. (2005) ASP Conf. 341, Astron. Soc. Pacific
Lada, C. J. and Lada, E. A. (2003) *Ann. Rev. Astron. Atrophys.*, 41, 57-115.
Lada, C. J. (2009) *Phil. Trans. Royal Soc. A*, in press.
Lauretta, D. S. and McSween, H. Y. eds. (2006) Univ. Arizona Press.
Mercer, E. P. et al. *Astron. J.*, 138. 7-18.
Pallavicini, R. et al. (1981), *Astrophys. J.*. 248. 279-290.
Pascucci, I., et al. (2007) *Astrophys. J.*. 663. 383-393.
Pravdo, S. H. et al. (2001) *Nature*. 413. 708-711.
Pravdo, S. H. et al. (2009) *Astrophys. J.*. 704. 1495-1505.
Preibisch, T. and Feigelson, E. D. (2005) *Astrophys. J. Suppl.*. 160. 390-400.
Robrade, J.,. Schmitt, J. H. M. M. (2007) *Astron. Astrophys.*. 473. 229-238
Reipurth, B. and Bally, J. (2001) *Ann. Rev. Astron. Astrophys.*. 39. 403-455.
Seward, F. D. and Chlebowski, T. (1982) *Astrophys. J.*. 256. 530-542.
Skinner, S. L., et al. (2009) *Astrophys. J.*. 701. 710-724.
Stelzer, B. and Scholz, A. (2009) *Astron. Astrophys.*. 507. 227-240.
Telleschi, A. et al. (2007) *Astron. Astrophys.*, 468. 425-442.
Townsley, L. K., et al. (2003) *Astrophys. J.*, 593. 874-905.
Townsley, L. K. (2009) Cambridge Univ. Press, 60-73.
Tsujimoto, M. et al. (2007) *Astrophys. J.*. 665. 719-735.
Wang, J. et al. (2008) *Astrophys. J.*. 675. 464-490.
Wang, J. et al. (2009) *Astrophys. J.*. 696. 47-65.
Weaver, R. et al. (1977) *Astrophys. J.*. 218. 377-395.
Weisskopf, M. C. et al. (2002) *Pub. Astron. Soc. Pacific*. 114. 1-24.
Winston, E. et al. (2007) *Astrophys. J.*. 669. 493-518.
Wolk, S. J. et al. (2005) *Astrophys. J. Suppl.*. 160. 423-449.
Wolk, S. J. et al. *Astronomical Journal* 132. 1100.
Wolk, S. J. et al. (2008) *Astron. J.*, 693-721.

Chandra's First Decade

Harvey Tananbaum

It is with great pleasure and pride that we marked the 10th anniversary of the launch of *Chandra*. We celebrated this milestone with the Symposium "*Chandra's* First Decade of Discovery" held in Boston from Sept. 22-25, 2009. The 4 days of talks and presentations underscored how many new insights have come from *Chandra* data–and how many opportunities still await us in the years to come.

At the Symposium, it was a particular pleasure to welcome back the STS-93 astronauts – Eileen Collins, Jeff Ashby, Steve Hawley, Cady Coleman, and Michel Tognini – who launched *Chandra* on July 23, 1999 and shared some of their memories and "inside" stories with the attendees. Riccardo Giacconi, who in 1963 originated the plans for an Observatory with *Chandra's* capabilities, de-

livered the keynote address. Martin Weisskopf, the NASA Project Scientist for the entire course of the program, presented a "personal perspective" on the making of *Chandra*. Steve Murray, Claude Canizares, and Mark Bautz (on behalf of Gordon Garmire) shared some of the joys and growing pains experienced by the Instrument Principal Investigators and their teams. Bob Burke shared similar experiences from the perspective of TRW (now NGAS), the prime contractor for the mission. A takeaway message is that a real key to the *Chandra* success is the practically seamless teaming among NASA, industry, and the science community to design, build and operate the Observatory.

If the pictures in this issue have whetted your appetite, you can see more and enjoy the conference proceedings (*http://cxc.harvard.edu/symposium_2009/photos/* and *http://cxc.harvard.edu/symposium_2009/proceedings/*).

Congratulations to the whole team – those who designed and built *Chandra*, those who operate it and enable scientists world-wide to use it, and those who have advanced our knowledge and thrilled the public with *Chandra*'s stunning images and detailed spectra.

We also wish to single out our late colleague Leon van Speybroeck, the *Chandra* Telescope scientist, who had so much to do with making *Chandra* a reality with such spectacular capabilities. ✯

Project Scientist's Report

Martin Weisskopf

We celebrated *Chandra's* 10th anniversary with the symposium "*Chandra*'s First Decade of Discovery", in Boston. (See pages 3-31, 60) Riccardo Giacconi (2002 Nobel Laureate) delivered the keynote address. In a session on the history of *Chandra*, the STS-93 crew—Mission Commander Eileen M. Collins; Pilot Jeffrey S. Ashby; and Mission Specialists Catherine (Cady) G. Coleman, Steven A. Hawley, and Michel Tognini—recounted their experiences in launching and deploying *Chandra*. Also in this session, Project Science described the history of the development of the Observatory. Additionally to mark the 10th anniversary, Martin Weisskopf, Wallace Tucker, Harvey Tananbaum, Norbert Schartel, and Maria Santos-Lleo co-authored "The first decade of science with *Chandra* and XMM-Newton", a review published in Nature's December 24/31 issue.

Now into its 11th year of operation, *Chandra* continues to enable exciting, often unique science. Current and projected spacecraft and Observatory performance lead us to anticipate a full second decade of discovery. The success and longevity of the mission are due to the dedication, experience, and professionalism of the team of scientists and engineers that designed, built, tested, manage, and operate the Observatory. During the past year, this experienced team detected, analyzed, and dealt with a potentially serious anomaly—an apparent leak in the Momentum Unloading Propulsion System (MUPS). Ultimately, the team established that the culprit was a faulty sensor (rather than a hydrazine leak) and appropriately modified procedures to continue to use the MUPS. In the process, the team determined that—through judicious target selection and use of gravity-gradient torques—*Chandra* operations could continue indefinitely even without the MUPS!

The *Chandra* team (CXC, MSFC, and instrument teams) continues to refine the Observatory's calibration (including better modeling of contamination of the ACIS filter) and to adjust operations to accommodate normal hardware aging (especially long-term warming of the spacecraft). Currently, a major activity is the preparation of the *Chandra* proposal for the NASA Astrophysics Division's biennial Senior Review of Operating Missions. Considering all the recent accomplishments, we are looking forward to a successful review. ✯

Project Manager's Report

Roger Brissenden

Chandra marked ten years of successful mission operations with continued excellent operational and scientific performance. The milestone was celebrated with a wide-ranging series of papers at the symposium "*Chandra*'s First Decade of Discovery" held in Boston, September 22-25. The Symposium was attended by over three hundred scientists. All five astronauts from the Columbia mission that launched *Chandra* were reunited for the first time. Commander Eileen Collins led a fascinating panel session of the astronauts' recollections. Videos of the talks, including Ricardo Giacconi's keynote address, are at *http://cxc.harvard.edu/symposium_2009/proceedings/*.

This first decade of operational and scientific excellence was capped by the signing of a contract modification with NASA to continue *Chandra* operations through the next decade. It provides for three years of continued operations followed by two additional options of three years each, plus one year of operations allowing for the CXC to develop all final data products. While space is an unforgiving environment, there are no expected limits to the *Chandra*'s life over this time span.

Chandra observing time continues to be in high demand. In Cycle 11, over 700 proposals oversubscribed the available observing time by a factor greater than 5. The peer review of proposals was held in June, and in December 2009 the observing program officially transitioned from

Cycle 10 to Cycle 11. The call for Cycle 12 observations was issued in December, and planning is well underway for the peer review to be held 21-25, June, 2010.

The CXC solicits proposals and conducts a peer review of applicants for the NASA Einstein Fellowship program, which includes research areas related to the science goals of the Physics of the Cosmos program and its missions. This year, 162 young scientists applied for the ten Fellowships. The results have been announced (see article on page 45). The first Einstein Fellows symposium was held at the Harvard-Smithsonian Center for Astrophysics, 27-28 October 2009, where 21 of the fellows presented their recent research. The presentations can be viewed at *http://cxc.harvard.edu/fellows/program_2009.html*.

A science workshop, "SNR and Pulsar Wind Nebulae in the *Chandra* Era," was held 8-10 July 2009, at the Double Tree Guest Suites Hotel, Boston. Presentations can be viewed at *http://cxc.harvard.edu/cdo/snr09/program.html*.

The CXC mission planning staff continued to maximize observing efficiency in spite of temperature constraints on spacecraft pointing. Competing thermal constraints continue to require some longer observations to be split into multiple short-duration segments, to allow the spacecraft to cool at preferred attitudes. Overall the average absolute observing efficiency in 2009 was 69% of total time, compared with 68% in the prior year. The maximum efficiency possible, limited by the need to turn off *Chandra's* instruments when in the Earth's radiation belts, is about 70%.

Three flight software patches helped mitigate potential effects of the long-term warming of the spacecraft. One patch added an important safety factor by enabling use of the HRC anti-coincidence shield as an auxiliary radiation monitor, to compensate partially for the continual degradation of the EPHIN radiation detector due to heating. The other two patches improved safety and observing efficiency by mitigating contingencies associated with eclipses.

Operational highlights over the past year included four "fast" observations of targets of opportunity, and five other operational events that required the mission planning and flight teams to reschedule and interrupt the on-board command loads. *Chandra* passed through the 2009 summer and winter eclipse seasons with nominal power and thermal performance. For the third year in a row the sun was quiet, causing no interruptions due to solar activity. With the clear onset of solar cycle 24, we are prepared for solar interruptions during the coming year.

A significant concern was an anomalous reading of the momentum unloading propellant pressure that occurred suddenly in July. As discussed in an accompanying article (see "The MUPS Anomaly", pg 26), after extensive evaluation this event proved to have the most benign outcome possible: a faulty pressure transducer. It is remarkable that during the evaluation, and despite added constraints on pointings to control temperatures and balance momentum, normal science observing was maintained with no loss of time! *Chandra* continues to have had no safe mode transitions since the first year of operation.

Both focal plane instruments, the Advanced CCD Imaging Spectrometer and the High Resolution Camera, have continued to operate well and have had no significant problems. ACIS, along with the overall spacecraft, has continued to warm gradually. Following tests conducted during 2008 and 2007, an additional heater was turned off on the Science Instrument Module, with an immediate beneficial reduction in the average ACIS focal plane temperature.

Significant improvement of calibrations during the year included improved knowledge of the HRMA effective area at low energies, and of the contamination on the ACIS optical blocking filters. The former improves the internal consistency of spectra measured by *Chandra* using different instrument energy bands, and the latter better extrapolates the (small) increase in attenuation for low energy measurements by ACIS.

Chandra data processing and distribution to observers continued smoothly, with the time from observation to delivery of data averaging less than 2 days. The *Chandra* archive holdings grew from 6.6TB to 7.4TB (compressed) and now contain 27 million files.

The Data System team released software updates to support the Cycle 11 proposal submission (March 2009), the Cycle 11 Peer Review (June) and the Cycle 12 Call for Proposals (December). *Chandra* Source Catalog (CSC) version 1.0 was officially released in March 2009. The catalog includes public ACIS data representing point and compact sources. In addition the team upgraded the catalog generation software to allow HRC data to be included in catalog version 1.1, planned for release in spring 2010. Version 4.2 of CIAO was released in December, with important enhancements to Sherpa and Chips, and an updated CalDB 4.2.0 was released to support the latest CIAO. A release was also made of the CXC data processing system software, supporting a migration to Solaris 10.

The Education and Public Outreach group issued 18 *Chandra* press releases (*http://chandra.harvard.edu/press*) and a comparable number of additional image releases. An exciting 3-D image wall - a virtual museum that contains all publicly released *Chandra* images - was completed (*http://chandra.harvard.edu/photo/3d_gallery/*) and the team contributed to the International Year of Astronomy with the 'From Earth To the Universe' display featured in over 60 countries and over 20 locations across the US.

We look forward to an eleventh year of smooth and efficient operations, yielding rich and exciting science results. ✯

Instruments: ACIS

Paul Plucinsky, Royce Buehler, Nancy Adams-Wolk, & Gregg Germain

The ACIS instrument continued to perform well over the past year with no failures or unexpected degradations. The charge-transfer inefficiency (CTI) of the FI and BI CCDs is increasing at the expected rate. The CIAO software and associated calibration files correct for this slow increase in CTI over time. The contamination layer continues to accumulate on the ACIS optical-blocking filter. The CXC calibration group has recently released an update to the contamination model which more accurately represents the absorption due to the contamination layer during recent years (discussed elsewhere in this newsletter). There was one unexpected reboot of the ACIS Back-End Processor (BEP) on 25 January 2010, which resulted in the loss of a small amount of science observing time. The flight SW patches were re-installed and the BEP was quickly rebooted since the reboot was caused by a power transient which erased the patches in memory. ACIS has operated nominally since the reboot.

The control of the ACIS focal plane (FP) temperature continues to be a major focus of the ACIS Operations team. In April 2008, the ACIS Detector Housing (DH) heater was turned off to provide more margin for the FP temperature control. In August 2009, a heater on the Science Instrument Module (SIM) Focus Assembly (FA) was turned off to provide yet more margin (the so-called "SIM FA6" heater). Figure 6 shows the average ACIS FP temperature during science observations from 2007 to 2010. The desired operating temperature is -119.7˚C. The FI CCDs have a narrower tolerance on the FP temperature than the BI CCDs. For the FI CCDs, the gain changes by 0.3% at 1.5 keV if the FP temperature warms to -119.2˚C and for the BI CCDs, the gain changes by 0.3% if the FP temperature increases to -118.2˚C. The plot shows that there was a significant reduction in the average FP temperature after the DH heater was turned off, and there was an additional reduction after the SIM FA6 heater was turned off. The red line shows the FI CCD limit of -119.2˚C and the blue line shows the BI CCD limit of -118.2˚C. There are two main factors which lead to warmer than desired ACIS FP temperatures; first the Earth can be in the FOV of the ACIS radiator (which provides cooling for the FP and DH) and second, for pitch angles larger than 130 degrees, the Sun illuminates the shade for the ACIS radiator and also heats the rear surfaces of the SIM surrounding the ACIS DH. The ACIS Ops team is working with the *Chandra* Flight Operations Team to develop a model which will more accurately predict when the Earth is in the ACIS radiator FOV, so that those observations can possibly be rescheduled to reduce or eliminate the excursions of the FP temperature.

One change was made to the default grade rejection for CC mode observations. Up to this point in the mission, the default grade selection for CC mode observations had been to reject **ASCA** grade 7 events. The default grade rejection for TE mode observations has been to reject ACIS flight grades 24, 66, 107, 214, & 255. The grade rejection

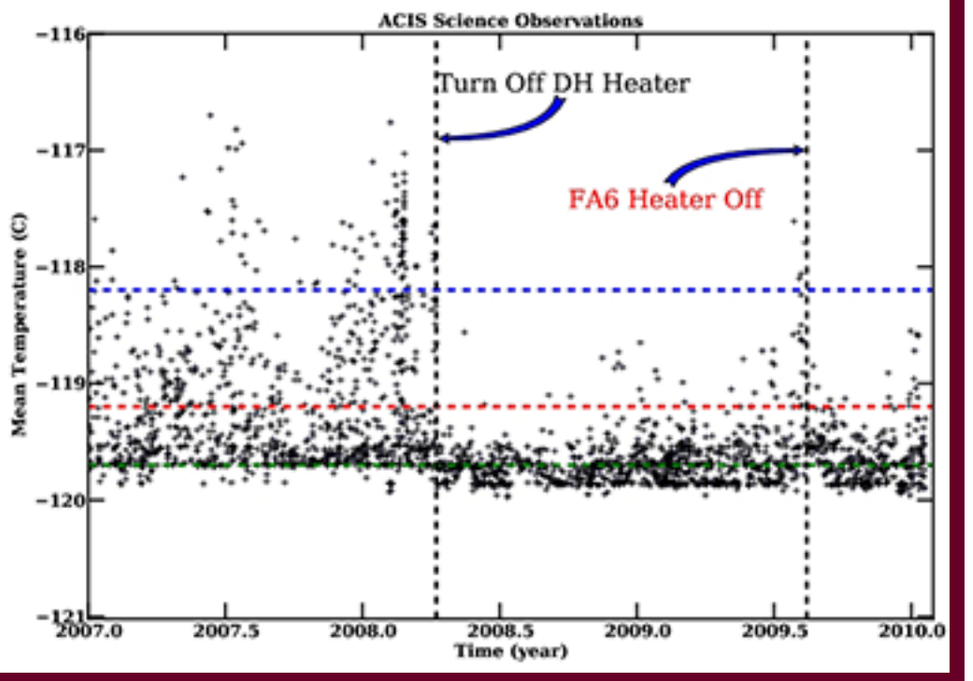

FIGURE 6: The average ACIS focal plane temperature for sciencee observations from 2007 until January 2010. The dashed vertical line at 2008.3 indicates the day on which the ACIS detector housing heater was turned off and the dashed line at 2009.6 indicates the day the SIM FA6 heater was turned off. The green dashed horizontal line indicates the desired FP temperature of -119.7 C. The red dashed line indicates the temperature (-119.2 ˚C) at which the gain of the FI CCDs changes by 0.3% and the blue dashed line indicates the temperature (-118.2 ˚C) at which the gain of the BI CCDs changes by 0.3%.

filter had been selected to be more inclusive for CC mode since the effective background is higher in CC mode than TE mode and the assumption is that one is observing a bright source in CC mode. Because the row-to-row transfer time differs between CC and TE modes, CTI has different effects in CC mode. The CXC calibration team has determined that a significant fraction of the good X-ray events end up in flight grade 66. In order to recover these events for future use, the CXC decided to change the default grade rejection in CC mode to reject ACIS flight grades 24, 107, 127, 214, 223, 248, 251, 254, & 255. This grade rejection optimizes the selection of valid X-ray events compared to background events. The change was implemented in November 2009. *Chandra* GOs should notice that their CC mode level 1 events lists now include flight grade 66 events in observations taken after November 2009.

Supernova Remnants in the ChASeM33 Survey

Paul Plucinsky, Knox Long, Terrance Gaetz, and the ChASeM33 Team

The Chandra ACIS Survey of M33 (ChASeM33) is a VLP program to survey the inner regions of the M33 galaxy. The survey consists of 7 different fields observed for 200 ks (each field observed twice for ~100 ks), covering most of the galaxy inside the D25 isophote. Details of the survey and the first source catalog are contained in Plucinsky et al. 2008. One of the key projects of the ChASeM33 survey is to characterize the SNR population in M33. M33 is a particularly appealing target for such a study because it is nearby (D 817 kpc), it is relatively face-on (i ~ 56 degrees), and the Galactic foreground absorption is relatively low (N_H ~ 6.0 × 10^{20} cm^{-2}). At the distance of M33, one arcsecond subtends about 4.0 pc, offering the possibility of resolving structure in SNRs with diameters of 20 pc or more. Previous optical and radio surveys had identified about 100 SNRs, relying mostly on optical interference-filter imaging to determine the ratio of S II to Hα to distinguish SNRs from H II regions.

We supplemented the existing list of M33 SNRs with new SNR candidates based on the emission line survey from the Local Group Galaxy Survey (LGGS) and our own observations acquired with 0.6m Burrel Schmidt telescope at the Kitt Peak National Observatory. In addition, we acquired new images of M33 at 6 cm and 20 cm with the VLA in its A configuration which offered 0.5 and 2.0 arcsecond resolution at 6 and 20 cm, respectively, with typical noise levels between 15 and 25 uJy. We also acquired optical spectra of some of the candidates using the Blue Channel Spectrograph and Hectospec instruments on the MMT Observatory. Finally, the ChASeM33 data were also searched for candidate SNRs by looking for objects with soft, thermal spectra which may also appear to be extended. The result of combining the above searches is 137 SNR and SNR candidates, of which 131 lie within the region covered by the ChASeM33 survey.

The X-ray emission properties of these 131 confirmed and candidate SNRs are reported in Long et al. 2010. We detect 58(82) of the SNRs and SNR candidates at the 3(2) sigma level in the ChASeM33 data. This represents the largest sample of SNRs detected in both the X-ray and the optical of any galaxy, including the Milky Way. The high angular resolution and sensitivity of *Chandra* are crucial for this project, especially in crowded regions of the galaxy. Figure 7 is a close up of the southern spiral arm of M33 which has a high density of SNRs. The top panel shows the X-ray data which has been color-coded such that sources with soft spectra appear red and sources with hard spectra appear blue. The middle panel is a combination of the Hα, S II , and O III from the LGGS survey which illustrates the complexity of the interstellar medium in this region of the galaxy. The bottom panel overlays the positions of the SNRs on the continuum-subtracted Hα image showing that there are about 30 SNRs in this region of the galaxy alone. The brightest SNR (GKL98-21) has over 9,000 counts in the ChASeM33 data, while the faintest (GKL98-34) has only 13 counts. The luminosities of the SNRs in the 0.35-2.0 keV band range from 2.0 × 10^{34} erg/s to 9.0 ×10^{36} ergs/s assuming a thermal plasma spectrum with a kT=0.6 keV and an absorbing column of 6.0 × 10^{20} cm^{-2}. A comparison of the M33 SNR luminosity function to that of the LMC and SMC (Figure 8) shows a striking difference at the high luminosity (L) end. The LMC has more high L SNRs than M33 and the SMC has as many high L SNRs, while having significantly fewer SNRs overall. The reasons for these discrepancies are not clear. The LMC and M33 have similar star formation rates so one naively expects the number of core-collapse supernovas (SNe) to be similar for the two galaxies, while the SMC has a star formation rate about 1/4 that of M33 such that the number of SNRs should be significantly less than M33. One possibility is that SNRs are evolving faster in the LMC and SMC, such that it is less likely to catch an older, fainter remnant and a younger remnant might be more luminous because it is expanding into a dense medium. Another possibility is that the LMC and SMC may not have been surveyed as deeply as M33 across their entire extent, such that incompleteness sets in at a higher L than in M33. If that is the case, recent observations of the SMC and LMC should help to fill in the LF.

There are seven SNRs in the ChASeM33 survey which have more than 750 counts such that a detailed analysis of

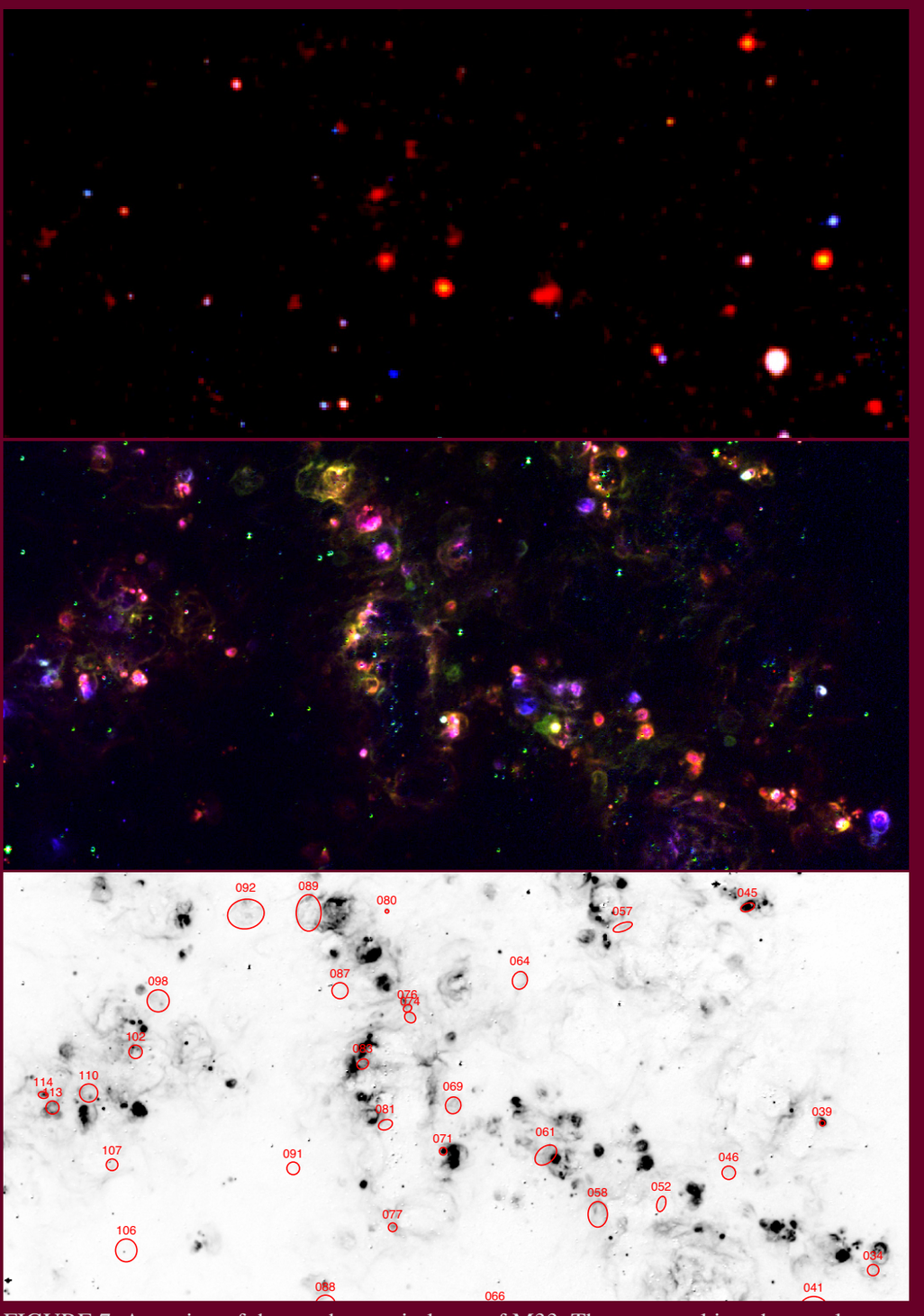

FIGURE 7: A portion of the southern spiral arm of M33. The top panel is a three-color rendition of the *Chandra* X-ray mosaic image (red: 0.35–1.1 keV; green: 1.1–2.6 keV; blue: 2.6–8.0 keV). The center panel is a three-color optical image from the continuum-subracted LGGS data (red: H α; green: S II; blue: O III). The bottom panel shows the continuum-subtracted H α image with the SNRs marked. In the center panel, SNRs generally appear as green or yellow, while hii regions are generally magenta or red. The field measures 12.2′ × 5.8′ and is oriented N up, E left. (Reprinted from ApJS)

the images and spectra are warranted. The brightest SNR in M33 (GKL98-21) has already been studied in detail by Gaetz et al. 2007. GKL98-21 has a diameter in X-rays which is about 5 arcseconds or about 20 pc. The *Chandra* image (Figure 9: Figure 2 in Gaetz et al 2007) beautifully resolves the X-ray emission into a limb-brightened shell with the eastern side of the remnant being significantly brighter than the rest. Interestingly, a detailed comparison of the X-ray image with the optical image shows that where the X-rays are brightest the S II is faintest. The ChASeM33 data have resolved structure in a SNR in M33 in the X-rays for the first time. We performed detailed spectral fits of these seven brightest SNRs with a non-equilibrium, plane-parallel shock model. Five of the spectra were fit reasonably well with abundances typical of M33, but two fits showed large residuals with M33 abundances, especially around the Mg lines. We refit these two spectra (GKL98-31 and GKL98-35) and found a significant improvement in the fit when O, Ne, Mg, and Fe were allowed to vary. These fits showed that O, Ne, and Mg were significantly enhanced compared to Fe, indicating that these two remnants are most likely the result of core-collapse SNe. Therefore, the quality of the ChASeM33 spectra allow us to perform detailed spectral fits for the first time in order to constrain the progenitors of the observed SNRs.

It is interesting to ask if counterparts of the the historical SNRs in the Galaxy (the Crab, Cas A, Tycho, Kelper, and SN 1006) in M33 would have been detected in the ChASeM33 survey. The question is somewhat complicated by the varying sensitivity across the seven fields in the ChASeM33 survey and the uncertainty introduced in taking the observed, more absorbed spectrum of Galactic remnant and extrapolating that to a less-absorbed spectrum at the distance of M33. Nevertheless, we can say with some confidence that if there were an object similar to the Crab, Cas A, Kepler, or Tycho in M33, it would have been detected in our survey. However, an SN 1006 analog would have been just above or just below our detection limit depending upon its position in M33. Therefore, it seems likely that an SN 1006 analog would not have been classified properly as a SNR or not detected. Since the star formation rate of M33 is significantly less than the Galaxy, it is not surprising that analogs of the Crab or Cas A were not found in our survey. ✯

References

Plucinsky, P. P., et al. 2008, ApJS, 174, 366
Gaetz, T. J., et al. 2007, ApJ, 663, 234
Long, K.S., et al., 2010, ApJS, in press
Williams, R. M., Chu, Y.-H., Dickel, J. R., Gruendl, R. A., Shelton, R., Points, S. D., & Smith, R. C. 2004, ApJ, 613, 948
Williams, R. M., Chu, Y.-H., Dickel, J. R., Petre, R., Smith, R. C., & Tavarez, M. 1999, ApJS, 123, 467
Haberl, F., & Pietsch, W. 1999, A&As, 139, 277
Bamba, A., Ueno, M., Nakajima, H., Mori, K., & Koyama, K. 2006, A&A, 450, 585
Filipovic, M.D., et al. 2008, A&A, 485, 63
van der Heyden, K. J., Bleeker, J. A. M., & Kaastra, J.S. 2004, A&A, 421, 1031

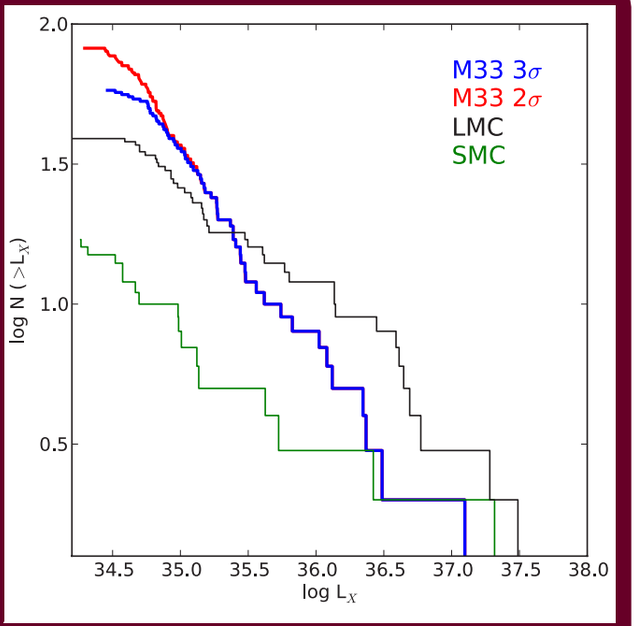

FIGURE 8: The 0.35–2 keV luminosity function for SNRs in M33. The sources detected at 3σ or greater are shown in blue; those only detected at 2σ are shown in red. For comparison, the luminosity functions for SNRs in the Large and Small Magellanic Clouds are also shown in black and green, respectively. For the LMC, we used data from Williams 1999, Williams 2004, Haberl 1999 and Bamba 2006; for the SMC we used Filipovic 2008 and van der Heyden 2004. In all cases we converted count rates to luminosities assuming simple thermal plasma models with kT_e of 0.6 kev and an absorbing N_H of $5 \times 10^{20} cm^{-2}$. We assumed distances of 50 and 60 kpc for the Large and Small Clouds, respectively. (Reprinted from ApJS)

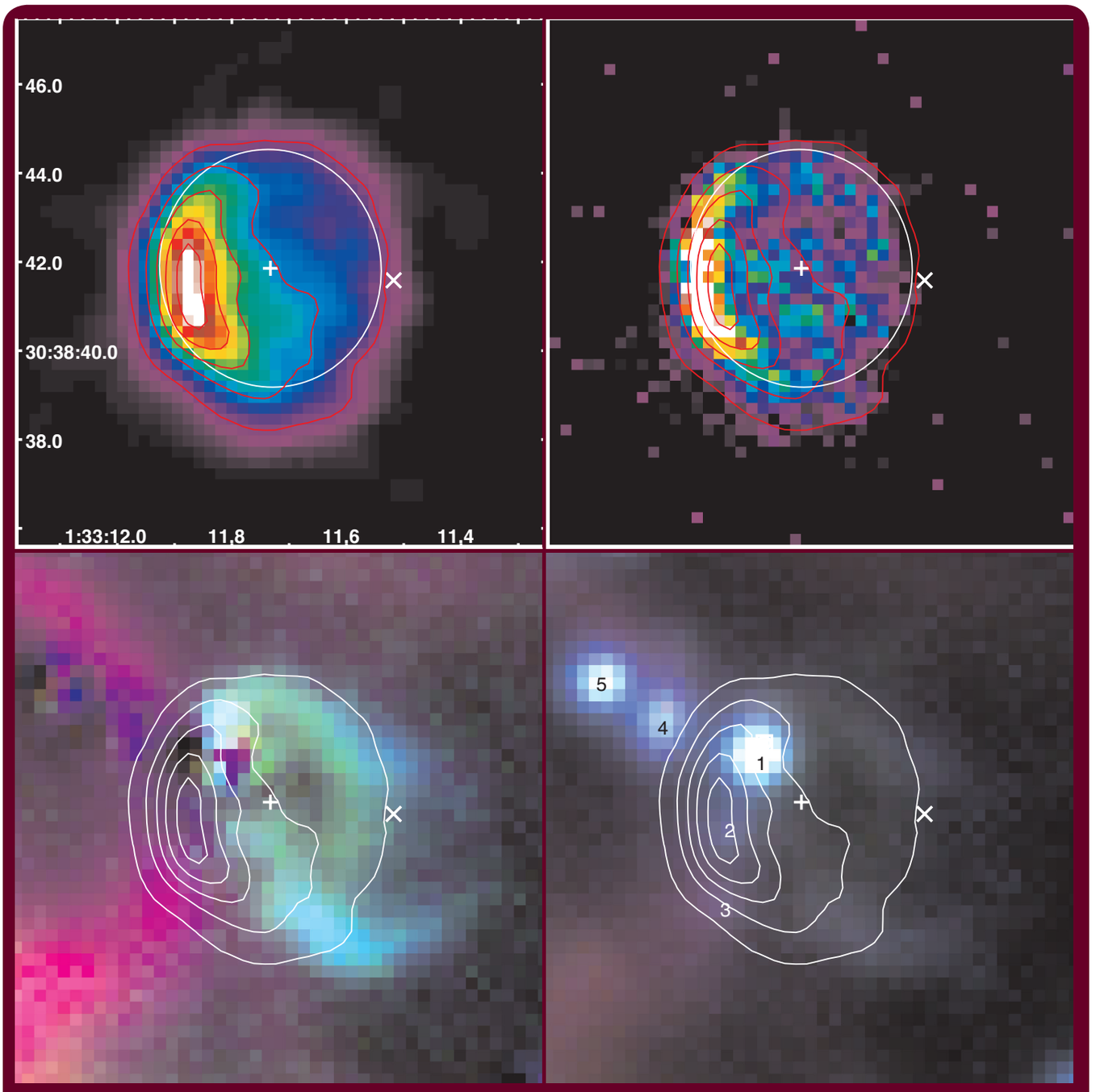

FIGURE 9: Top left: Exposure-corrected (0.35–4keV) *Chandra* image of G98-21, binned by 0.5 ACIS pixels in each direction and smoothed with a 3-bin radius Gaussian. The coordinate axes are labeled with J2000 coordinates. The red contours are from a similarly smoothed image for total counts, ranging from 2–18 counts/bin in steps of 4 countst/bin; the background level is 0.03 counts/bin. The white ellipse shows the dimensions of an elliptical shell model. The central white "+" is the X-ray center, and the white "×" to the west is the centroid position for the nonthermal radio source. Top right: The result of 10 iterations of the Lucy-Richardson deconvolution algorithm. The slight shift of the bright ridge to larger radii is an artifact. Bottom panels: False color RGB composite of the optical images, with Hα (red), S II (green), O III (blue). Bottom left: Continuum subtracted LGGS images, overlaid with X-ray contours. Bottom right: LGGS images prior to continuum subtraction, overlaid with X-ray contours. The numbers identify stars from the LGGS catalog. (Reprinted from ApJ)

Chandra Related Meetings

Upcoming

Check our website for details:
http://cxc.harvard.edu/

Chandra Users' Committee Meeting
April 27-28, 2010
Cambridge MA
http://cxc.harvard.edu/cdo/cuc/

Chandra Workshop: Accretion Processes in X-rays:
From White Dwarfs to Quasars
July 13 - 15, 2010
DoubleTree Guest Suites, Boston, MA
http://cxc.harvard.edu/cdo/accr10/

Einstein Fellows Symposium
Fall 2010
http://cxc.harvard.edu/fellows/

Past

7th *Chandra*/CIAO Workshop
February 1-3, 2010
Cambridge, MA
http://cxc.harvard.edu/ciao/workshop/feb10/

Supernova Remnants and Pulsar Wind Nebulae
July 8-10, 2009
Cambridge MA
http://cxc.harvard.edu/cdo/snr09/

Chandra Calibration Review
September 21, 2009
Cambridge MA
http://cxc.harvard.edu/ccr/

Chandra's First Decade of Discovery
Sept. 22-25
Cambridge MA
http://cxc.harvard.edu/symposium_2009/

Einstein Fellows Symposium
October 27-28, 2009
Cambridge, MA
http://cxc.harvard.edu/fellows/

Chandra Users' Committee Meeting
October 29-30, 2009
Cambridge, MA
http://cxc.harvard.edu/cdo/cuc/

Instruments: HRC

Ralph Kraft, Almus Kenter

The theme of this year's HRC contribution to the *Chandra* newsletter is 'On The Road (Again)'. The big news of course is that the HRC principal investigator, Dr. Stephen Murray, is leaving SAO after nearly thirty-seven years of service to take a faculty position at Johns Hopkins. He will continue to lead a number of ongoing projects at SAO, and will be involved in a variety of projects in his new role, including developing innovative mission concepts for IR astronomy. He will continue to be the PI of the HRC after moving to Baltimore, but all other HRC-related activities, including both laboratory and mission operations, as well as all other HRC IPI-team personnel will remain in Cambridge. On behalf of all the HRC instrument team members and other colleagues at SAO, we want to wish Steve the best in his future endeavors at JHU. He will be sorely missed here at SAO. A brief description of Steve's enormous contribution to SAO, to the *Chandra* program, and to the high energy astrophysics community more generally is contained elsewhere in this newsletter. Additionally, the HRC lab is on the move again. We had been sharing space in the high-bay area of the Cambridge Discovery Park facility. We are currently in the process of moving the lab into our own area in the same building. The HRC POC (Proof of Concept electronics, i.e. the HRC backup that is in the lab to diagnose any potential electrical or mechanical problems) and other laboratory operations should be fully functional before the publication of this newsletter.

HRC flight operations continue smoothly with no anomalies or interruptions. The instrument gain continues to slowly decline with increasing charge extraction, but we are still many years away from having to increase the operating voltage to offset the gain loss. Another routine year of HRC operations, with hopefully many more to come!

The HRC has been used over the past year to make a wide variety of scientific investigations. One of the most interesting has been an HRC-I observation of SN1987A (Ng et al. 2009). The ring structure of the SNR that was previous reported based on deconvolution of the lower spatial resolution ACIS-S observation (Burrows et al. 2000) was confirmed by direct imaging with the HRC. The X-ray radius of the shell is found to be ~0.96" and is identical to the radius of the radio shell, contrary to earlier reports that the X-ray shell was smaller than the radio shell. A montage of raw, deconvolved, and smoothed HRC, ACIS, and radio (9 GHz ATCA) images of the SNR is shown in Figure 10. The ring-like structure of the remnant is clearly visible in the HRC images at the top left. No point source is ob-

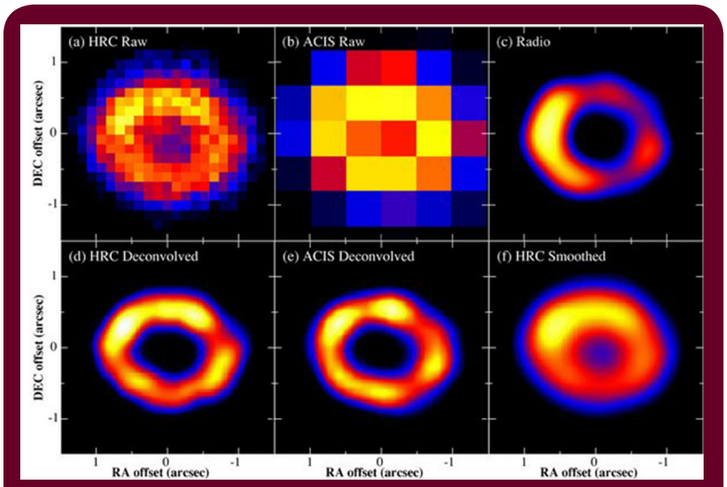

FIGURE 10: (a) Raw HRC data of SNR 1987A taken on 2008 April 28-29. The image was binned into the HRC detector pixel and centered at R.A. = 05h35m28s, decl. = –69°16'11.2" (J2000). (b) Raw ACIS data taken on 2008 January 9. The image is in 0.3-8 keV energy range and was binned into the ACIS detector pixel. (c) Super-resolved radio image at 9 GHz taken by ATCA on 2008 April 23 (Ng et al. 2008). (d) Deconvolved HRC image using the data set shown in panel (a). (e) Deconvolved ACIS image using the data set shown in panel (b), in 0.3-8 keV energy range (Racusin et al. 2009). (f) HRC data in panel (a) smoothed to 0.4" to match the resolution of the radio image in panel (c). All panels are on the same spatial scale. (Image and figure captions taken from The Astrophysical Journal Letters).

served at the center of the remnant, and the upper limit to the flux conclusively rules out the presence of any neutron star with surface temperature, T∞, greater than 2.5 MK, a pulsar wind nebulae, or a magnetar. ✯

References

Ng et al. 2009, ApJ, 706, L100
Burrows et al. 2000, 543, L149
Ng et al. 2008, ApJ, 684, 481
Racusin et al. 2009, ApJ, 703, 1752

Instruments: HETG

Dan Dewey, for the HETG Team

The HETG continues to perform as well as ever and successfully completed its first 10 years of high-resolution observations with an observation of SN 1987A in July 2009 and began its next decade with an observation of Eta Car in September 2009. Why the August gap you ask? Well, a "failed" limit switch on a grating mechanism began working again which surprised the patched-assuming-a-failed-switch flight software which had to then be redesigned to ignore the limit switch rather than count on it in a failed state. Thanks again to the operations team for keeping the observatory working so well over the past decade.

At the *Chandra*'s First Decade conference, HETG PI Prof. Claude Canizares presented a brief history of the HETG over its three decades (Canizares 2009), adding more human details to the HETG's design and fabrication (Canizares et al. 2005.) What was the HETG recipe for spectroscopy? Get about a dozen technicians and engineers, provide invar frames, silicon wafers, liquids, gasses, and energy, and in a few years with lots of sweat out come HETG gratings!

TGCat: The Armchair Spectroscopist

The *Chandra* Transmission Grating Data Catalog and Archive, TGCat, is up and running with a new web interface, see it at: *http://tgcat.mit.edu/*. TGCat (Huenemoerder et al. 2009, Mitschang et al. 2010) provides easy access to analysis-ready products for *Chandra* HETG and LETG observations. Unlike the *Chandra* archive which is organized around pointings of the telescope (observations), TGCat includes a source catalogue of the 300+ distinct sources that have *Chandra* grating spectra. Given a source it is possible to get all the TGCat extractions of that source, view summary plots of them, make combined custom spectral plots from them, and download standard products (pha, arf, rmf files) to carry out analyses. Because of the relatively limited number of sources it is possible for the TGCat curators to provide customized attention to the sources and extractions, assessing data quality, etc. TGCat is available from just a web browser, so when you are reading a paper with HETG results, e.g., Figure 11, you can find and view the data yourself, Figure 12, and download it all in a couple of minutes. In an effort to support multiwavelngth use, the interactive custom plotting of TGCat (Figure 12, 13) allows making plots with many choices for the units of the axes besides common X-ray ones, for example: νF_ν, mJy, and Hz. Of course, the TGCat curators are happy to receive your feedback to make this a most useful resource for X-ray spectroscopy.

HETG Science: Not Your "Vanilla" White Dwarfs

Two recent papers describe HETG observations of X-rays from white dwarf (WD) binary systems, both of these are unique even within the context of X-ray-bright WD systems. The line-rich X-ray spectrum from the AE Aquarii system, Figure 14, includes clear im-

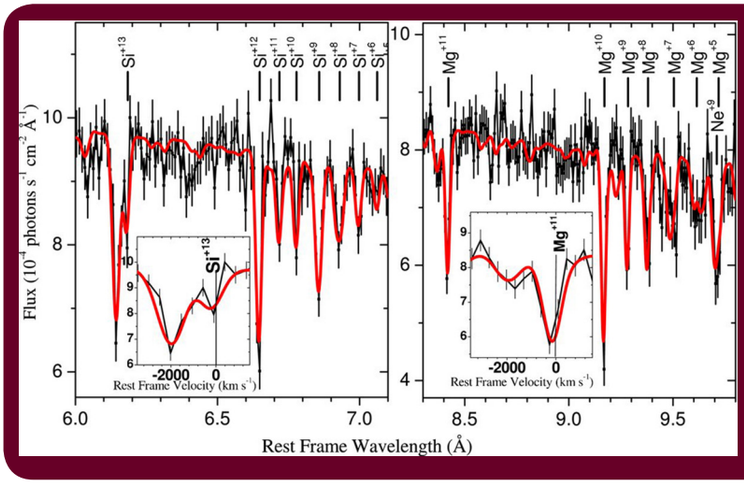

FIGURE 11: HETG spectral regions seen in the Seyfert 1 active galactic nucleus (AGN) MCG -6-30-15. Ionized absorption of Si and Mg ions show slow and fast velocity components (insets) w.r.t. the rest frame, z = 0.007749. This is Figure 3 of Holczer et al. (2010).

prints of the WD spin; see the spectrum in Mauche (2009b) or use TGCat! As well as seeing flux changes at the WD spin frequency, the HETG data were used to measure small changes in the average emission line wavelengths that, remarkably, are seen to vary with the WD spin, Figure 16. A two-spot emission model, initally suggested by HST UV data, can reproduce the qualitative aspects of the measurements, Figure 15. These HETG observations were made as part of a multiwavelength campaign that included amateur observations as well (Mauche 2009a).

A second WD system, SS73 17, is one of the "hard X-ray emitting symbiotics" that was seen at high energies by *INTEGRAL* and *Swift* and follow-up observations by *Suzaku*. A recent HETG observation (Eze et al. 2010) clearly separates the Fe-K lines, Figure 17, whose flux ratios confirm that the Fe XXV and FE XXVI lines are from thermal emssion at a temperature that is consistent with the temperature measured by the highly-absorbed continuum emission.

Of course further observations and analyses could be

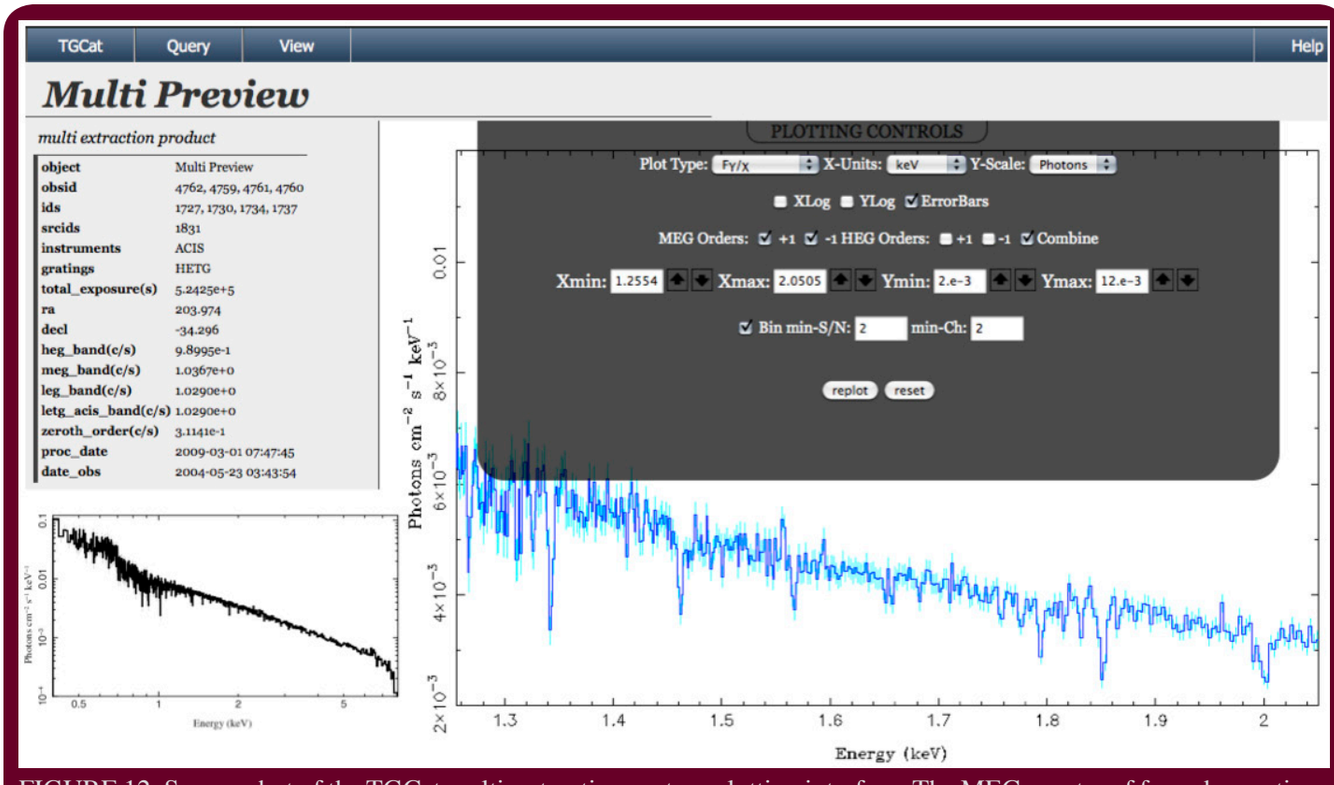

FIGURE 12: Screen-shot of the TGCat multi-extraction custom plotting interface. The MEG spectra of four observations of MCG -6-30-15 have been combined and plotted vs observed energy. The absorption features seen in Figure 11 are seen here as well, flipped left-to-right: Mg from 1.255 to 1.482 keV and Si from 1.733 to 2.050 keV. This view can be created in a minute or two using just a web browser.

done to learn more about these systems with current observatories and especially with future observatories like *IXO* with its larger collecting area and improved spectral resolution (Mauche 2009b). ✯

References

Brickhouse, N.S. et al. (2010), ApJ, TBD, TBD.
Canizares, C.R. et al. (2005), PASP, 117, 1144.
Canizares, C.R. (2009), a talk at *Chandra*'s First Decade of Discovery, Session 4: *http://cxc.harvard.edu/symposium_2009/proceedings/session_04.html*
Eze, R.N.C. et al. (2010), ApJ, 709, 816.
Holczer, T. et al. (2010), ApJ, 708, 981.
Huenemoerder, D.P. et al. (2009), *Chandra* Newsletter, issue 16, p.39.
Mauche, C.W. (2009a), a talk at The 14th North American Workshop on CVs and Related Objects: *http://www.noao.edu/meetings/wildstars2/talks/wednesday/Mauche_AEAqr_WildStars2.pdf*
Mauche, C.W. (2009b), ApJ, 706, 130.
Mitschang, A.W. et al. (2010), ADASS XIX, arXiv:1001.0039
.

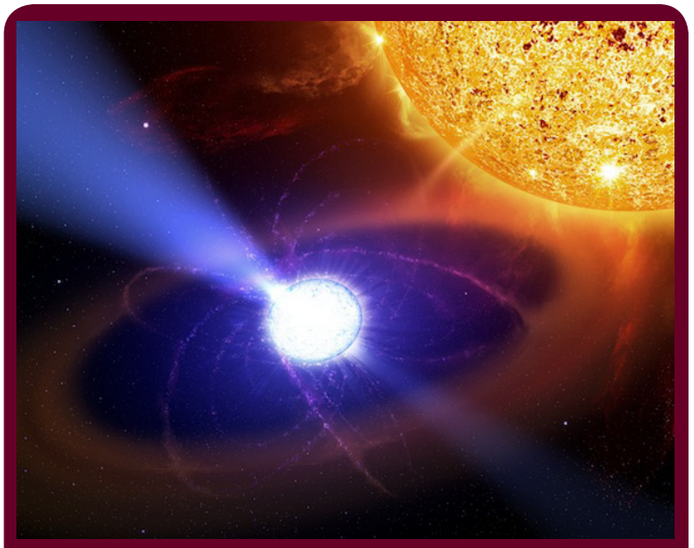

FIGURE 14: In the nova-like binary system, AE Aqarii, a magnetic white dwarf (WD) orbits its companionK star in a "year" taking only 9.88 hours while spinning with a 33.08 second "day".(Image credit: Casey Reed; NASA/GSFC)

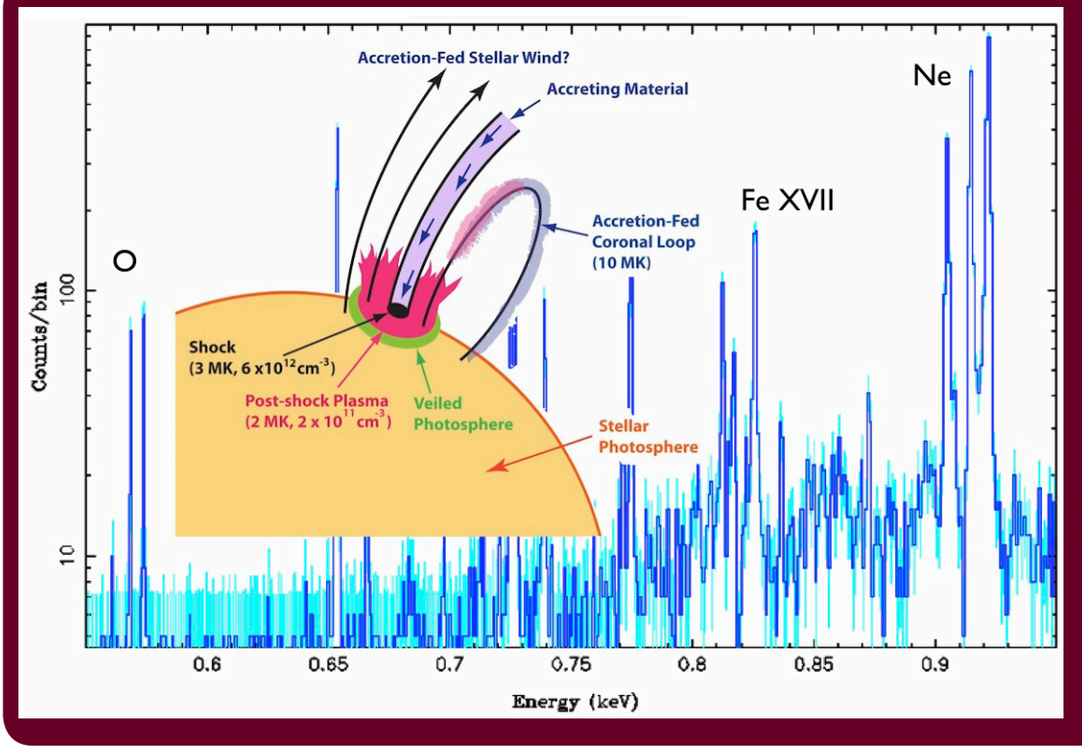

FIGURE 13: Another example of TGCat custom plot output. Here TGCat data from the accreting young star TW Hydrae are shown in the range from the oxygen to neon He-like triplets. For reference, a schematic of the proposed emission geometry is over-plotted (Figure 10 of Brickhouse et al. 2010).

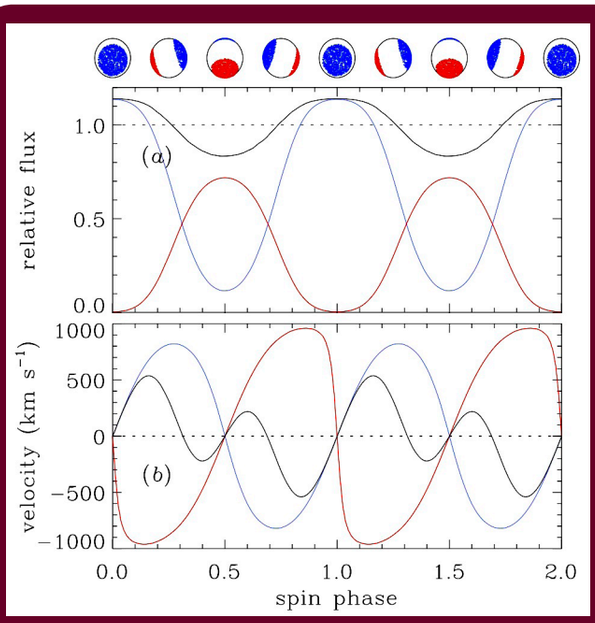

FIGURE 15: simple two-spot emission model can explain both the flux variations (a) and the period-doubled character of the Doppler velocities (b). (From Mauche (2009b) Figure 11.)

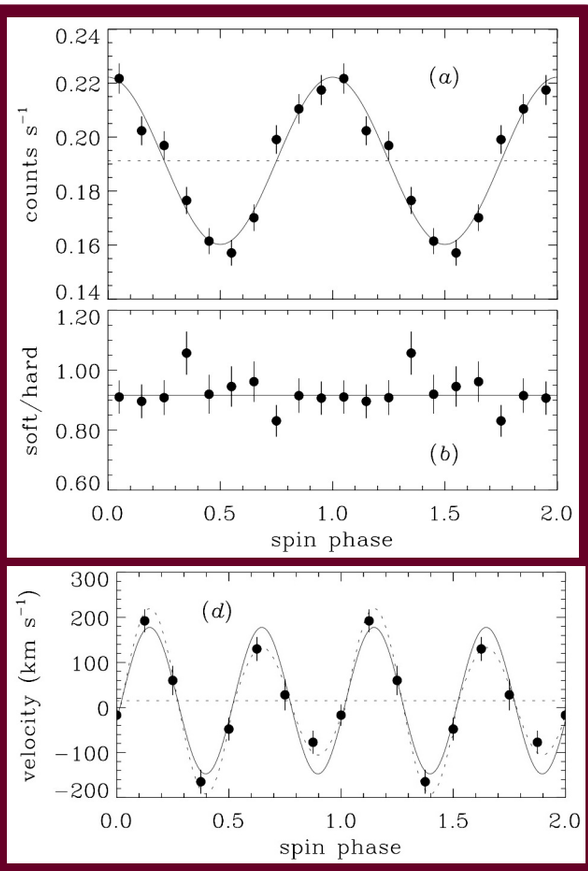

FIGURE 16: These panels show the variation of flux (top), softness ratio (middle), and the Doppler velocity line shifts (bottom) with the WD spin phase from the HETG observation. The frequency-doubled velocity curve is particularly intriguing; the observed velocities are a fraction of the WD's equatorial speed of 1330 km/s. (from Mauche (2009b) Figure 3 and Figure 10(d).)

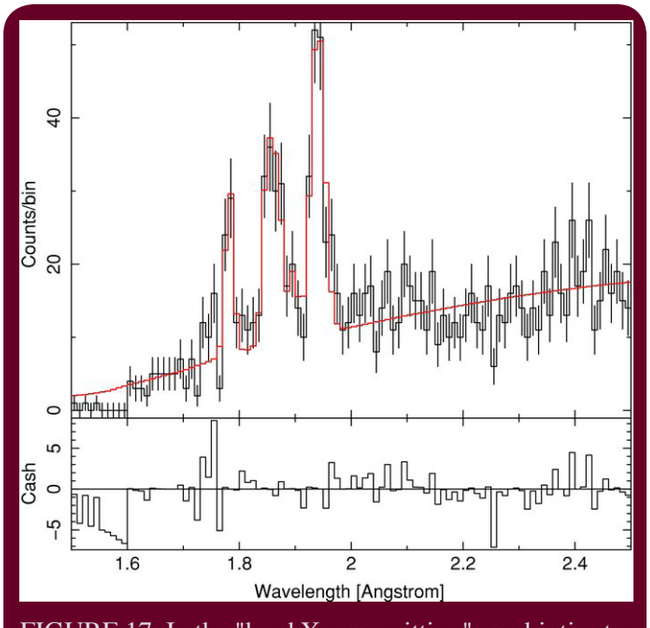

FIGURE 17: In the "hard X-ray emitting" symbiotic star SS73 17, a white dwarf accretes mass from a red giant companion. In this short-wavelength view, the HETG clearly separates the Fe XXVI H-like, the Fe XXV He-like, and the neutral Fe flourescent lines (l-to-r) modeled on top of a bremsstrahlung continuum. (From Eze (2010) Figure 1.)

Instruments: LETG

Jeremy Drake

LETGS: Out of Order

Obtaining new astronomical observations and making immediate scientific discoveries that smack you in the face as soon as you look at the image or spectrum doesn't happen to me very often. I do occasionally get smacked in the face for other reasons, but with astronomical discoveries it's usually more of a slow-motion, gradual process, involving tedious steps like "data analysis", and doing "model calculations" and other things that should by rights be completely unnecessary.

I do remember one though, while I was at the University of California in Berkeley working on the *Extreme Ultraviolet Explorer* program. Passing through the Control Room one day, one of the payload controllers handed me a plot of the registered counts from one of the survey detectors—the Al/Ti/C filter of Scanner A. There was a bright source there at a position that did not correspond to any known bright EUV object. Indeed, we had looked at that part of the sky before and seen only a very faint source that we could attribute to a very small UV leak from a B star, β Cen. With rare exceptions, B-stars do not generally exhibit flares and violent transient behaviour, and we were seeing a couple of orders of magnitude difference in count rate. Promising! A new pinhole in the detector filter could be ruled out because they gave rise to a characteristic halo and not a point source, and do not follow the spacecraft dither pattern.

At this point we started to get quite excited—it was in some ways what we had been waiting for since the start of a mission that was looking at the sky at wavelengths never explored in any detail before: new discoveries of astrophysical phenomena not conspicuous at other wavelengths. At least that is what it said in the brochure. A target of opportunity observation was rapidly approved to use the spectrometers and get an EUV spectrum of this new bright source. In less than a day, even before we could mobilize ground-based observational follow-up, we had the data! A few of us had gathered in the control room on Sunday to see what it looked like when it came in. And when it did there was ..... nothing. There was no sign of a source in the Lexan/B filter of the Deep Survey telescope that was co-aligned with the spectrometers. We had missed it! Since we had not caught the rise, the timescale for the transient was unknown, but perhaps it was just due to a giant flare on an unseen late-type companion to the B star.

On Monday, we returned to the observation we had interrupted, and tweaked the satellite roll angle to get β Cen back into the Scanner A field of view. On passing through the Control Room, once again one of the payload controllers handed me a plot of the registered counts on one of the survey detectors—the Al/Ti/C filter of Scanner A. Once again, here was a bright source there at a position that did not correspond to any known bright EUV object. It was at the position of a known B star, β Cen. So we had indeed discovered dramatic EUV transient behaviour after all!

At least that thought might have been entertained for a split second. Before cooler, more cynical reasoning kicked in, born of the bruises, scratches and scars of the usual scientific career that gives nothing back without the ritual amount of hard work.

Why are we seeing two transients now, when we had not seen any for the first couple of years of the mission?

John Vallerga worked out that the transmittance of the Al/Ti/C filter for UV/FUV light had increased in an approximately grey fashion by more than 3 orders of magnitude, with a slew of tiny pinholes perhaps caused by a space debris event being the favored explanation (i.e. we still have no clue what happened). Armed with this experience of having helped discover in-flight filter degradation through UV leaks I was not to be fooled ever again, oh no—there was an old saying at the Center for EUV Astrophysics, probably at the CXC too, that goes, erm, "fool me once, shame on you; fool, erm...you can't get fooled again."

Last Orders Please

B stars were also legitimate EUV sources, two of them at least. Adhara (ε CMa), a piece of the leg of Canis Majoris and a B2 II star, dominates the local stellar radiation field at wavelengths $\lambda > 450$ Å and is sited along a low-density "tunnel" in the local interstellar medium (Vallerga & Welsh 1995). *Chandra* observed Adhara as a GO target for 150 ks with the LETG+HRC-S to capture a high-resolution spectrum of its soft X-ray emission in 2006 July (P.I. D.J. Hiller). In 2008, David Huenemoerder of the HETG MIT team contacted me about a peculiarity of the observation: a splodgy extended halo to the 0th order. But I knew immediately what this was. Fool me once, shame..... fool again... This was a clear sign of a UV leak from what is a whoppingly bright UV source: *Chandra* is the best X-ray telescope ever made, but CXC mirror expert Diab Jerius once described it to me as "a lousy optical/UV telescope". The telescope optical PSF is broadened by diffraction effects of the mirror shells and support structures that become negligible for X-ray photons of 100-1000 times smaller wavelength.

But there was more. There were also some diffuse, splodgy signatures in the **dispersed** spectrum between 20—40Å or so (Figure 18). If the signal is dispersed out this far then it *has* to be X-rays. UV photons are dispersed at much larger angles corresponding to positions on the focal plane way past the end of the detector and are probably

blocked much earlier in the optical path. So it could not be UV. The relative intensities of the 0th order and first order splodges were also not too different from the expected ratio if they were X-ray signals: The checks were done and the signal was an X-ray one. The diffuse X-rays were not present in an XMM observation obtained 5 years earlier. Adhara appears to lie a bit blue-ward of the β Cephei instability strip and is not expected to vary significantly: obviously something exciting and unexpected was happening warranting further follow-up.

David Huenemoerder obtained a 10ks ACIS imaging observation of Adhara in 2008 November. It showed... nothing, no diffuse emission at all. Just a point source sitting there in a smattering of sparse background. *Chandra* had discovered variable diffuse X-ray...!

Fool me once, shame... complete and utter fool again...

There **was** actually one clue in the LETG+HRC-S data. The diffuse signal started at 20Å or so—close to the boundary of the additional 486Å of UV-blocking Al that covers the "imaging region" in the middle of the HRC-S central plate. But how do you disperse UV photons to typical first order X-ray positions on the detector? The main gold LETG grating bars are supported by two sets of thicker gold bars, referred to as "fine" and "coarse" support structures. The fine support bars run parallel to the dispersion axis and make the characteristic cross-dispersed "cat's whiskers" pattern seen in observations of bright targets, as illustrated by a recent ToO observation of the very bright nova KT Eri in Figure 19. The fine support structure cannot be to blame.

What about the coarse support structure? This is a triangular mesh easily visible to the human eye; a photograph of a grating facet flight spare—the LETG comprises about 180 of these arranged behind the HRMA in a hinged support assembly—is reproduced in Figure 20. It is this triangular mesh that gives rise to the pretty 0th order star pattern that is easily visible in the 0th order of KT Eri shown in Figure 19. The period is 2 mm—2000 times that of the main grating period of 0.9912 μm.

The UV sensitivity of the HRC-S is very small and not very accurately calibrated, but it drops off sharply toward longer wavelengths and is non-zero for $\lambda \leq 2500$Å (Zombeck et al. 2000). For a star like Adhara, any UV signal is likely to originate in the FUV, in the 1000–2000 Å range. The first order coarse support signal for these wavelengths should be dispersed to, say $1500 \times 0.9912\mu m/2mm$, or about the position of 1 Å X-rays. Hmm. But the coarse support diffraction efficiency as a function of spectral order is quite different to that of the main grating. This is dictated by the ratio of the bar width to spacing—a ratio of 68μm/2000μm for the coarse support, compared with 1 for the main grating: the coarse support diffraction efficiency decreases only very slowly as a function of spectral order, whereas the main grating is designed to have close to zero efficiency in every even spectral order. In fact, the extent of the 0th order star due to X-ray diffraction is only visible because it is seen in tens of orders that stretch further and further from the 0th order.

So, UV light will be diffracted in many overlapping spectral orders of the coarse support structure and can reach out to dispersion distances corresponding to tens of Å in first order main X-ray diffraction. For 1000–2000Å, the observed dispersed fuzzy signal corresponds to orders ~ 20–30 or so. It then only remains to be seen if the observed diffuse dispersed signal matches expectations. We can scale the expected **direct** UV leak (i.e. with no grating) based on *IUE* observations of different hot stars, passed through the HRC-S UV model response for that part of the detector—several counts/s for ε CMa based on Zombeck

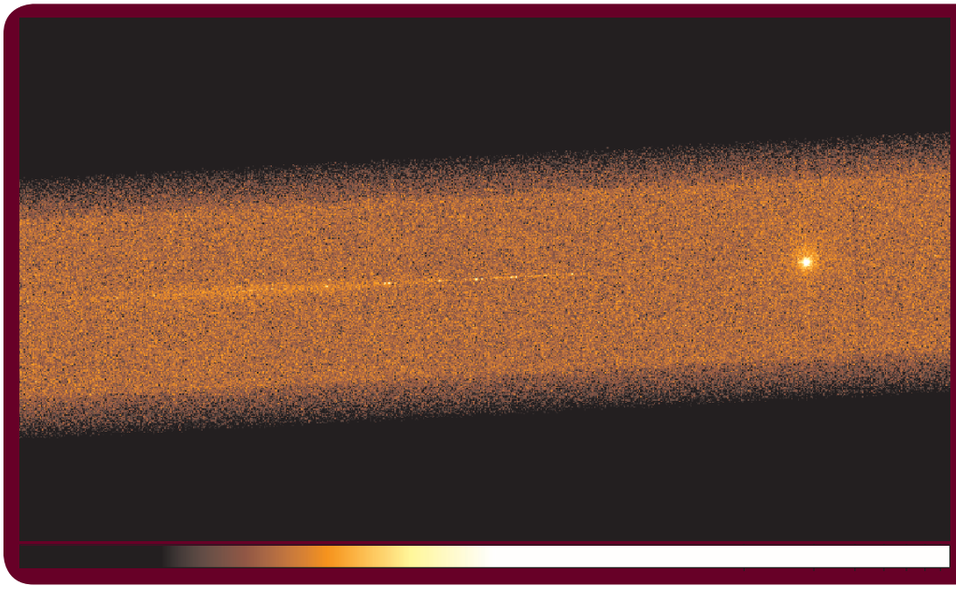

FIGURE 18: The HRC-S image of the LETG observation of ε CMa on one side of the central plate. The 0th order is shown to the right, together with one side of the dispersed spectrum. The keen observer will be able to discern the UV leak "halo"' around the 0th order, and the diffuse signal in the left half of the image extending vertically either side of the traditional narrow X-ray trace that could fool inexperienced LETG users into thinking it is an exciting transient diffuse X-ray signal. The diffuse signal runs from approximately 20-40Å.

& Wargelin (2002). Then we need to multiply this by the coarse support diffraction efficiency. The summed efficiency for orders 20–30 amounts to about 3×10^{-4}. Within a factor of ten or so this is the observed signal.

But the coarse support diffraction is star shaped—where is the rest of the star? The other arms are diffracted off the detector so we do not see the characteristic pattern that would have given it away immediately. What about the reasonably close match between the 0th order signal and the coarse support diffracted signal? The factor of a few 10^{-4} in coarse support diffraction efficiency is compensated reasonably closely by the difference in UV transmittance of the thick (0th order) and thin (20–40Å) parts of the HRC-S UVIS.

Not too long ago, David Huenemoerder was looking at the LETG+HRC-S observation of α Crux (B0.5 IV) obtained in 2008 August (P.I. L. Oskinova). He was responding to a Helpdesk query concerning a mysterious dispersed diffuse X-ray signal...

New Order

In 2004, Brad Wargelin completed a long and painstaking analysis of LETG+ACIS-S observations of continuum sources aimed at building a better understanding of the higher order LETG diffraction efficiencies. The energy resolution of ACIS allows the separation of the spectral orders that the HRC-S does not, and, at least in principle, provides a means to investigate their relative throughput. This work can be found just off the main LETG calibration web page (*http://cxc.harvard.edu/cal/letg/HO2004/*).

Prompted by a request of Marty Weisskopf to look into a possible discrepancy between the observed higher order signal seen in an LETG+HRC-S observation of the Crab pulsar and the observed first order signal folded through the higher order response, Brad has been re-investigating the efficiencies derived in his 2004 analysis. It turns out that a difference between the spatial extraction regions used in that analysis and in pipeline processing and CIAO gives rise to systematic differences of 2-10% in the effective higher order efficiencies for orders m = 2–7. An update is being made to the CALDB to bring the diffraction efficiencies into line with standard extracted spectra.

Order out of Chaos

In the last Newsletter, I described the beginning of a large project to revise the calibration of the LETG+HRC-S effective area using new multi-core Mac Pro systems. The project aimed to make use of the powerful 'Garage Band'

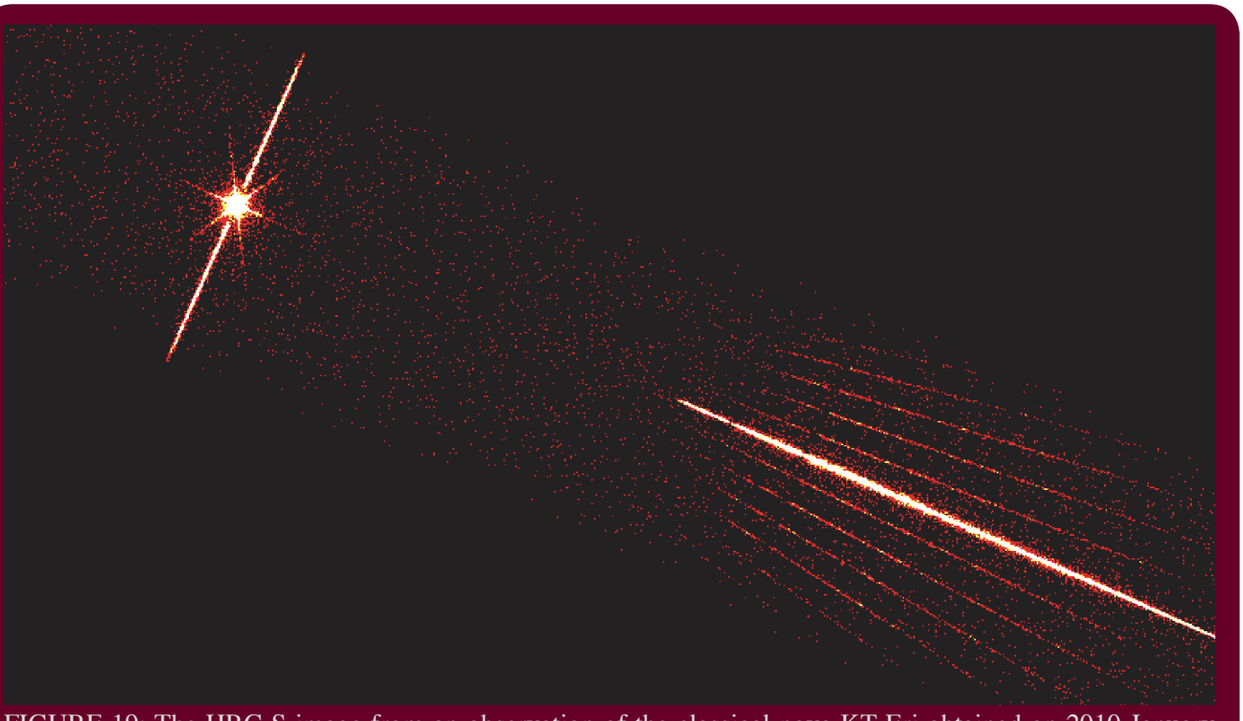

FIGURE 19: The HRC-S image from an observation of the classical nova KT Eri obtained on 2010 January 31. The 0th order is shown to the upper left, together with the coarse support structure 'star pattern'. The 'cat's whiskers' fine support structure cross-dispersion signal is also clearly visible. This observation had an elapsed time of only 5 ks. But the source was so bright—about 200/s in the *Swift* XRT at the time—that the LETGS count exceeded HRC-S telemetry limit of 180 count/s. As a result, the was close to 50%: *Chandra* obtained a quality resolution spectrum of KT Eri in a net exposure of only 2.7ks.

data analysis package. While I did not quite understand the inner workings of the code, and at some point during the work smoke was coming from my computer—from a board that someone told me was the "sound card" or something—we did manage to complete the first stage of the project: a revised effective area for energies above the carbon edge (0.28< E < 10 keV). This was released, together with a revised quantum efficiency uniformity map for the outer HRC-S plates, in CALDB 4.2. The new effective area is consistent with revisions to the HRMA effective area that were implemented in CALDB 4.2. ✯

Acknowledgments

JJD thanks John Vallerga for his reminiscences and detailed memo on The β Cen Incident that filled local bubble-sized gaps in my memory, and Dave Huenemoerder for his help in unravelling The ε CMa Incident.

References

Vallerga, J. V., & Welsh, B. Y. 1995, ApJ, 444, 702

Zombeck, M. V., Barbera, M., Butt, Y., Drake, J. J., Harnden, F. R., Jr., Murray, S. S., & Wargelin, B. 2000, X-Ray Astronomy 2000 (Cambridge: CfA), *http://hea-www.harvard.edu/HRC/calib/palermopaper.ps*

Zombeck, M. V., & Wargelin, B. 2002, *Chandra* Calibration Workshop, *http://cxc.harvard.edu/ccr/proceedings/02_proc/presentations/m_zombeck/index.html*

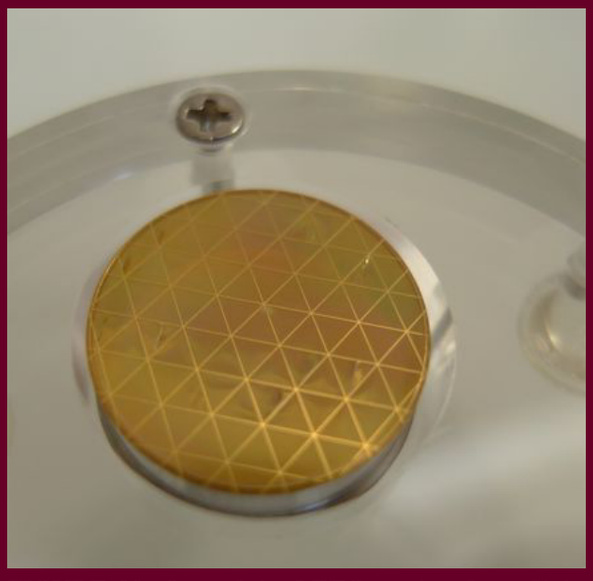

FIGURE 20: One of the LETG grating facet flight spares. The LETGS comprises 180 of these facets arranged in circular configurations behind the HRMA on a grating support structure than swings in and out of the optical path. The triangular coarse support structure is easily visible; the triangles are 2 mm high and the facet is the size of a US dime.

SDSS J1254+0846: A Quasar Pair Captured During Galaxy Collision

Paul Green

A joint *Chandra*/NOAO program to study a sample of rare binary quasars has led to the discovery of the first luminous, spatially resolved binary quasar that clearly inhabits an ongoing galaxy merger (Green et al. 2010, ApJ, 710, 1578).

The program (Paul Green, PI) imaged quasar pairs discovered from the SDSS by Adam Myers and collaborators, focusing on those with the smallest transverse and velocity separations. The number of close quasar pairs exceeds what we expect from larger-scale clustering measurements. This program investigates the properties of close quasar pairs to try to distinguish between two competing theories explaining the statistics of binary quasars: interaction-triggered quasar activity, versus close projections of overdense regions that normally spawn isolated quasars.

SDSS J1254+0846 are two luminous z=0.44 radio quiet quasars, separated on the sky by 3.6 arcsec (21 kpc). Followup imaging at NOAO's Mayall 4m telescope revealed faint tidal tails spanning some 75 kpc at the quasar redshift (A. Myers, W. Barkhouse observing). Spectroscopy at the Magellan telescope with IMACS (J. Mulchaey observing) revealed a radial velocity difference of just 215 km/sec.

Numerical modeling (T.J. Cox) suggests that the system consists of two massive disk galaxies prograde to their mutual orbit, caught during the first passage of an active merger. This demonstrates rapid black hole growth during the early stages of a merger between galaxies with pre-existing bulges. Neither of the two luminous nuclei show significant instrinsic absorption by gas or dust in our optical or X-ray observations, illustrating that not all merging quasars will be in an obscured, ultraluminous phase. Based on the optical spectra, the Eddington ratio for the fainter component B is normal, while for the brighter component it is quite high compared to quasars of similar luminosity and redshift, possible evidence for strong merger-triggered accretion. More such mergers should be identifiable at higher redshifts using binary quasars as tracers. ✯

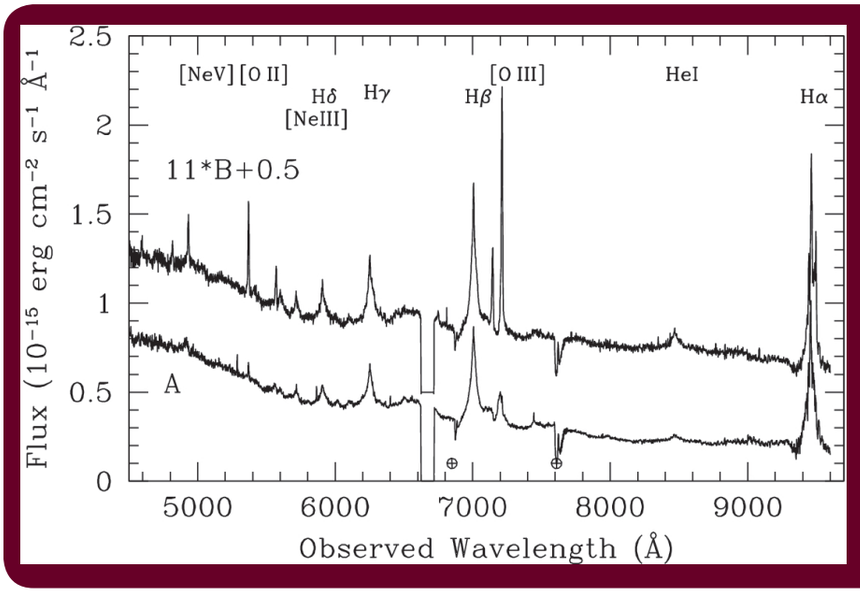

FIGURE 21: Simultaneous Magellan/ IMACS spectra of the two quasar components of SDSS\,J1254+0846, with the fainter 'B' component scaled up and shifted for clarity. Despite the factor of 11 difference in flux, the redshift, continuum and broad line shapes are all remarkably similar. Major emission line species are labeled along the top. The most striking difference is in the equivalent widths of the narrow emission lines; all the forbidden lines are relatively much stronger in B. Atmostpheric absorption bands (marked with circumscribed crosses) and CCD gaps are evident in both spectra. Excerpted from the ApJ article. Reprinted from ApJ.

FIGURE 22: This composite image shows the *Chandra* point sources shown in blue, overlaid on a Magellan r-band optical image shown in yellow (*http://www.chandra.harvard.edu/photo/2010/sdss/)*.

Important Dates for *Chandra*

Cycle 12 Proposals due: March 18, 2010

Users' Committee Meeting: April 27-28, 2010

Cycle 12 Peer Review: June 21-25, 2010

Workshop: July 13 - 15, 2010
Accretion Processes in X-rays: From White Dwarfs to Quasars

Cycle 12 Budgets Due: September 17 2010

Einstein Fellows Symposium: Fall 2010

Users' Committee Meeting: Fall, 2010

Cycle 12 Start: December, 2010

Cycle 13 Call for Proposals: December, 2010

The MUPS Anomaly

Tom Aldcroft, Belinda Wilkes, and Pat Slane

A scary story with a happy ending

The Scary Bit

On Sunday July 19 an e-mail announced a significant spacecraft anomaly that had occurred several hours earlier:

> On DOY 200 [July 19] during the 1950-2205 GMT pass, G_LIMMON reported the MUPS tank pressure at 233.2 psia, well below its yellow caution low of 250 psia. Upon further investigation, it was discovered that a few hours into the JUL2009A loads at 1750 GMT the tank pressure suddenly dropped ~21 psi over 45 minutes, from 255 psia to 234 psia. It stabilized until 2100 GMT and then began a slow drop to the last known value of 228.5 psia at 2205 GMT (end of track).
>
> There were no significant changes in rates, momentum, or propulsion system temperatures. As a precautionary measure, the crews closed the MUPS bank-A isovalve at the end of the track by executing script P_ISO3 with inputs of C for Close and F for Forward.

In simple terms, the problem was a sudden and unexpected drop in the pressure reading for the hydrazine tank within the Momentum Unloading Propulsion System (MUPS). This drop and two other significant events in the timeline are shown in the figure (Figure 23). At the time of this e-mail the Flight Operations Team (FOT) at the Operations Control Center (OCC) in Cambridge, MA had already completed the initial on-console anomaly response and determined that *Chandra* was in a stable state with all other systems operating nominally. But for many scientists and engineers supporting *Chandra* operations this was a scary first glimpse of a very serious situation. Even after discounting the momentary visions of Apollo 13 and a tumbling spacecraft, the possibility of a ruptured propellant line leaking kilograms of corrosive hydrazine fuel into the spacecraft represented the gravest threat that *Chandra* had faced in its first decade of operation.

MUPS overview

When *Chandra* maneuvers it does so by electrically changing the spin rates of six Reaction Wheel Assemblies and storing spacecraft angular momentum in the wheels. In addition to maneuvers, external torques such as gravity gradient forces can inject angular momentum to the spacecraft. The MUPS is used to remove momentum from the reaction wheels by despinning the wheels while applying countertorque with the gas thrusters. At the top level the MUPS consists of a tank of pressurized hydrazine propellant connected to redundant banks of four thrusters that catalyze the fuel and generate significant thrust.

While conceptually straightforward, the system contains over 30 meters of tubing, valves galore, and the spherical MUPS fuel tank with a membrane separating the fuel from the helium pressurant. The engineering drawings are a marvel to see. Unfortunately there is no redundant pressure transducer so when the reading dropped precipitously in the span of 45 minutes there was no immediate way to know if there was a real leak or if the sensor had malfunctioned. There were compelling arguments both for and against each possibility.

Anomaly response and investigation

The full team anomaly response began on Sunday July 19 with the discovery of the anomalous pressure reading. After determining the spacecraft was stable the immediate priority was a dedicated effort to maximize the communication time available for monitoring the spacecraft to watch for another sudden drop in pressure and allow for a realtime response. Declaring a spacecraft emergency would give access to unlimited Deep Space Network (DSN) communication time but requires imminent loss of spacecraft or a major subsystem. Because all indications apart from the pressure reading were nominal an emergency was not declared. Instead, the *Chandra* program owes a huge debt to JPL DSN and a number of other missions that accommodated the requests to allocate all spare or unneeded time to *Chandra*. To support this nearly continuous communication time the FOT operations crew expanded their daily 2-shift schedule from the normal 20 hours up to 24 hours of coverage.

Starting on Monday July 20 a daily anomaly status telecon began at the OCC with a regular agenda to review spacecraft status, vendor discussions, fault tree development and technical analyses. The anomaly investigation and continuing spacecraft monitoring became the primary focus for much of the FOT as well as a substantial support team including people from Northrup Grumman factory, the Science Operations Team (SOT) and Marshall Space Flight Center Project Science. Hundreds of pages of analysis and presentation charts were generated in under 6 weeks, spanning topics from the time-dependent thermal behavior of propulsion lines to the potential observability from the ground of vented hydrazine to using heater cycling data to infer the mass of remaining fuel. One especially memorable moment occurred when a propulsion expert patiently explained to the science team why there was no chance that the iridium-coated HRMA could explode should hydrazine find its way to the mirror surfaces, even though iridium is the very material used as the catalyst in the thrusters.

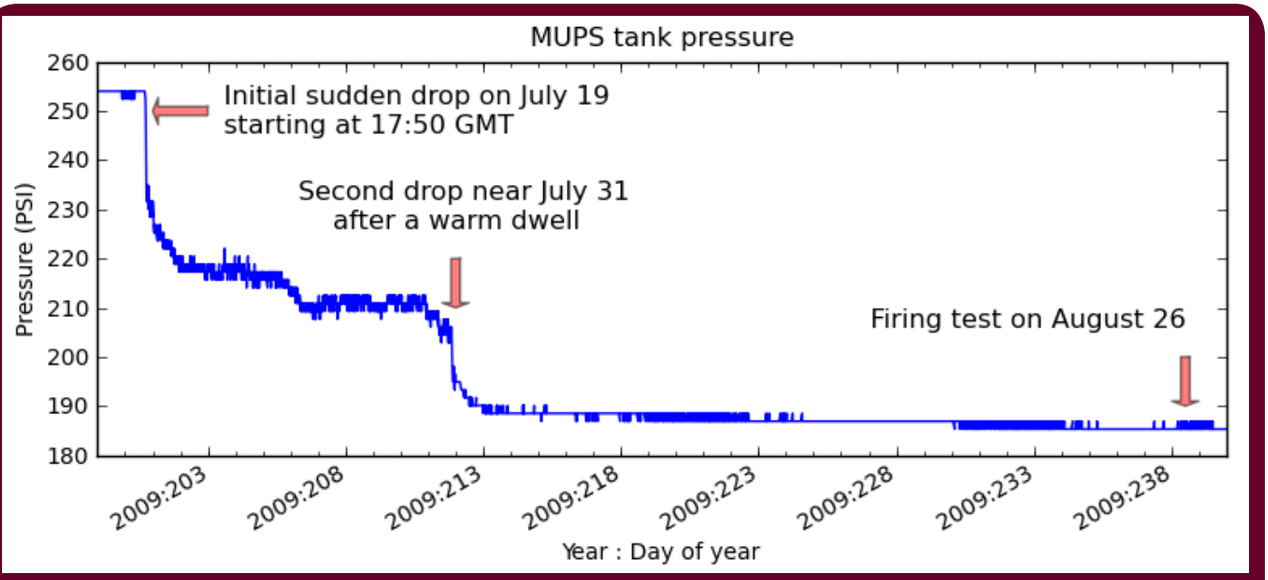

FIGURE 23: MUPS tank pressure

During the investigation the *Chandra* science mission continued and maintained a typical science observing efficiency. Behind this apparently normal situation was actually a storm of activity occurring across town from the OCC at the *Chandra X-ray Center* within the Center for Astrophysics. There the SOT mission planning team and *Chandra* Director's Office were struggling to assemble targets and contact observers in a radical replan of the science schedule that was driven first by the halting of momentum dumps and then by a pitch angle restriction imposed to keep the MUPS cool. The next article contains the details of this effort.

Another bump in the night

During the first two weeks after the initial drop there were no additional thermal or attitude restrictions on mission planning. This changed when another significant drop in the pressure reading was observed one evening following a long dwell at forward-sun pitch where the propulsion components heat up. The fear was that a "self-sealed" leak was somehow melting and allowing additional fuel to be leaked within the spacecraft. Shortly after this drop occurred a new mission planning guideline was put in place to restrict attitudes to sun pitch angles of greater than 130 degrees to keep the propulsion components cool. This resulted in over a month of "tail-sun" attitudes which the SOT mission planning team was able to accommodate by pulling certain observations forward from the long term schedule. This restriction was not without consequence however, as the constant illumination of the tail of the Science Instrument Module caused the ACIS CCD to occasionally operate up to few degrees warmer than the desired setpoint, impacting the gain stability for a number of calibration and some science observations.

The Mystery: leak or transducer failure?

At the end of a comprehensive fault tree analysis the investigation boiled down to one question: was there really a physical leak or was the drop due to a transducer malfunction? The profile of the initial sudden drop bore a striking resemblance to what could be expected for a self-sealing leak in which ice accumulates at the leak site and eventually stops or slows the flow. Such leaks had been seen in ground tests of similar propulsion system components. Adding to the case was the transducer vendor stating that the profile was unlike anything they had ever seen in ground or flight data. No credible mechanisms, either mechanical or electrical, for generating such a failure could be identified. This evidence implied it had to be a real leak.

But a real leak involving several kilograms of hydrazine would surely have produced a noticeable signature either as an angular impulse or a temperature drop. However the measured limits from *Chandra's* sensitive gyros were a factor of 100 to 1000 below what would be expected from the inferred leak rate if the material had a reasonable vent path to space. This would then require that the leak be almost fully contained, at which point one would expect significant ice and associated cooling near the leak point. No such cooling was seen anywhere. More evidence against a real leak came from a thermistor on a propulsion line very near the tank. During the 45 minute pressure drop it stayed at a cool temperature despite what would have been a substantial flow of warmer hydrazine past that point. Finally, after the pressure drop event the readout data from the transducer suddenly became noisier at a level which could not be due to physical pressure oscillations. So this other evidence implied it had to be a transducer failure!

A definitive test: fire the thrusters

Through the first half of August the analysis continued and while the strongest evidence implicated a transducer failure there was still no smoking gun. At the same time pressure of another kind was building. The 24/7 high-alert operational posture had now been been in place for several weeks and could not be sustained indefinitely with the existing staffing. Around this time the operations team began seriously discussing doing a MUPS thruster firing test. This had been recognized early as a definitive method to determine the actual tank pressure since the thrust is a simple function of tank pressure. There is obvious risk in activating a system with a known failure and possible leak, but at the same time there was an increasing risk in maintaining the status quo. After an exhaustive evaluation and risk assessment, a telecon was convened on August 24 and all parties agreed to go forward with a firing test. Two days later a later a 141 second momentum dump was commanded with all eyes watching.

A happy ending

The firing test was done under controlled conditions and with a stack of contingency procedures at the ready. Fortunately none of these were needed and within 20 minutes the answer came back: the momentum imparted by the thruster firing was exactly that expected for a MUPS tank pressure that agreed with pre-anomaly measurements, and wholly inconsistent with the pressure currently being read from the transducer. There was no leak; it was a faulty reading from the pressure sensor. Operations were returned to normal immediately and this was the time for popping the champagne.

Maintaining Observation Efficiency During the Anomaly

The timing of the anomaly was such that the Cycle 11 targets had been approved but they had not yet been ingested into the ObsCAT (the observation database) nor had they been reviewed by the CXC or the observation PIs in order to approve them for observation. This approval process has two stages: (1) a high-level check by PIs (Initial Proposal Parameters Signoff, IPPS) which is sufficient to allow the Mission Planning group (MP) to plan out the Long-Term Schedule (LTS) (2) a detailed check of all observation parameters, overseen by the User Interface group (USINT) and required before an observation can be included in a Short-term Schedule (STS)

In response to the anomaly, the initial restriction of no MUPS firing resulted in an increase in scheduling constraints to avoid the need for a momentum dump. MP needed to fully replan the upcoming weeks of the mission allowing for the new constraints. A larger than usual "pool" of unconstrained targets was needed from which to draw in order to find enough observable targets to maintain the observing efficiency. The approved Cycle 11 targets were ingested into the ObsCAT immediately and the IPPS emails were sent out to PIs on 24 July 2009. As targets were checked-off by the PIs and approved by CDO, they were immediately released for USINT review, a process which usually begins in September.

As well as moving up the observation parameter review process, the detailed technical feasibility review of approved targets, which is primarily concerned with highly constrained targets and Targets of Opportunity (TOOs), was placed on hold during the anomaly, freeing up the staff to work on the pool target check-off. This review was completed later, after normal operations resumed, with no affect on long-term planning.

With the subsequent pitch angle restriction of >130˚ to moderate the temperature, the available target pool became significantly smaller. In parallel to the target sign-off, MP selected Cycle 11 targets that would be observable in the next few weeks in the required pitch range. Working from this list of high priority targets, CDO and USINT contacted individual PIs directly to speed up their checks. As sign-offs were received, targets were released to MP for scheduling.

A notice was sent to the general *Chandra* mailing list on 5 August 2009 explaining that some Cycle 11 targets would be observed over the next few weeks and asking for prompt response to any CXC requests for confirmation of observing parameters. In addition PIs were notified that, in the case of a non-response, the CDO and USINT teams would carry out detailed checks, document any updates made and release the target for scheduling if this became necessary. No details of the MUPS anomaly itself were included at this time because the situation was very fluid and uncertain.

The accelerated process was sufficiently harried that the lack of observable targets at times threatened the observing schedule only 1 or 2 days ahead. Despite this, the observing efficiency was maintained at normal levels throughout the 5-week anomaly period. This was due to a great team effort, including that of many *Chandra* observers who responded very quickly to our requests and to whom we owe our thanks!

Once normal operations were resumed in late August the IPPS check-off resumed its usual process, which was completed in September. The USINT/PI review of observing parameters resumed its usual schedule, starting in September, ensuring that pool targets are approved early in the observing cycle and that constrained targets are approved prior to their inclusion in a STS. ✯

Chandra Calibration

Larry P. David

Chandra Calibration - Update to the ACIS Contamination Model

ACIS observations of astronomical sources as well as its own external calibration source (ECS) have shown that molecular contamination has been building up on the optical/UV blocking filters since launch. To prevent radiation damage, ACIS is stowed during each perigee pass, i.e., the HRC is at the focal point. When ACIS is stowed, it is illuminated by its ECS, which consists of a bare Fe55 source, an Al fluorescence source and a Ti fluorescence source. To monitor the build-up of contamination on the ACIS filters, data is collected from the ECS before and after each perigee pass. The ECS has a strong Mn-K line at 5.9 keV and Mn-L and F-K lines that comprise most of the line emission around 660 eV. Since the Mn-Kα line at 5.9 keV is not affected by absorption, the optical depth of the contaminant can be monitored by measuring the flux ratio between the blended lines at 660 eV and the Mn-Kα line. In addition to ECS data, LETG/ACIS-S observations of blazars have been extensively used to monitor the increasing optical depth of the ACIS contaminant at the C, O and F-K edges.

The previous version (N0004) of the ACIS contamination model was released to the public in CALDB 3.0 on Dec. 14, 2004 and provided a good fit to the ECS data up until about 2006 (see Figure 24). This figure shows that the optical depth of the contaminant predicted by version N0004 underestimates the optical depth derived from the ECS data after this time. This figure also shows that the time dependence of the contamination build-up changed around 2005. Figure 25 shows the discrepency between the measured optical depth at the C-K edge from LETG/ACIS-S observations of blazars and the predictions of version N0004.

An updated version (N0005) of the ACIS contamination model was released to the public in CALDB 4.2 on Dec. 15, 2009. A major change to the new contamination model is an adjustment in the time dependence to account for the accelerated build-up of contaminant relative to extrapolations from version N0004. Also, the improved gain corrections for the S1 and S3 chips (released in CALDB 3.4.3 on March 31, 2008) at a focal plane temperature of -110˚ (the ACIS operating temperature during the first 3 months after launch), permit a more accurate measurement of the contamination buildup early in the *Chandra* mission. A more in-depth discussion of the adjustments in the CALDB 4.2 version of the ACIS contamination model can be found on the CXC Calibration web page.

Comparison of Versions N0004 and N0005

The oxygen rich supernova remnant E0102-72 has been observed at least once per year since launch to monitor the low energy gain and QE of the ACIS CCDs. Figure 26 shows the 0.3-1.16 keV flux in these observations derived with version N0004 of the ACIS-S contamination model. The blue data points were obtained in full-frame mode and the red data points were done with a sub-array. The fluxes for the sub-array measurements are slightly higher due to pile-up. Notice that there is some time dependence to the derived fluxes, especially a 10% decrease over the past few years in the sub-array measurements. Figure 27 shows the same data with fluxes derived using version N0005 of the ACIS-S contamination model. Notice that the full-frame and sub-array fluxes are less time-dependent.

Figure 28 shows the ACIS-S spectrum from a 1999 observation of the Coma cluster. The solid curve is the best-fit absorbed single temperature model with the absorption fixed to the galactic value. Figure 29 shows the ACIS-S spectrum from a 2009 observation of the Coma cluster using the same extraction region as that used for the 1999 spectrum. The solid curve is the best-fit model to the 1999 spectrum using version N0004 of the ACIS-S contamination model. Notice the 10% deficit below 1 keV due to the underestimate in the depth of the absorption at recent times in the N0004 model. Fitting the 2009 spectrum using the N0004 model with N_H treated as a free parameter gives an excess absorption above the galactic value of ~2.0×10^{20} cm^{-2}. Figure 30 shows the same 2009 ACIS-S spectrum and model derived using the N0005 version of the ACIS contamination model. Notice the significant improvement in the fit below 1 keV.

Figure 31 shows the spectrum of an LETG/ACIS-S observation of Mkn 421 fitted to an absorbed power-law model using version N0004 of the ACIS contamination model. Figure 32 shows the same spectrum fitted to an absorbed power-law model using version N0005 of the ACIS contamination model. Notice the significant improvement across the C-K edge.

Caveats

Residuals near the C-K edge in LETG/ACIS-S spectra

The deep LETG/ACIS-S observation of Mkn 421 shows that there are residuals up to 0.5 optical depths in the 43.2-43.5Å (0.285-0.287 keV) band using version N0005 of the ACIS-S contamination model. This 0.3Å range samples the resolved C-K edge and the user is advised to filter out this array range with high S/N LETG/ACIS-S data.

(continued on page 32)


Chandra's First Decade of Discovery
The fifth in a series, this symposium highlighted key science results from the first ten years of operation of the Chandra X-ray Observatory.
It was held in Boston Sept. 21-25 2009


Chandra's First Decade of Discovery
Several of the talks will be featured in a special issue of the Publications of the National Academy of Science (PNAS). The abstracts, presentation slides, and videos can be accessed at:
http://cxc.harvard.edu/symposium_2009/proceedings

Low energy residuals in ACIS imaging data.

There can be scatter in the residuals in ACIS imaging data below 0.8 keV using version N0005 of the ACIS contamination model (see the plot of the 2009 Coma spectrum in Figure 30). ✯

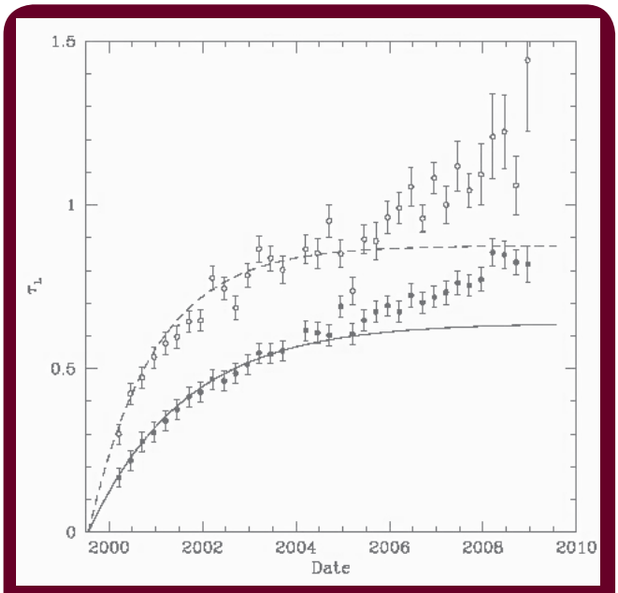

FIGURE 24: Optical depth at 660 eV on S3 as a function of time as measured by ECS data. The lower (solid) data points show the optical depth measured in the center of S3 and the upper (open) data points show the optical depth measured near the bottom of S3. The lines give the predictions from version N0004 of the ACIS contamination model.

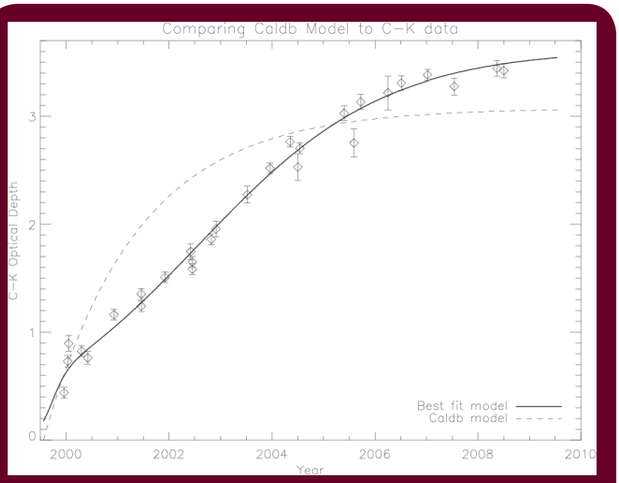

FIGURE 25: Measurements of the optical depth at the C-K edge from LETG/ACIS-S observations of blazars, compared to the predicted edge depth using CALDB version N0004 of the ACIS contamination model (dashed line). For a typical galactic N_H to one of these blazars, the optical depth at C-K would be about 0.10.

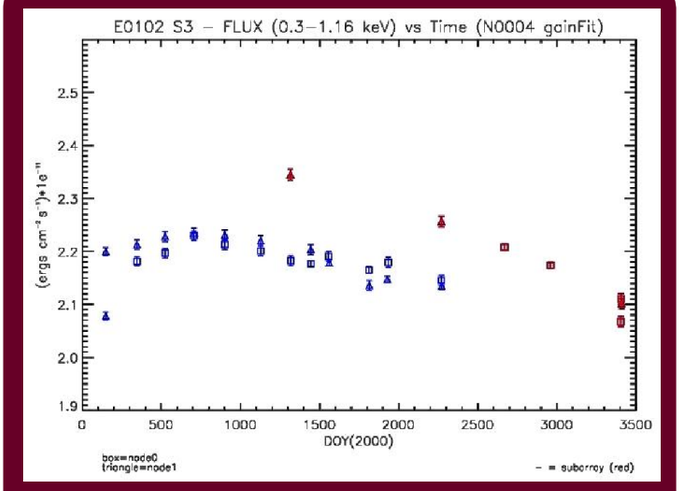

FIGURE 26: The 0.3-1.16 keV flux in E0102-72 observations derived using version N0004 of the ACIS-S contamination model. The blue data points were done in full-frame mode and the red data points were done with a sub-array. Due to pile-up, the fluxes derived from the sub-array data are slightly higher than those derived from the full-frame data. The square data points refer to observations done on Node 0 of ACIS-S3 and the triangular data points refer to observations done on Node 1 of ACIS-S3. The data point at the lower right was taken toward the read-out where the contamination is thicker.

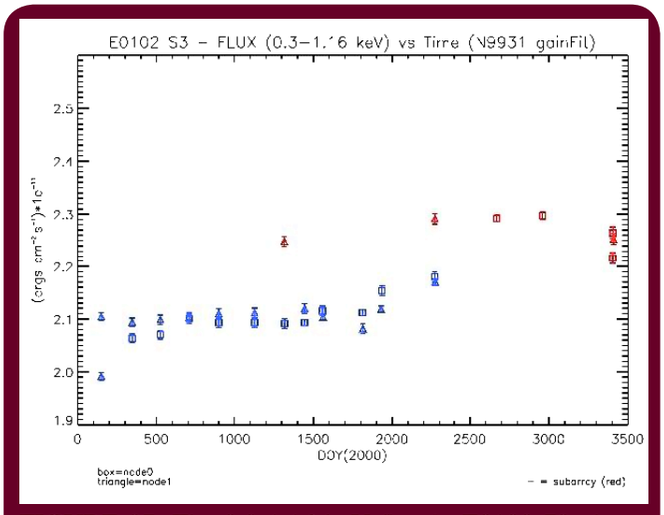

FIGURE 27: The 0.3-1.16 keV flux in E0102-72 observations derived using version N0005 of the ACIS-S contamination model. The symbols and colors used for the data points are described in the caption to Figure 26.

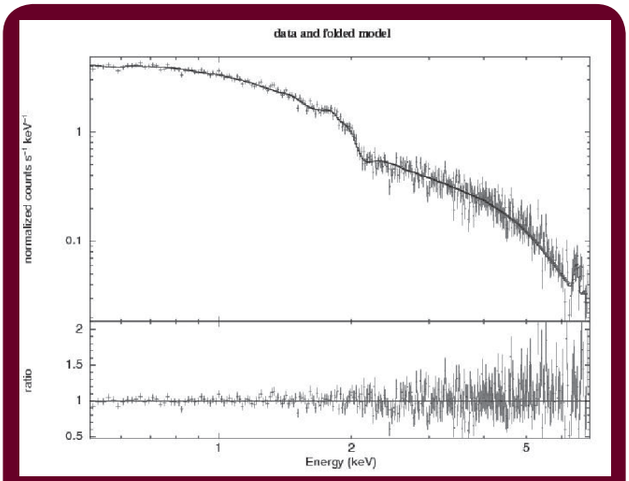

FIGURE 28: 1999 ACIS-S spectrum of the Coma cluster. The solid curve is the best fit absorbed single temperature model with the absorption fixed to the galactic value.

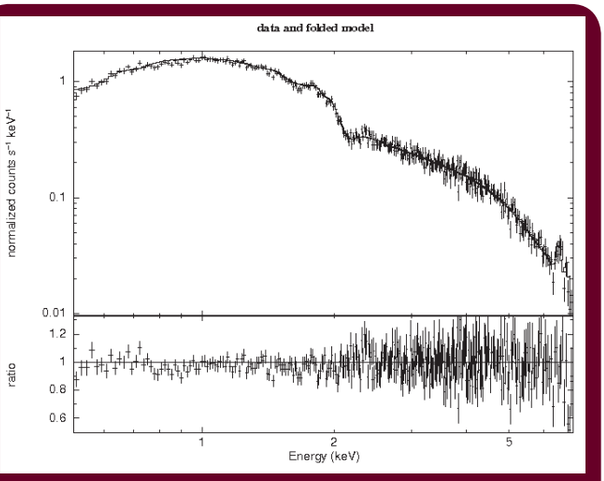

FIGURE 30: 2009 ACIS-S spectrum of the Coma cluster. The solid curve is the best fit model to the 1999 spectrum using version N0005 the ACIS-S contamination model.

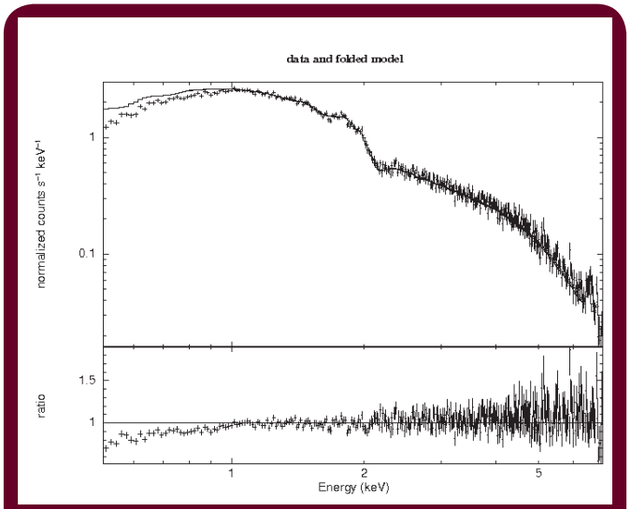

FIGURE 29: 2009 ACIS-S spectrum of the Coma cluster. The solid curve is the best fit model to the 1999 spectrum using version N0004 the ACIS-S contamination model.

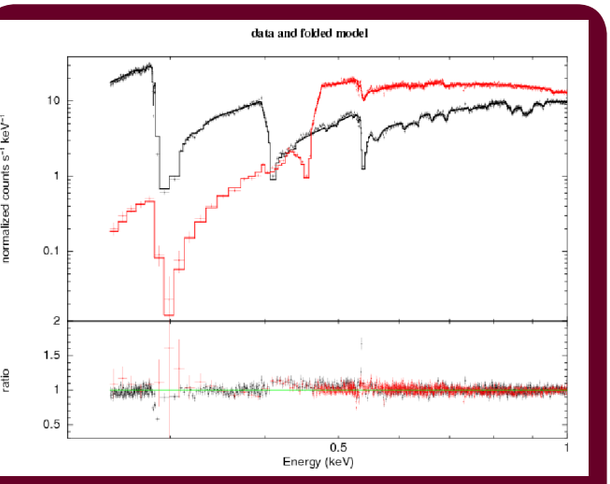

FIGURE 31: A LETG/ACIS-S spectrum of Mkn421 fitted to an absorbed power-law model using version N0004 of the ACIS contamination model. The plot shows the plus (red) and minus (black) first order spectra.

FIGURE 32: A LETG/ACIS-S spectrum of Mkn421 fitted to an absorbed power-law model using version N0005 of the ACIS contamination model. Colors are the same as the previous figure.

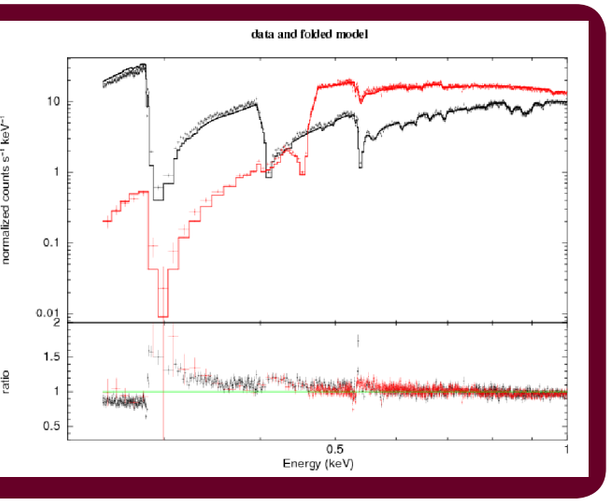

Chandra Calibration Review 2009

Vinay Kashyap and Jennifer Posson-Brown

As has become traditional, the Calibration team took the opportunity of the *Chandra*'s First Decade of Discovery Symposium to organize a Calibration Review (CCR). The CCR is a forum to disseminate detailed information about the workings of the *Chandra* instruments to the general community. It was held on Sep 21, 2009, the day before the Symposium began, at the same location as the Symposium. Approximately sixty people attended the CCR, which featured 15 talks and an additional 8 posters. All presenters were given the opportunity to present a poster on the same subject during the rest of the Symposium, and more than half did so.

The CCR was led off by a summary of the state of *Chandra* by CXC Director Harvey Tananbaum, who discussed the MUPS tank pressure anamoly, and pronounced that the state of the spacecraft is good, and barring unforeseen circumstances we should expect many more years of telescope operations. The Review started with a summary of HRC performance (PSF, spectral response, gain, degap, bad pixels, low-energy QE, etc.), and moved on to a summary of the optics, dealing with the revisions made to the HRMA effective area based on a reanalysis of *XRCF* data, and descriptions of the stability of the telescope pointing. The second session dealt predominantly with ACIS issues, such as CTI correction, CC mode calibration, and updates to the contamination model. Following a Poster Haiku session where short descriptions of parameterizing the PSF, dealing with calibration uncertainties, HRC background maps and gainmaps were presented, we ended the day with a session devoted to cross-calibration. All the presentations are now available online, at *http://cxc.harvard.edu/ccr/proceedings/2009/* and are also accessible via the Cal Presentations tag index at *http://cxc.harvard.edu/ccr/tags/*.

Useful Chandra Web Addresses

To Change Your Mailing Address:
http://cxc.harvard.edu/cdo/udb/userdat.html

CXC:
http://chandra.harvard.edu/

CXC Science Support:
http://cxc.harvard.edu/

CXC Education and Outreach:
http://chandra.harvard.edu/pub.html

ACIS: Penn State
http://www.astro.psu.edu/xray/axaf/

High Resolution Camera:
http://hea-www.harvard.edu/HRC/HomePage.html

HETG: MIT
http://space.mit.edu/HETG/

LETG: MPE
http://www.mpe.mpg.de/xray/wave/axaf/index.php

LETG: SRON
http://www.sron.nl/divisions/hea/Chandra/

CIAO:
http://cxc.harvard.edu/ciao/

Chandra Calibration:
http://cxc.harvard.edu/cal/

MARX simulator
http://space.mit.edu/ASC/MARX/

MSFC: Project Science:
http://wwwastro.msfc.nasa.gov/xray/axafps.html

Accretion Processes in X-Rays:
From White Dwarfs to Quasars

Current X-ray observatories have revolutionized the study of accretion in diverse astrophysical settings. *Chandra* and XMM-Newton gratings have enabled the detection of small velocity shifts and weak but vitally important lines, and the central engine in nearby accreting sources has been revealed in new detail. It is now possible to detect extremely faint sources, enhancing our understanding of accretion power throughout the universe and low-level accretion within the Milky Way. *Chandra* has also revealed unexpected parallels between accretion onto pre-main sequence stars, white dwarfs, neutron stars, stellar-mass and super-massive black holes.

The goals of this meeting are: (1) to bring together a broad scientific community interested in probing accretion physics from the X-ray perspective, (2) to leverage the rich accretion phenomenology and diverse theoretical approaches toward the understanding of accretion, and (3) to look ahead to the next ten years with *Chandra,* and future X-ray missions as well.

DEADLINES

WEDNESDAY, APRIL 28, 2010

Final deadline for contributed talk abstract submission

WEDNESDAY, MAY 26, 2010

Final deadline for general registration and poster abstract submission

Hosted by the
Chandra X-ray Center
July 13-15, 2010

at the
DoubleTree Guest Suites
Boston, MA

Scientific Organizing Committee

Meeting Chairs:
Aneta Siemiginowska (CXC)
John Raymond (SAO)

Monika Balucinska-Church (Birmingham)
Mitch Begelman (JILA)
Tomaso Belloni (INAF)
Omer Blaes (UCSB)
Joel Kastner (RIT)
Jon Miller (U. Mich)
Koji Mukai (GSFC)
Daniel Proga (UNLV)
Marina Romanova (Cornell)
Jeno Sokoloski (Columbia)

Local Organizing Committee

LOC Chair:
Paul Green

Ryan Foltz
Tara Gokas
Lisa Paton
Malgosia Sobolewska
Laura Brenneman

CXC 2009 Press Releases

Megan Watzke

Date	PI	Objects	Title
January 6	Dan Patnaude (SAO) Tracey Delaney (MIT)	Cas A	Cassiopeia A Comes Alive Across Time and Space
February 2	K. Kuntz (JHU)	M101	NASA's Great Observatories Celebrate the International Year of Astronomy
February 24	K. Arcand (SAO)	image exhibitions	'From Earth to the Universe' Project Launches Around Globe
February 25	N. Evans (SAO)	Einstein Fellows	NASA Announces 2009 Astronomy and Astrophysics Fellows
February 26	George Pavlov (Penn State)	PSR J0108-1431	Geriatric Pulsar Still Kicking
March 25	Joseph Neilsen (Harvard)	GRS 1915+105	Erratic Black Hole Regulates Itself
April 2	N/A	24-hr webcast for International Year of Astronomy	NASA Joins 'Around the World in 80 Telescopes'
May 28	Andy Fabian (IoA)	HDF 130	Ghost Remains After Black Hole Eruption
July 13	K. Arcand (SAO)	image exhibitions	The Universe Comes to the Nation's Capitol
August 12	Konstantin Getman (Penn State)	Cepheus B	Trigger-Happy Star Formation
October 22	Stefano Andreon (INAF)	JKCS041	Galaxy Cluster Smashes Distance Record
November 4	Craig Heinke	Cas A	Carbon Atmosphere Discovered on Neutron Star
November 10	Daniel Wang (UMass)	Galactic Center	NASA's Great Observatories Celebrate International Year of Astronomy
December 17	Laura Lopez (UC Santa Cruz)	various SNRs	Supernova Explosions Stay in Shape

CIAO 4.2: With the Power of Python!

Antonella Fruscione

Version 4.2 of the *Chandra* Interactive Analysis of Observation (CIAO) and CALDB 4.2.0, the newest versions of the CIAO software and the *Chandra* Calibration Database, were released in December 2009.

CIAO 4.2 includes a slew of enhancements and bug fixes with respect to previous CIAO versions and in particular:

- The Sherpa modeling and fitting package has a number of enhancements including a new algorithm for calculating confidence, simulations to probe model parameter space and calculate flux uncertainties, full support for wavelength analysis, and a "save_all" command to save the session in ASCII format. It also has capabilities to run parallel processing. Refer to the "Sherpa Latest Updates" page for more information.
- The ChIPS plotting application includes beta support for displaying images and colorbars, as well as the ability to create an editable ASCII save file.
- Two new tools - create_bkg_map and dmimgpm - enable users to create spatial background maps equivalent to those in the *Chandra* Source Catalog and useful for source detection and for detection sensitivity maps.
- acis_build_badpix allows users more control over customizing the bad pixel files.
- hrc_process_events, combined with files released in CALDB 4.2.0, applies time-variable gain calibrations. Using the gain-corrected PI values can reduce the background.
- tg_create_mask has improved the custom mask settings.

Of particular note is the inclusion in the CALDB 4.2.0 of the new ACIS QE Contamination Model which will primarily affect modeling of the low-energy absorption components between the C-K edge (0.283 keV) and 1.2 keV. We strongly suggest that CIAO users read the section of the Release Notes "How CIAO 4.2 and CALDB 4.2.0 Affect Your Analysis" at *http://cxc.harvard.edu/ciao/releasenotes/ciao_4.2_release.html#HowCIAO4.2andCALDB4.2.0AffectYourAnalysis*

The improvements and new features that CIAO 4.2 provides, allow new and powerful analysis capabilities. The following are some examples from Sherpa, ChIPS and DS9.

Sherpa 4.2 parallel processing capabilities have been used to model crucial temperature behaviors in *Chandra*. Figure 33 shows the predicted model temperature (blue) of the *Chandra* ACIS Power Supply and Motor Controller (PSMC) unit compared to the actual telemetered temperature). The PSMC has the potential to overheat in certain configurations, so a physically-motivated 13 parameter thermal model was developed to predict the unit temperature in advance of uplinking weekly command loads. This complex model was calibrated by making predictions for the last year of on-orbit data and using the Sherpa-Nelder-Mead fit method to optimize the 13 parameters. With just a little additional Python code the model evaluation was distributed across 30 CPUs, resulting in a dramatic improvement in fit speed (courtesy of Tom Aldcroft).

ChIPS, the CIAO plotting package, can now display images, color bars and overplot images and spectra. In figure 34 the "add_fov_region" command has been used to display the coverage of the *Chandra* observations of the COSMOS survey. The FOV files used come from the *Chandra* archive. In figure 35 a spectrum extacted from the TGCAT is plotted and overlayed onto a ground-based image (both figures courtesy of Douglas Burke).

Several CIAO tools can now be invoked directly from the DS9 CIAO "Analysis" Menu, which is automatically loaded in the version of DS9 distributed with CIAO (or can be set up in the DS9 Analysis Preferences). Figure 36 (courtesy of Kenny Glotfelty) shows an example of a light curve and a spectrum extracted directly from the source and background regions defined in the DS9 display window.

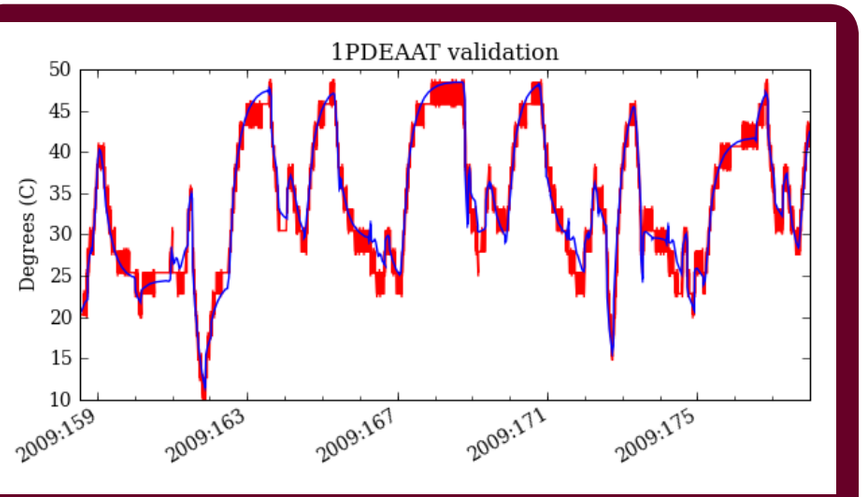

FIGURE 33: The predicted model temperature (blue) of the *Chandra* ACIS Power Supply and Motor Controller (PSMC) unit compared to the actual telemetered temperature (red).

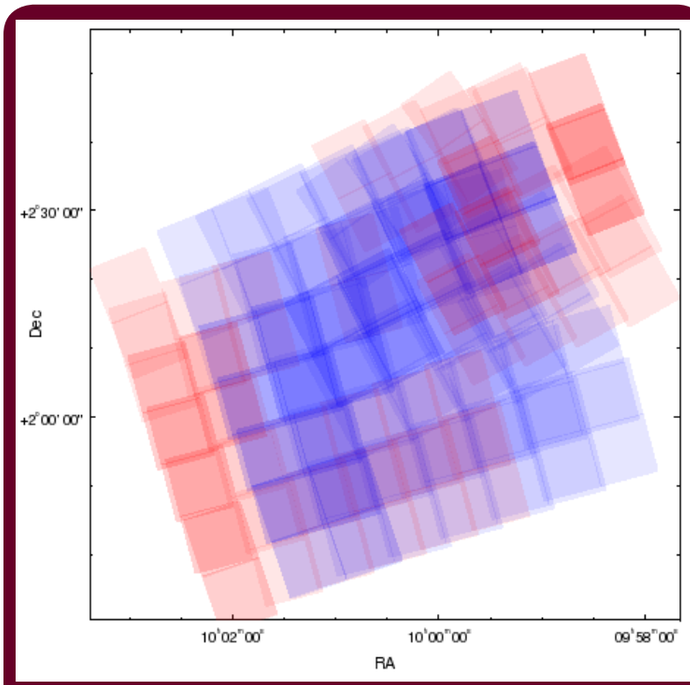

FIGURE 34: The *Chandra* COSMOS observations plotted with ChIPS.

More information on CIAO can be found at *http://cxc.harvard.edu/ciao/*

To keep up-to-date with CIAO news and developments subscribe to chandra-users@head.cfa.harvard.edu (send e-mail to 'majordomo@head.cfa.harvard.edu', and put 'subscribe chandra-users' (without quotation marks) in the body of the message).

Appendix A: A few important notes for CIAO users:

1. S-LANG

The CXC is phasing out support for the S-Lang interface in CIAO (including Sherpa and ChIPS). Only the Python interface will be supported after CIAO 4.2. This decision was made based on the results of the 2009 CIAO Software Survey and on input from the Users' Committee

We are currently planning to stop distributing the slsh application and the CIAO S-Lang modules as well. (slsh can be downloaded from *http://www.jedsoft.org/slang/slsh.html*). A variety of other CXC-developed and maintained S-Lang modules will still be suppored and can be obtained from *http://space.mit.edu/cxc/software/index.html*.

Please let us know via Helpdesk if this decision will badly affect your ability to conduct *Chandra* data analy-

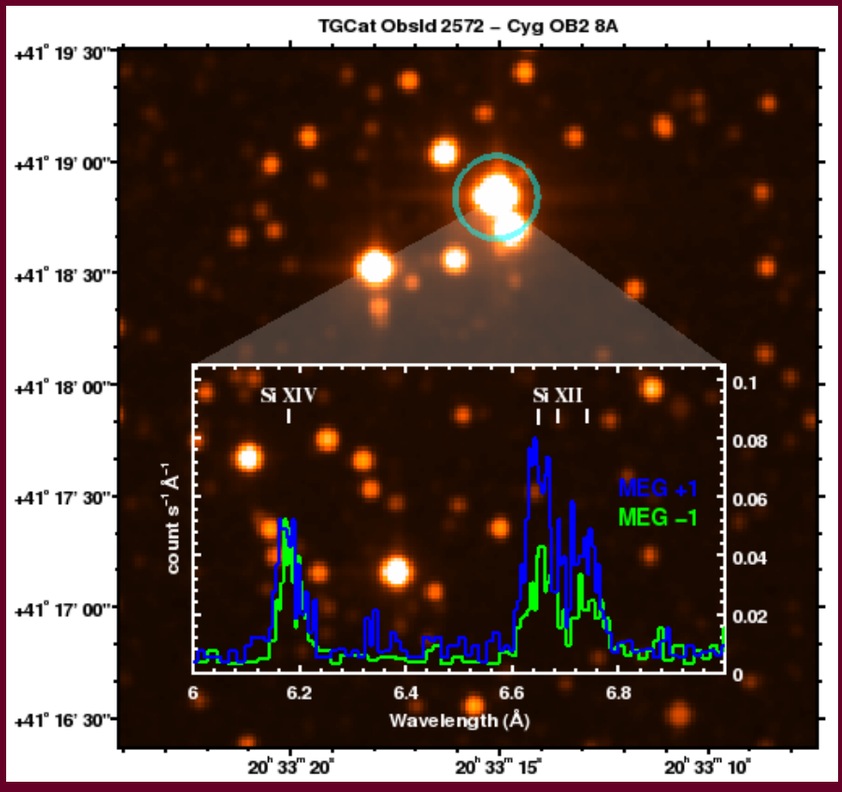

FIGURE 35: A spectrum from TGCAT overlaid on a ground-based image using ChIPS.

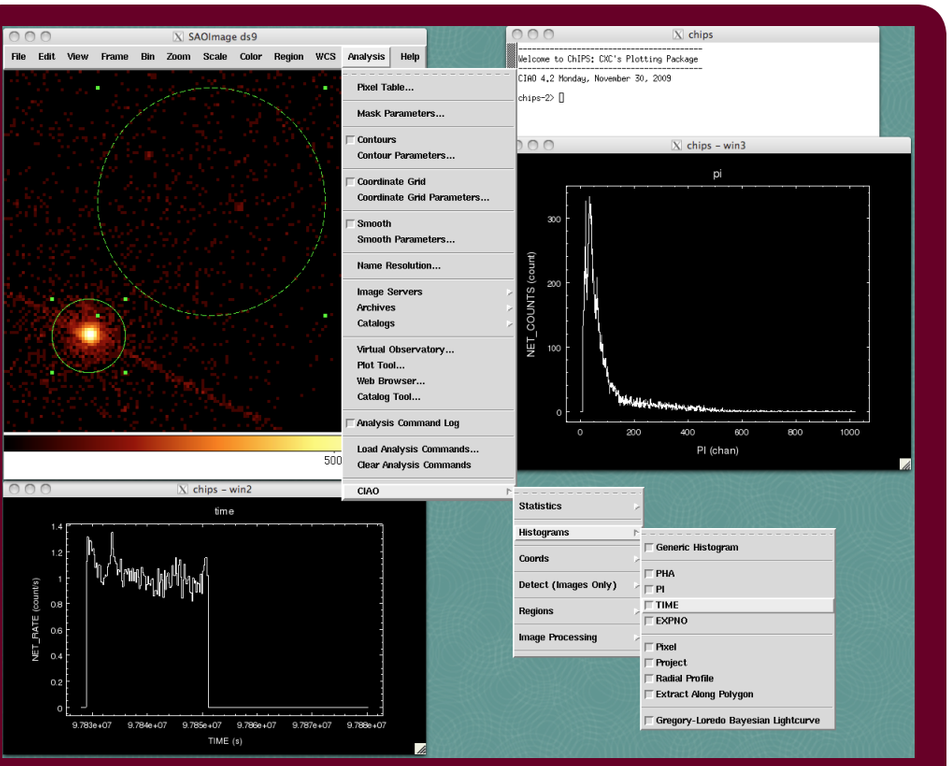

FIGURE 36: A light curve and a spectrum extracted directly from the source and background regions defined in the display window.

sis. New users of CIAO 4 should learn the Python syntax for ChIPS and Sherpa. The CXC is committed to helping existing S-Lang users transition to Python; contact Helpdesk if you need assistance.

2. SherpaCL

Version 0.23 of the experimental sherpacl application that allows users to use CIAO 3.4 syntax for Sherpa and ChIPS commands in CIAO 4 has been released. This version works with CIAO 4.2 (it will not work with earlier CIAO releases). Several additions and enhancements have been made. See 'AHELP CHANGES' from within SherpaCL for further details.

3. Mac OS X Power PC and Solaris Support

CIAO 4.2 will be the last CIAO release with support for the Mac OS X 10.4 PPC . We encourage users to acquire newer systems.

We are evaluating support for Solaris in future CIAO releases. Please let us know via Helpdesk if Solaris is still your only option for your CIAO data analysis.

4. CIAO 3.4 and CALDB3.x

The CXC no longer supports CIAO 3.4 however the CIAO3.4 webpages will stay on-line for the foreseeable future. Similarly there will be no more updates for version 3.x of the CALDB: CALDB3.5.5 is the last CALDB updated for CIAO3.4. For example the new ACIS QE Contamination Model vN0005 is not included in CALDB 3.x. We encourage users to migrate to CIAO 4.2 and CALDB 4.x. We also note that CALDB 4.x is not compatible with CIAO3.4. ✯

The 7th *Chandra*/CIAO Workshop

Antonella Fruscione

The first 3 days of February 2010 saw 19 participants descending into Cambridge, MA (or - in some cases - moving to the Phillips Auditorium from their offices!) for the 7th *Chandra*/CIAO workshop. The *Chandra*/CIAO workshops aim at helping users to work with the *Chandra* Interactive Analysis of Observations (CIAO) software.

The workshop included oral presentations by CXC "experts" and several hours of hands-on session where students could try to use CIAO "for real" with the constant support of CIAO team members. Every presentation for this - and all previous - workshop can be found at *http://*

cxc.harvard.edu/ciao/workshop/index.html. In many cases these presentations are a very good starting point for new and old *Chandra*/CIAO users looking for an introduction or a summary of a specific subject (e.g. Pileup Modeling, Scripting in CIAO etc.).

The students (from undergraduates to full professors!) who attended the talks and the hands-on session, arrived with a variety of background and expertise in X-ray data analysis and put the CIAO tools and documentation to a real test!

As in previous years, a "formal" feedback survey will be distributed very shortly, so we can learn what we did well and what we can improve. But in the meantime we are all very satisfied with the many positive comments we, and the CIAO software, received during the three days.

Thanks to all for coming and look out for the next announcement! ✯

FIGURE 40: Discussing pileup with the experts.

FIGURE 37: Participants hard at work under the vigilant eyes of the "experts"

FIGURE 39: Helpdesk experts Liz Galle and Nick Lee solving problems on-the-fly

FIGURE 38: Group photo on the last day.

"From Earth to the Universe" Wins Award

Congratulations to Kim Arcand and Megan Watzke of the *Chandra* EPO group who have won the IAU International Year of Astronomy 2009 (IYA2009) prize for Excellence in Astronomy Education and Public Outreach for the "From Earth to the Universe" (FETTU) exhibit project.

http://chandra.harvard.edu/press/10_releases/press_022610.html

http://www.fromearthtotheuniverse.org/event_photos.php

From Earth to the Universe in NYC, October 2009

Chandra Source Catalog

Ian Evans

It's hard to believe that a year has already passed since the first release of the *Chandra* Source Catalog (CSC) was made public. Much of the effort during this past year has concentrated on providing improved access to the catalog for users.

Release 1 of the CSC includes 94,676 sources, with fluxes that are at least 3 times greater than their estimated 1σ uncertainties, detected in ACIS imaging observations released publicly prior to the start of 2009. Release 1 includes point and compact sources with observed spatial extents < 30 arcsec, and in general, observations of fields containing highly extended sources are not included.

The CSC includes numerous raw measurements, as well as scientifically useful source properties (and associated errors) derived from each observation in which a source is detected. These properties include estimates of the source position, raw and deconvolved source extents, and aperture photometry fluxes in several energy bands. Cross-band spectral hardness ratios are reported for all detected sources, and absorbed power-law and black-body spectral fits are performed for sources with at least 150 net counts. Several source variability measures are included, both within a single observation of a source and between multiple observations that include the same source.

In addition to these tabulated properties, the CSC provides FITS (and in some cases, JPEG) format data products that include full field event lists, multi-band images, exposure maps, and limiting sensitivity maps, as well as per-source-region event lists, multi-band images, exposure maps, pulse-invariant spectra, spectral response matrices, and optimally binned light curves.

The CSC website (*http://cxc.cfa.harvard.edu/csc/*) provides access to the catalog, as well as a large bank of user documentation. The latter describes in detail the content and organization of the catalog, and lists important caveats and limitations that should be reviewed by prospective users. The various user interfaces are described, and there are several examples and user threads that demonstrate the use of these tools to access the catalog. The user documentation on the catalog website is continually improved as new features and capabilities are added.

Catalog Data Access

There are several ways in which users can interact with the catalog.

CSCview (Figure 41) is a powerful, web-based interface that allows the user to query tabulated catalog properties to identify sources that satisfy a set of user-supplied constraints. Selected properties for matching sources can then be either displayed on the screen or saved to a data file, and any of the file-based data products that are associated with the matching sources can be downloaded. Although *CSCview* has a highly flexible query interface that is well-suited for data-mining, this flexibility brings some degree of complexity. To simplify *CSCview* usage for new or infrequent users, we now provide a set of pre-defined "Standard Queries" designed to address the most common user requests. The set of standard queries will continue to be augmented as usage patterns emerge. A new pop-up "Getting Started" help window leads novice *CSCview* users through the steps necessary to perform both standard and custom queries, and retrieve data products. Although *CSCview* is primarily a forms-based interface, under the hood the queries are constructed using the Astronomical Data Query Language (ADQL), which is an International Virtual Observatory Alliance (IVOA) standard. Advanced users can bypass the forms and enter their query directly in ADQL if desired. The ADQL language interface is also accessible directly via a URL, so that users can query the catalog directly from the UNIX command line using cURL or wget.

Users who prefer a visual interface may choose to use *CSC Sky* in Google Earth (Figure 42). Using Google Earth (in "Sky" mode) installed on your personal workstation, three-color full-field images and field-of-view outlines can be displayed for all observations included in the CSC. A simple file download from the catalog website is all that is required. *CSC Sky* provides a quick and simple way to visualize the coverage of the catalog on the sky. In addition to images and fields-of-view, markers that identify the locations of catalog sources can optionally be displayed. Clicking on a marker pops-up a balloon that contains basic summary properties for the source. In the future, we expect to be able to provide pop-up graphics such a spectral plots and light curves for sources, as well as direct access to file-based data products. *CSC Sky* can also optionally display color-coded field-of-view outlines (but not images) for *all* completed *Chandra* observations, allowing the user to visualize easily which regions of the sky have been observed throughout the mission. The *CSC Sky* interface has proven to be enormously popular with both professionals and amateurs alike, and typically receives several thousand hits per day.

Instead of using *CSC Sky* to visualize catalog coverage, a user can instead choose to query the prototype *CSC Sensitivity Map Service* to determine whether one or more user-specified celestial locations are included in the fields-of-view of any of the observations that comprise the catalog. If so, the approximate limiting sensitivity of the CSC (photons cm^{-2} s^{-1} in the ACIS broad energy band needed for a point source to be included in the catalog) is returned for each specified location. Since this service is a proto-

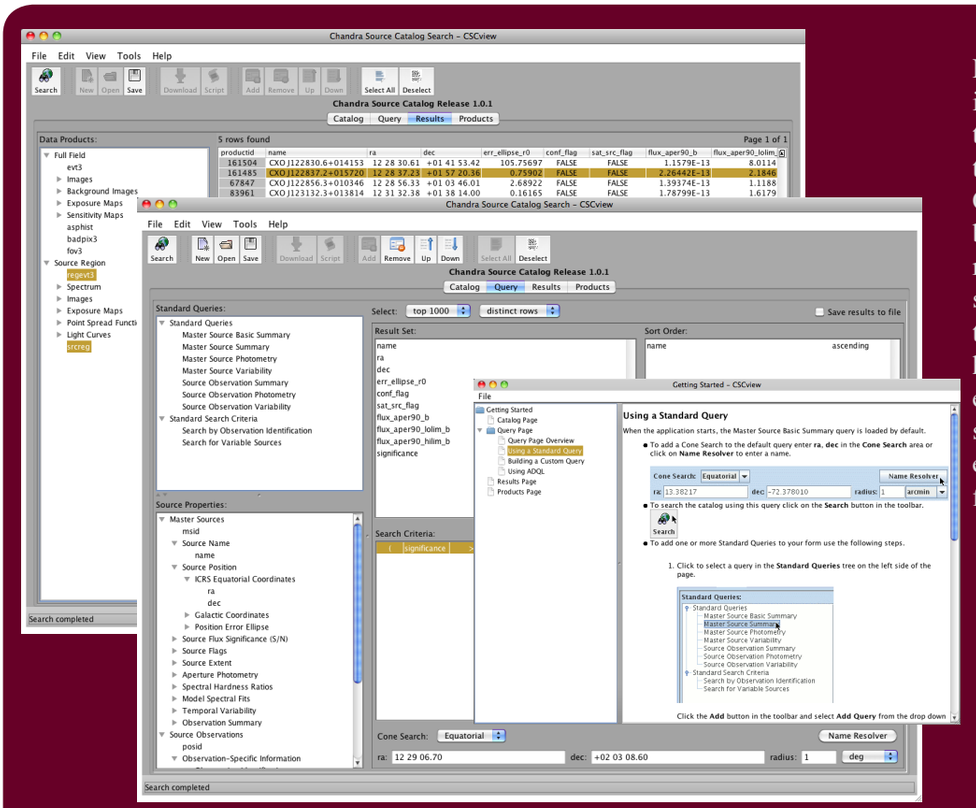

FIGURE 41: The CSCview query interface to the CSC allows users to search the catalog for sources that match their search criteria. Common searches are addressed by pre-defined "Standard Queries" or users can perform custom searches of the source properties. A pop-up "Getting Started" help window leads first-time users through the steps required to search the catalog, return tabulated source properties, and retrieve file-based data products.

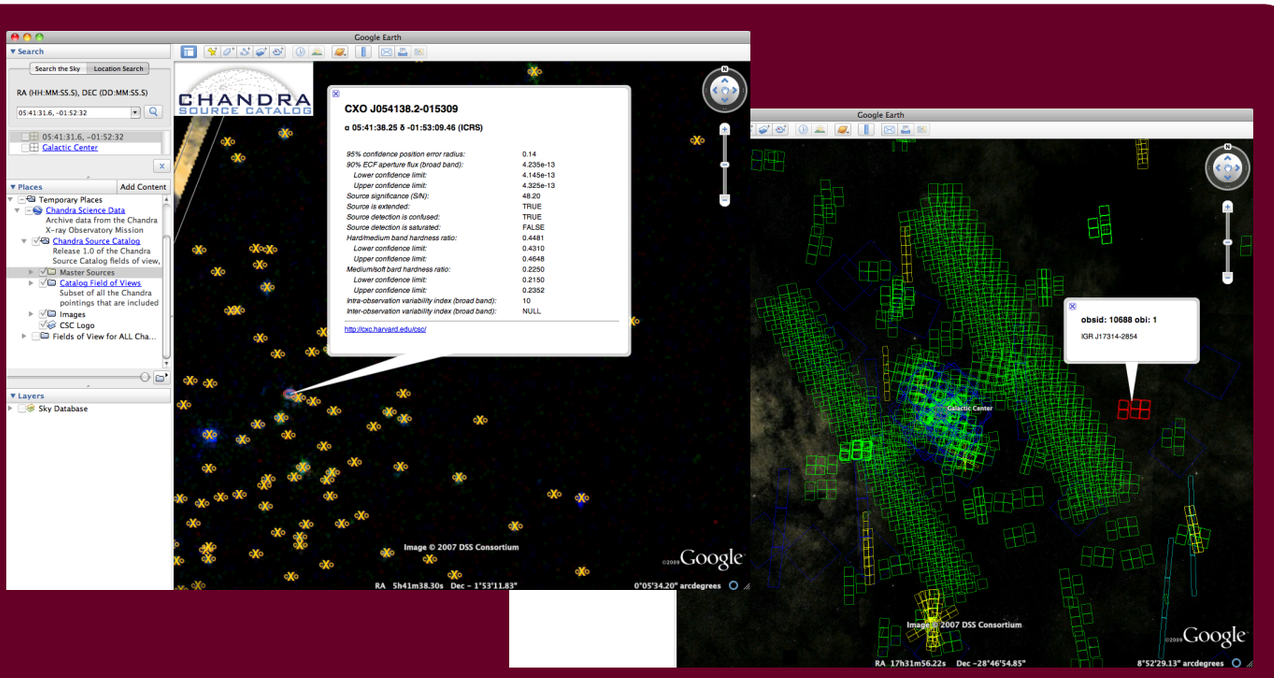

FIGURE 42: CSC Sky in Google Earth can be used to view 3-color images of the observations included in the CSC (left). Markers identify catalog sources, and clicking on a marker opens a balloon that summarizes key source properties. Field-of-view boundaries for observations included in the CSC can be displayed so that the user can readily visualize the region of the sky included in the catalog. A recent update to CSC Sky allows display of all *Chandra* observations (right), color-coded by instrument.

type, the user is advised to review the associated caveats described on the *CSC Sensitivity Map Service* web page.

An IVOA standard *Simple Cone Search* interface allows users of Virtual Observatory (VO) portals such as DataScope (*http://heasarc.gsfc.nasa.gov/vo/*), or VO-aware applications such as TOPCAT (*http://www.star.bris.ac.uk/~mbt/topcat/*), to directly search for catalog sources near a user-specified position.

Finally, as a convenience to our users, and in collaboration with the Sloan Digital Sky Survey, we provide a *CSC-SDSS Cross-match Catalog* that tabulates the list of sources common to both Release 1 of the CSC and Data Release 7 of the SDSS. This catalog was compiled by applying a Bayesian cross-match algorithm (developed at JHU by Tamas Budavari and Alex Szalay) that considers catalog positions and position errors, and the coverage areas of the CSC and SDSS, and contains about 17,000 CSC-SDSS source pairs, about 8,000 of which are classified by SDSS as stars, and ~9,000 as galaxies. The *Cross-match Catalog* service can return either all matching sources, or the subset of sources that satisfy optional user-specified search criteria. ✯

Mining the *Chandra* Data Archive and the Literature

Sherry Winkelman and Arnold Rots, for the Archive Operations Team

Linking the *Chandra* Data Archive and the astronomical literature (through the ADS) together provides a powerful data mining tool. Right now, one can link from a paper at the ADS to the data sets in the CDA that were used for the publication, and from an observation in the CDA to the papers published on that observation. But it is also possible to browse both simultaneously though the CDA's bibliography interface: *http://cxc.harvard.edu/cgi-gen/cda/bibliography*.

This interface also provides access to papers that are relevant to *Chandra* but do not present any specific observations, such as articles on software, operations, and instruments; and it allows searching on keywords. The CDA and the ADS have plans to expand the mining capabilities through much more extensive semantic linking, but the current tool is already quite powerful and a great research aid.

There are two ways in which you, our users, can help us in the expansion:

- We will be happy to host any significant custom data products that you may have generated for a paper, such as highly processed images, spectra, light curves, and tables. We will link them to the paper, and make them available to the community. For instance, highly processed images, spectra, light curves, tables. Drop an email to arcops@head.cfa.harvard.edu. Your colleagues will be grateful.
- Instead of arcops guessing which ObsIds you used for a particular paper (or our bugging you about it), you can include that information in your manuscript in a very easy and painless manner, at least for AAS journals. It takes the guesswork out of the linkings, it is more accurate, and it will give you a warm feeling that you have done something nice for the community.

See:

http://cxc.harvard.edu/cda/datasetid.html
http://dopey.mcmaster.ca/AASTeX/
http://dopey.mcmaster.ca/datasets/datasetlinking.html

Thank you for adding to the data mining capabilities! ✯

CXC Contact Personnel

Director:	Harvey Tananbaum	Calibration:	Christine Jones
Associate Director:	Claude Canizares	Development and Operations:	Dan Schwartz
Manager:	Roger Brissenden	Mission Planning:	Pat Slane
Systems Engineering:	Jeff Holmes	Science Data Systems: Deputy:	Jonathan McDowell Mike Nowak
Data Systems:	Pepi Fabbiano	Director's Office:	Belinda Wilkes
Education & Outreach:	Kathy Lestition	Media Relations:	Megan Watzke

Note: E-mail address is usually of the form: <first-initial-lastname>@cfa.harvard.edu
(addresses you may already know for nodes head.cfa.harvard.edu or cfa.harvard.edu should work also)

Einstein Postdoctoral Fellowship Program

Nancy R. Evans

FIGURE 43: Fellows at the 2009 Symposium; from left to right (including former *Chandra* and *Fermi* Fellows): Bence Kocsis, Norbert Werner, Uri Keshet, John Fregeau, Prateek Sharma, Ian Parrish, Jeremy Schnittman, Bret Lehmer, Brian Metzger, Eduardo Rozo, Ezequiel Treister, Kevin Schawinski, Jesper Rasmussen, Aurora Simionescu, Vasiliki Pavlidou, Eran Ofek, Orly Gnat, Rodrigo Fernandez, Ed Cackett, Matt McQuinn, Nat Butler

The Chandra Postdoctoral Fellowship program has now had 13 groups of Fellows, including the new 2010 Einstein Fellows: *http://cxc.harvard.edu/fellows/fellowslist.html*. As always, you are invited to enjoy the exciting projects they are involved in at the fall Einstein Fellows Symposium. The Symposium last year was particularly interesting because of the addition of *Fermi* Fellows, as well as the new group of Einstein Fellows.

The Call for Proposals for Fellowship applications will be posted on the web in the summer. ✯

Einstein Fellows 2010

	PhD Institution	Host Institution
Giacintucci, Simona	Bologna University	Smithsonian Astrophysical Observatory
Katz, Boaz	Weizmann Institute	Institute for Advanced Studies
Kerr, Matthew	University of Washington	Stanford University
Kistler, Matthew	Ohio State University	California Institute of Technology
Levesque, Emily	University of Hawaii	University of Colorado
Liu, Xin	Princeton	Harvard
Mroczkowski, Tony	Columbia	University of Pennsylvania
O'Leary, Ryan	Harvard	University of California at Berkeley
Poznanski, Dov	Tel Aviv University	Lawrence Berkeley National Laboratory
Yunes, Nicolas	Pennsylvania State University	Massachusetts Institute of Technology

The Results of the Cycle 11 Peer Review

Belinda Wilkes

The observations approved for *Chandra*'s 11th observing cycle are now in full swing and the Cycle 12 Call for Proposals was released on 15 December 2009. Cycle 10 observations are close to completion.

Cycle 11 observations began unusually early this year, in July/August, due to a spacecraft anomaly (the "MUPS anomaly") which is described in a separate article in this Newsletter. During a 5-week period of highly constrained observational parameters, observable targets were selected from a pool of unconstrained targets from both Cycle 10 and Cycle 11 in order to efficiently fill the observing schedule.

The Cycle 11 observing and research program was selected as usual, following the recommendations of the peer review panels. The peer review was held 23-26 June 2009 at the Hilton Boston Logan Airport. More than 100 reviewers from all over the world attended the review, sitting on 14 panels to discuss 668 submitted proposals (Figure 44). The Target Lists and Schedules area of our website provides lists of the various types of approved programs, including abstracts. The peer review panel organization is shown in Table 1.

Table 1: Panel Organization

Topical Panels	
Galactic	
Panels 1, 2	Normal Stars, WD, Planetary Systems and Misc
Panels 3, 4	SN, SNR + Isolated NS
Panels 5,6,7	WD Binaries + CVs, BH and NS Binaries, Galaxies: Populations
Extragalactic	
Panels 8,9,10	Galaxies: Diffuse Emission, Clusters of Galaxies
Panels 11,12,13	AGN, Extragalactic Surveys
Big Project Panel	LP and VLP Proposals

The over-subscription rate in terms of observing time for Cycle 11 was 5.3, similar to that in previous cycles (Figure 46), with the total time request being ~ 90 Msecs, again similar to past cycles (Figure 45). All proposals were reviewed and graded by the topical panels, based primarily upon their scientific merit, across all proposal types. The topical panels produced a rank-ordered list along with detailed recommendations for individual proposals where relevant. A report was drafted for each proposal by one/two members of a panel and reviewed by the Deputy panel chair before being delivered to the CXC. The topical panels were allotted *Chandra* time to cover the allocation of time for GO observing proposals based upon the demand for time in that panel. Other allocations made to each panel were: joint time, Fast and Very Fast TOOs, time constrained observations in each of 3 classes and money to fund archive and theory proposals. Many of these allocations are affected by small number statistics in individual panels so allocations were based on the full peer review over-subscription ratio. Panel allocations were modified, either in real time during the review or after its completion, transferring unused allocations from one panel to other panels which requested more.

Large (LP) and Very Large Projects (VLP) were discussed by the topical panels and ranked along with the other proposals. The topical panels' recommendations were recorded and passed to the Big Project Panel (BPP). The BPP discussed the LPs and VLPs and generated a rank-ordered list. BPP panelists updated review reports, as needed, both at the review and remotely over the following 2 weeks. The schedule for the BPP included time for reading and for meeting with appropriate panel members to allow coordination for each subject area. The BPP meeting extended into Friday morning to allow for additional discussion and a consensus on the final rank-ordered list to be reached.

The resulting observing and research program for Cycle 11 was posted on the CXC website three weeks later, 17 July 2009, following detailed checks by CXC staff and approval by the Selection Official (CXC Director). All peer review reports were reviewed by CXC staff for clarity and consistency with the recommended target list. Formal letters informing the PIs of the results, budget information (when appropriate) and providing the report from the peer review were e-mailed to each PI in August.

Joint Time Allocation

Chandra time was also allocated to several joint programs by the proposal review processes of XMM-Newton (3 proposals).

The *Chandra* review accepted joint proposals with time allocated on: Hubble (14), XMM-Newton (2), NRAO (10), NOAO (3) and RXTE (1).

Constrained Observations

As observers are aware, the biggest challenge to efficient scheduling of *Chandra* observations is in regulating the temperature of the various satellite components (see POG Section 3.3.3). In Cycle 9 we instituted a classification scheme for constrained observations which accounts

for the difficulty of scheduling a given observation (CfP Section 5.2.8). Each class was allocated an annual quota based on our experience in previous cycles. The same classification scheme was used in Cycles 10 and 11. There was a large demand for constrained time so that not all proposals which requested time constrained observations and have a passing rank (>3.5) could be approved. Effort was made to ensure that the limited number of constrained observations were allocated to the highest-ranked proposals review-wide. Detailed discussions were carried out with panel chairs to record the priorities of their panels should more constrained observations become available. Any uncertainty concerning priorities encountered during the final decision process was discussed with the relevant panel chairs before the recommended target list was finalized. Please note that the most over-subscribed class was: "EASY" while "AVERAGE" was only marginally oversubscribed. In practice we combined these two classes in order to determine which observations should be allocated time. The same 3 classes will be retained so as to ensure a broad distribution in the requested contraints. *We urge proposers to specify their constraints as needed by the science*.

Large and Very Large Projects

The full 6 Msecs of observing time available for Large and Very Large Projects (LPs, VLPs) was combined so that projects of both types competed for the full amount. In principle this allows projects requesting as much as 6 Msecs to be proposed, and approved. The Big Project Panel recommended 12 LPs and 1 VLP totalling 6.08 Msecs altogether. The over-subscription for LP+VLPs in Cycle 11 was a factor of 6.65, higher than the GO proposals, as has been typical since Cycle 4. Discussion with the *Chandra* Users' Committee following two cycles of experience with combining the two categories resulted in endorsement to continue in Cycle 12.

Cost Proposals

PIs of proposals with US collaborators were invited to submit a Cost Proposal, due in Sept 2009 at SAO. As in past cycles, each project was allocated a "fair share" budget based on their observing program, as described in CfP Section 8.4. Cost proposals requesting budgets at or lower than the allocated "fair share" budget were reviewed internally while those requesting more (7% of the cost proposals) were sent for an external review by a subset of the science peer reviewers. For these, final budgets were allocated based on the recommendations of the external review. The results were announced in late November, in good time for the official start of Cycle 11 on 1 Jan 2010. Cycle 11 projects for which observations were started in 2009 were processed in order of the date of their first observation starting in early December, as the availability of Cycle 11 funds allowed.

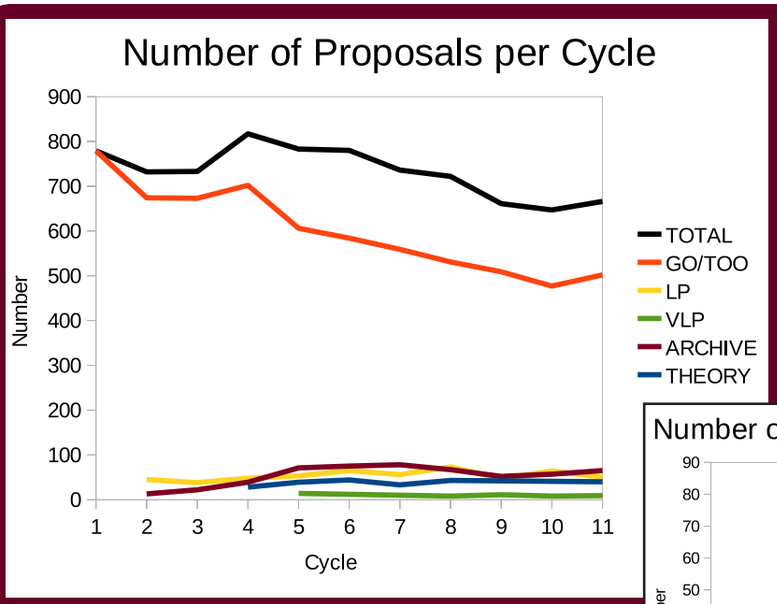

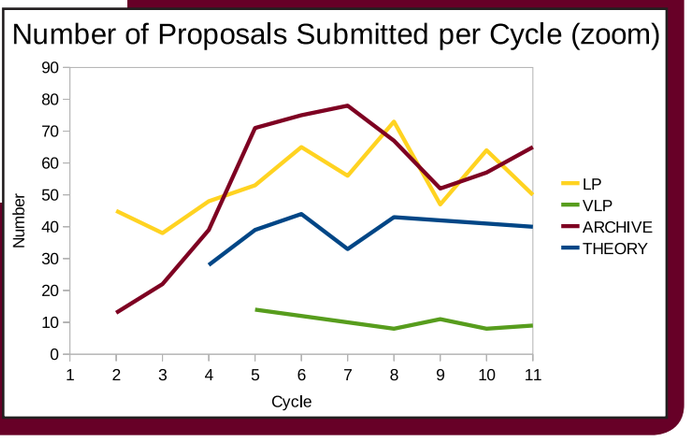

FIGURE 44: Left: The number of proposals submitted in each proposal type (e.g. GO, LP, Archive etc.) Right: zoom on lower curves. as a function of cycle. Since more proposal types have become available in each cycle, the number classified as GO has decreased as other types increase. The total number of submitted proposals is remarkably constant.

Proposal Statistics

Statistics on the results of the peer review can be found on our website: under "Target Lists and Schedules": select the "Statistics" link for a given cycle. We present a subset of these statistics here. Figure 47 displays the effective over-subscription rate for each proposal type as a function of cycle. Figures 48, 49 show the percentage of time allocated to each science category and to each instrument combination. Table 2 lists the numbers of proposals per country of origin. ✯

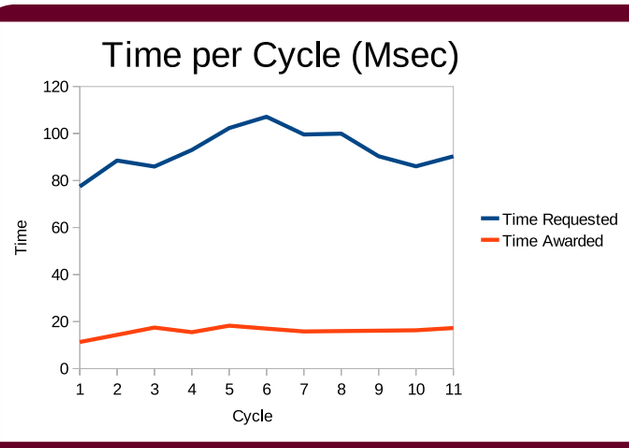

FIGURE 45: The requested and approved time as a function of cycle in ksecs.. This increased in the first few cycles, the largest effect being due to the introduction of VLPs in Cycle 5.

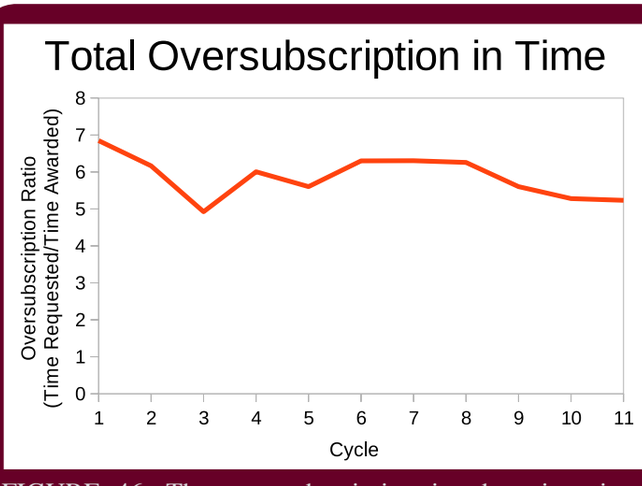

FIGURE 46: The over-subscription in observing time based on requested and allocated time in each cycle. Again the numbers are remarkably constant.

Table 2: Number of Requested proposals by Country*

Country	Requested		Approved	
	# Proposals	Time (ksec)	#Proposals	Time (ksec)
USA	489	67173.60	151	12809.25
Foreign	179	28056.84	56	5583.40

Country	Requested		Approved	
	# Proposals	Time (ksec)	#Proposals	Time (ksec)
Australia	5	276.0	1	80.00
Belgium	2	200.00	1	100.00
Canada	14	1067.92	5	504.00
Chile	1	110.30		
China	2	80.00		
Denmark	1	80.00		
France	10	942.00	4	327.00
Germany	22	1607.00	10	750.00
Greece	3	487.00	1	50.00
India	3	400.00		
Israel	1	33.00	1	33.00
Italy	28	3526.00	5	300.00
Japan	12	1251.00		
Neth	18	1373.50	6	461.00
Poland	1	60.00		
Spain	10	737.50	2	150.00
Switz	5	856.40	3	546.40
Taiwan	4	361.00	3	221.00
Turkey	1	100.00		
UK	36	14508.00	14	2160.00

* Note: Numbers quoted here do not allow for the probability of triggering TOOs

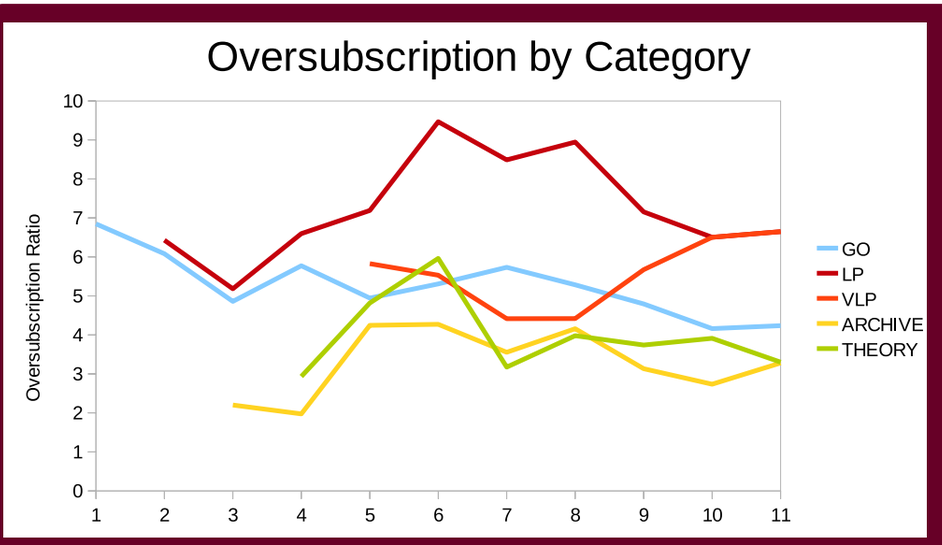

FIGURE 47: The effective over-subscription ratio in terms of observing time for each proposal type as a function of cycle. Please note that some of the fluctuations are due to small number statistics (e.g. Theory proposals).

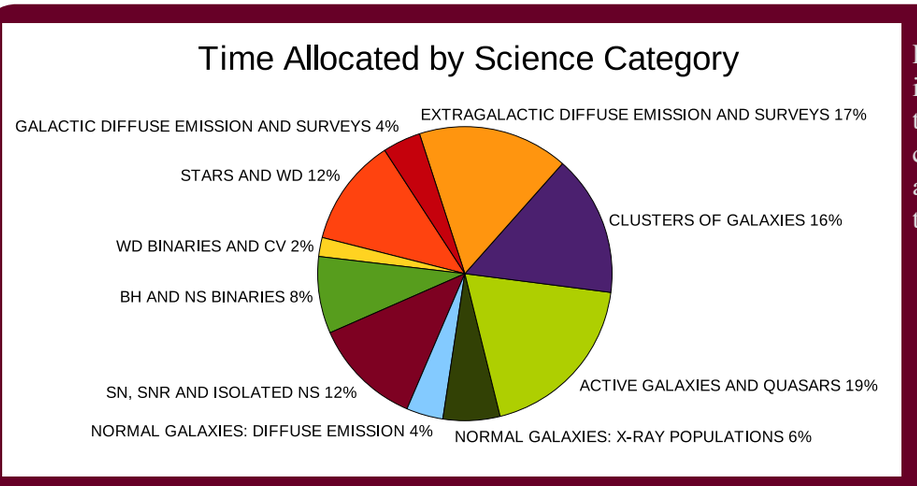

FIGURE 48: A pie chart indicating the percentage of *Chandra* time allocated in each science category. But note that the time available for each category is determined by the demand.

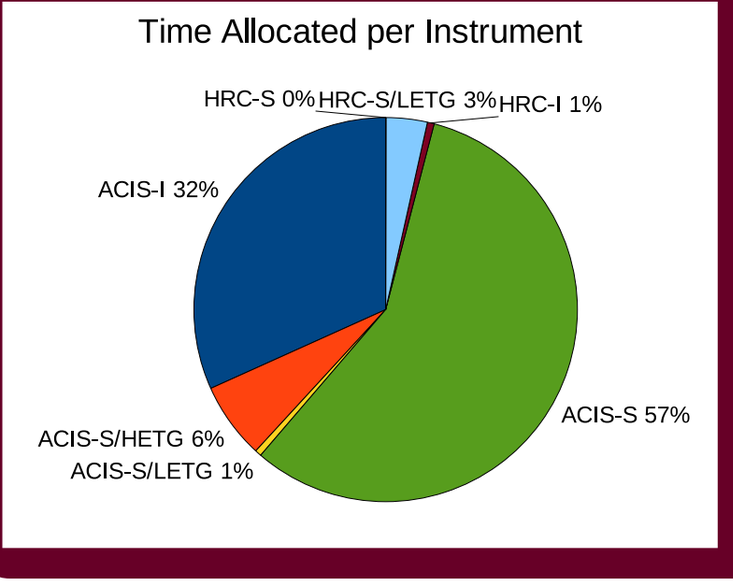

FIGURE 49: A second pie chart, shows the percentage of *Chandra* time allocated to observations for each instrument configuration.

Education and Public Outreach Proposals Selected in Cycle 11

Kathy Lestition

The Cycle 11 *Chandra* EPO Peer Review, conducted by the CXC, was held in Cambridge MA on Dec. 2-4, 2009. A panel representing science, education, museum, Forum, and NASA mission and management perspectives reviewed 9 proposals. Three individual and 2 institutional proposals were selected for funding. An overview of the selected proposals by type follows, alphabetically in order of PI last name.

Individual Proposals

Black Holes: A High Demand PD Workshop for Science Teachers

Science PI: Dr. William N. Brandt, Penn State University, (niel@astro.psu.edu)

EPO Co-I: Dr. Christopher Palma, Penn State University, (cpalma@astro.psu.edu)

Education Partner: Pennsylvania Space Grant Consortium

This proposal funds participation of teachers with a focus on underserved urban districts, in the annual teacher professional development workshops presented in partnership by the Penn State Department of Astronomy and the Pennsylvania Space Grant Consortium. The content draws heavily on results and hands-on educational materials developed by NASA missions, and includes the active participation of several NASA researchers.

Rooftop Variables: Observational PD for Inner City Teachers

Science PI: Prof. Eric Gotthelf, Columbia University (eric@astro.columbia.edu)

EPO Co-I: Dr. Marcel Agueros, Columbia University (marcel@astro.columbia.edu)

Education Partners: Summer Research Program for Teachers (SRP), Columbia University and American Association of Variable Star Observers (AAVSO), Cambridge MA

This program leverages the existing SRP program at Columbia to recruit teachers for the Astronomy program. Teachers are competitively selected to learn observational and data reduction techniques on amateur observing targets suggested by the AAVSO. The AAVSO monitors sources which can become targets of opportunity for NASA missions such as *Chandra*, and participants are expected to contribute data to the AAVSO data base for later use should targets be triggered. Teachers are also presented with astronomy teaching resources and participate in department-sponsored observing nights and field trips. Teachers use these experiences as the basis for developing their own astronomy-related teaching materials. The ultimate goal of the program is for participating teachers to establish astronomy clubs at their schools with the on-going mentorship of the Columbia astronomy department. Teachers are mentored by faculty and students in the astronomy department.

Addressing the Nature of Science Through a Telescope Loaner Program (CLUSTER)

Science PI: Dr. Gregory Sivakoff, University of Virginia (grs8g@virginia.edu)

EPO Co-I: Dr. Edward Murphy

Education Partner: University of Virginia Astronomy Dept.

This program addresses the nature of science, astronomy, and space science components of the Virginia Standards of Learning through a telescope loaner program and the development of associated materials. The program loans 13 telescopes retired by the University of VA astronomy department to teachers from area schools. Teachers are trained in the telescope use, in materials that engage students in the astronomy content, and in activities for use with students that address the nature of science. After training, teachers borrow the telescopes for 6-8 week periods for use in activities at their schools, including night observing with student groups. Students are connected to NASA through the use of NASA education materials and NASA science results.

Institutional Proposals

Enabling Students to Discover X-ray Astronomy: a Middle School Curriculum Module

Science PI: Dr. Smita Mathur, Ohio State University, (smita@astronomy.ohio-state.edu)

EPO Co-I: Dr. David J. Ennis, Ohio State University, (dje@astronomy.ohio-state.edu)

Education Partner: Center of Science and Industry (COSI) Columbus, Columbus Ohio

This program will leverage an on-going collaboration at COSI that combines the scientific expertise of OSU professors with the educational skills of COSI staff to produce lecture materials, classroom demonstrations, student events and teacher lesson plans focused on X-ray astronomy and the *Chandra* mission for middle school students. The resulting module will be utilized in the well-established COSI program that brings middle school students from central Ohio to COSI for day-long educational programs while their teachers participate in a professional development program based on the same material. The material will be further leveraged through the COSI "Electronic Experts" program which provides informal education through COSI on Wheels, Science Days, distance learning, the Agenda for Change (STEM) program, and a Digital Vizualization Lab under development.

Augmenting Elementary School Astronomy Education in Rural Albemarle County

Science PI: Dr. Gregory Sivakoff, University of Virginia, (grs8g@virginai.edu)

EPO Co-I: Kelsy Johnson, University of Virginia, (kej7a@virginia.edu), Dark Skies, Bright Kids program (UVA Astronomy Dept. and NSF)

This program will collaborate with the Dark Skies, Bright Kids (DSBK) program seeded by NSF and adopted by the Astronomy Department at UVA to target elementary school children in underserved, rural Albemarle County. The program will develop activities for an inexpensive mobile planetarium to augment the offerings of the DSBK afterschool astronomy club held weekly for students and their families. The planetarium programs will provide early engagement with expanded astronomy content as a next step in the NASA pipeline. Fifteen UVA undergraduate, graduate and postdoctoral astronomers have volunteered to help with the activities, enabling a secondary goal of encouraging and training young scientists to participate in science education and outreach activities. ✯

International X-ray Observatory (IXO) Update

Michael Garcia, for the *IXO* Team

Since the last *IXO* Update in the winter of 2009, the *IXO* team has completed the inputs to the Decadal (Astro2010) Survey Committee. The team responded to two separate 'Requests for Information' with written reports, and was one of a limited number of teams asked to make an oral presentation to the sub-committee on Electromagnetic Observations from Space at the June 2009 AAS meeting. You can find this presentation, along with many of our other presentations and submissions to the Decadal, on the *IXO* web site at ixo.gsfc.nasa.gov, under the 'resources' link. One item developed for the Decadal which you might find particularly useful is the '*IXO* Quick Reference Guide', shown here. A higher resolution version is available at: *http://ixo.gsfc.nasa.gov/technology/spacecraftQG.html*. A hearty THANK YOU to all of those (including many from Europe and Japan) who helped prepare these important inputs to the Decadal panels. It truly was a team effort. The results of the Decadal prioritization process are expected to be announced in the fall of 2010.

The equivalent to the Decadal process in Europe, 'Cosmic Visions (CV) 2015', began with presentations in October and December, 2009, by European industry partners on the design of the mission. The science input to this process takes the form of 40 pages in the 'Yellow Book' describing the mission. The effort to produce these 40 pages has started. While this effort will be tuned to match the already established science themes of the CV process, it will draw from the science inputs to the Decadal Survey. If you are on the '*IXO* Science Associates' email list you have already been invited to help in this effort. If you are not on this list and wish to, please email me (garcia@head.cfa.harvard.edu) and I will put you on the list. The draft of this science case will be one of the topics for discussion at the next *IXO* science meeting in Paris, April 27-29, 2010. This is an open meeting, so please attend if you are interested. More info is available at: *http:/ixomeeting.cesr.fr.*

As well as supporting the Decadal (and CV) processes, the technology teams have been hard at work making progress on the technologies needed for *IXO*! X-ray tests on a complete mirror module of silicon pore optics show an improvement in the angular resolution (half power diameter HPD) to ~10 arc sec, from the earlier 17 arc sec. We have fabricated slumped glass mirror segment pairs which, when aligned and mounted, are able to achieve 8 arcsec HPD images at 1 keV. This HPD is limited by the figure quality of the current forming mandrels which were fabricated to meet the original Con-X 15" HPD requirements. Since the transition of Con-X into *IXO* and the associated 5" HPD requirement, we have fabricated two pairs of forming mandrels that have a figure quality of 2.3" HPD for two reflections, which satisfies the *IXO* mandrel requirements.

The calorimeter team has manufactured the first sets of flight-sized 'inner' (2 arcmin FOV) arrays and measured 2.7eV resolution on them. The team is investigating several designs to populate the 'outer' array which will bring the FOV to 5x5 arcmin. Future calorimeter activities include making refinements to the fabrication process in order to meet the design goals and increasing the MUX bandwidth to handle the degree of multiplexing assumed for XMS (X-ray Microcalorimeter Spectrometer). ✯

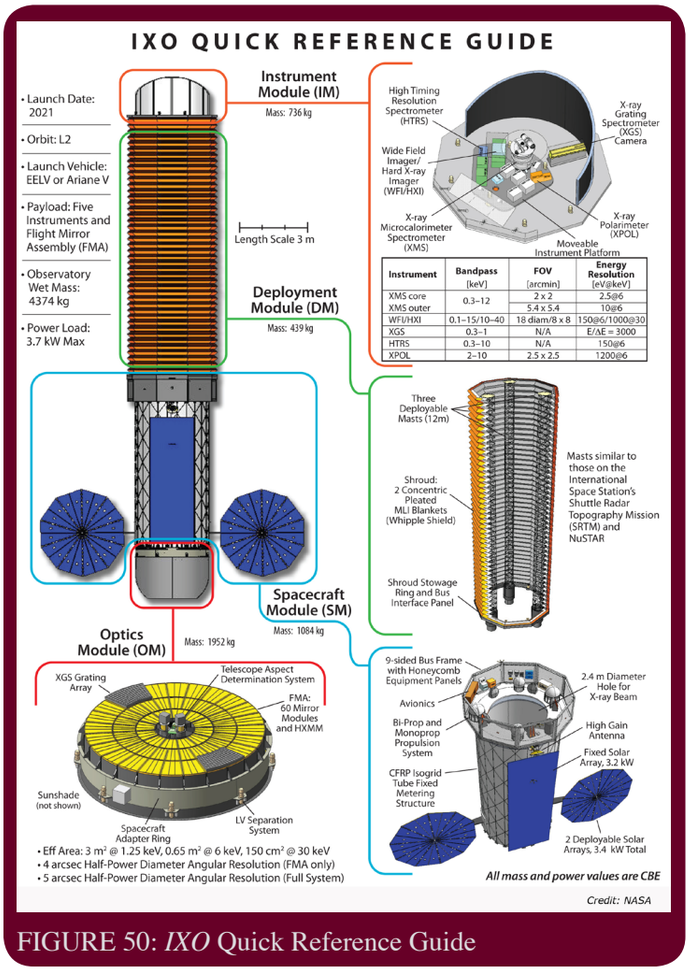

FIGURE 50: *IXO* Quick Reference Guide

Moving on: Steve Murray

Ralph Kraft, Almus Kenter, William Forman, Christine Jones, Charles Alcock, Harvey Tananbaum, Roger Brissenden

Our colleague and friend Steve Murray has accepted a faculty position at the Johns Hopkins University, and will head south at the end of March, 2010. Steve has been an SAO scientist for nearly thirty-seven years, and his record here is astonishing. He is a leading developer of scientific instrumentation for the study of X-rays in space. Steve built important instruments for *three* major missions: he was the Senior Project Scientist for the High Resolution Imager on Einstein, led the development of the the High Resolution Imager on *ROSAT*, and most recently the PI for the High Resolution Camera on *Chandra*. In addition, he was the Scientific Program Manager for the Einstein Data Center in the 1980's.

The two traits that best define Steve are his incredible hard work and his hands-on, can-do willingness to participate in any aspect of a project from the highest level discussions of future mission concepts to chasing vacuum leaks in a lab experiment. As a young scientist in the 70s, Steve, along with summer student Priscilla Cushman, wound the first Cross Grid Charge Detector, the readout used for microchannel plate readouts. Along with Jon Chappell and Jerry Austin, he also assembled the MCP stacks and UVIS for the *Chandra* flight HRC. When *ROSAT* was delayed, he started the program that ultimately became the Astrophysics Data System, for which he is still the PI. ADS has profoundly changed the relationship between all of us and our literature, permanently and for the better. Steve was on the red review team that critiqued SAO's original proposal for the AXAF Science Center. After pointing out some deficiencies in the original draft, he went on to lead (i.e. effectively, do) the re-write of the technical section for what ultimately became the highly successful blueprint for the creation of the *Chandra X-ray Center.*

Steve is deeply interested in the development of novel technologies for scientific instrumentation. His innovations contributed to the many successes of his flight instruments. With an eye on the future, he founded and led SAO's Center for X-ray Technology, a research center devoted to the development of the next generation of optics and detectors for high-energy astrophysics missions. He has branched out recently with a program to develop high speed, fully addressable CMOS imagers for use in both high energy and planetary missions.

With all of this, it is remarkable that Steve has had any time for his own scientific research, but he is a very original and productive astrophysicist. It is fair to say that Steve has dedicated his life to his work, and it is unusual to find an evening or a weekend when he is NOT working. He has a wide range of astrophysical interests, and actively participates in diverse research projects. Steve has used his share of *Chandra* GTO observing time to advance imaginative programs that otherwise might not have been carried out. These projects include studies of individual galaxy clusters as well as cluster surveys to measure the evolution of the cluster mass function and thus measure cosmological parameters. Steve has also committed significant effort and time to ensure the success of the XBootes Survey, involving the largest contiguous area (nine square degrees) surveyed by *Chandra*. This has now developed into a major multi-wavelength program including AGN studies, which, for example, show important differences in the environments of AGN selected in X-ray, IR, and radio bands. Steve's other interests include studies of radio galaxies, pulsars, pulsar wind nebulae, and the nucleus of M31, particularly when these utilize the unique timing capability of the High Resolution Camera.

Steve has been and remains an important leader in

FIGURE 51: AXAF Science Working Group photo - spring 1995. Left to right - Andrew Wilson, Andy Fabian, Jeff Linsky, Harvey Tananbaum, Alan Bunner, Steve Holt, Martin Weisskopf, Riccardo Giacconi, Bert Brinkman, Steve Murray, Gordon Garmire, Leon van Speybroeck, Claude Canizares, and Richard Mushotzky. Fast forward to pictures from "*Chandra*'s First Decade of Discovery" (page 60) for a 2009 pictures of Steve and many of his colleagues in this picture.

our field. He was the Associate Director for SAO's High Energy Astrophysics Division (1992-2003), and was recognized as SAO Scientist of the Year in 1999 (on behalf of the *Chandra* team). He was awarded the NASA Exceptional Service Award and Medal in 2000 for his leadership of the *Chandra* HRC, and he was Vice Chair of High Energy Astrophysics Division of the AAS (2004-2005) and Chair (2006-2007).

The entire *Chandra* community, and the high energy community more broadly, owes an enormous debt of gratitude to Steve for his hard work in making *Chandra* the success that it is. He will be sorely missed by his colleagues at SAO, but we wish him the best in his future work at JHU and look forward to collaborating with him in his continued role as HRC PI and on other projects. ✯

FIGURE 52: Two pictures of Steve at work. (left) Here in the astronaut crew cabin of the Shuttle Columbia just before the STS-93 launch of *Chandra*. (right) Here at TRWduring the *Chandra* thermal vacuum testing. Steve is front right. Other colleagues in disguise include Jerry Austin, Jon Chappell, Everett Johnston, and Martin Zombeck among others.

Cool Stories from the Hot Universe

Wallace Tucker, reprinted with permission from the full article and image set at: http://chandra.harvard.edu/chronicle/0309/cool/

While in the process of pulling together a list of the top ten *Chandra* science stories, colleague Peter Edmonds suggested that we also put together a list of *Chandra*'s coolest news stories.

Not being an especially cool person - at least I don't think I'm cool, and I don't remember anyone ever saying I'm cool, and as I understand cool, if you're cool, you know it - I was perplexed. This confirms one of Malcolm Gladwell's rules of cool: ". . . it can be only be observed by those who are themselves cool."

"Do you mean most popular?" I asked.

"Well," he hesitated, making me wonder if he wasn't also cool-challenged, "Yes."

The discussion then devolved into a debate about how to measure popularity: web stats - tricky because of the inflation of hits on the *Chandra* site over the years, coverage by the media - not a cool bunch by and large - or maybe just what we at the *Chandra* Education and Public Outreach (EPO) think is cool - a comment that made me think that Peter might be cool after all.

Then there is the incomparable and usually incomprehensible Marshall McLuhan's famous observation that "... Hot media are... low in participation, and cool media are high in participation or completion by the audience."

If this is true, then X-ray astronomy, (along with gamma-ray astronomy), is the coolest branch of astronomy, even though cosmic X-rays are produced in the hottest places in the universe! Because an X-ray photon is thousands of times more energetic than an optical or infrared photon, there are generally many fewer photons represented in a typical *Chandra* image as compared to Hubble or *Spitzer* Telescope images. So, some participation by the observer is needed to complete the interpretation (which is why we are grateful to have such good illustrators and animators on our EPO staff.)Add this to the fact that you can't go outside at night and "see" an X-ray star because they are invisible, and you begin to grasp the "coolness" of X-ray astronomy. It makes you think. In fact, this must be why all astronomical images are pretty cool. They make you wonder.

With the "wonder-full" criterion in mind, the *Chandra* EPO group put together the following list of cool *Chandra* stories, realizing that if too many people agree that they're cool, they may cease to be cool - see Gladwell's rules of cool. The list is not in any order of priority because we suspect that would be uncool.

Malcolm Gladwell's Rules of Cool

- Cool can only be observed by those who are themselves cool.
- Cool cannot be manufactured, only observed.
- Cool cannot be accurately observed at all, because the act of discovering cool causes cool to take flight.

"*The meaning of cool is beyond definition. And as I said, beyond modification. It just is, man.*" *Stephen King, best-selling author of horror novels and self-proclaimed authority on cool.*

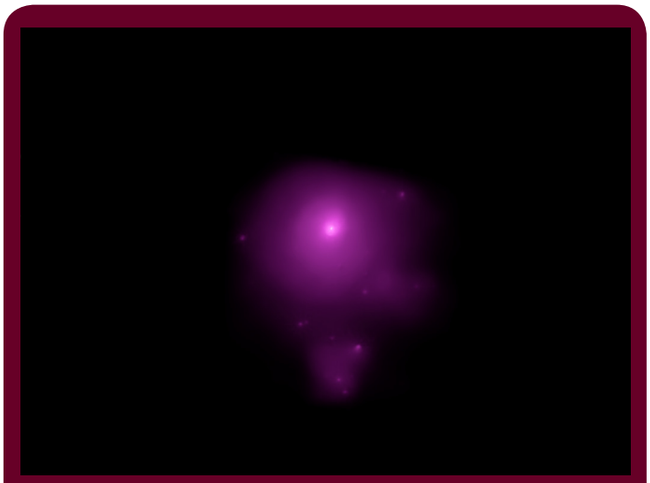

FIGURE 53: Abell 85 (*http://chandra.harvard.edu/photo/2008/darkenergy/*)

Dark Energy Found Stifling Growth in Universe

This story requires lots of effort on the part of the reader to know what we're getting at, but few if any things are more mysterious than the evidence that most of the energy in the universe is in some form that no one understands. See Figure 53.

PSR B1509-58: A Young Pulsar Shows its Hand

The "hand of God" stuff about this image probably got out of hand, but the image definitely makes you wonder, especially when you realize that a neutron star only twelve miles in diameter is responsible for this beautiful X-ray nebula that spans 150 light years. See Figure 54.

FIGURE 54: PSR B1509-58 (*http://chandra.harvard.edu/photo/2009/b1509/*)

Crab Nebula: Fingers, Loops and Bays in The Crab Nebula

What's really cool about this image are those circles in the center, and the jet, which are thought to be produced by electrons and antimatter electrons created near the surface of the neutron star in the center, and racing away from the star at near the speed of light. This antimatter is real, not just Angels and Demons fantasy.

The Galactic Center: Light Echo from the Milky Way's Black Hole, and, Milky Way's Giant Black Hole Awoke from Slumber

These stories are cool because they illustrate how not looking at an object can sometimes provide valuable information about the object. In this case, the object not looked at is Sagittarius A*, the supermassive black hole at the center of the Galaxy. Astronomers observed an increase in X-ray activity from two sets of gas clouds 50 and 300 light years away from Sgr A*, and deduced that these were light echoes produced by outbursts from the black hole 50 and 300 years ago. The one from 300 years ago indicates that Sgr A* was a million times more active than it is today. See Figure 55.

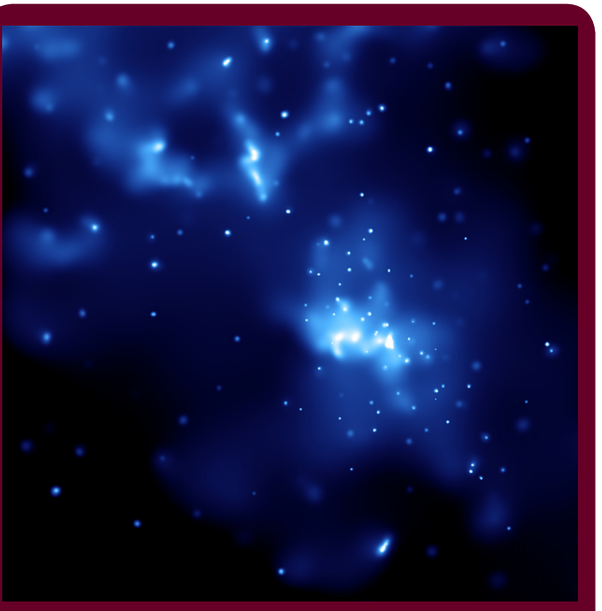

FIGURE 55: Sagittarius A* (*http://chandra.harvard.edu/photo/2007/gcle/*)

The Bullet Cluster: NASA Finds Direct Proof of Dark Matter

A high speed collision between thousands of galaxies, multimillion degree gas clouds more massive than all the stars in the galaxies, and even more massive clouds of dark matter. The best proof yet that most of the matter in the universe is in some mysterious form that astronomers

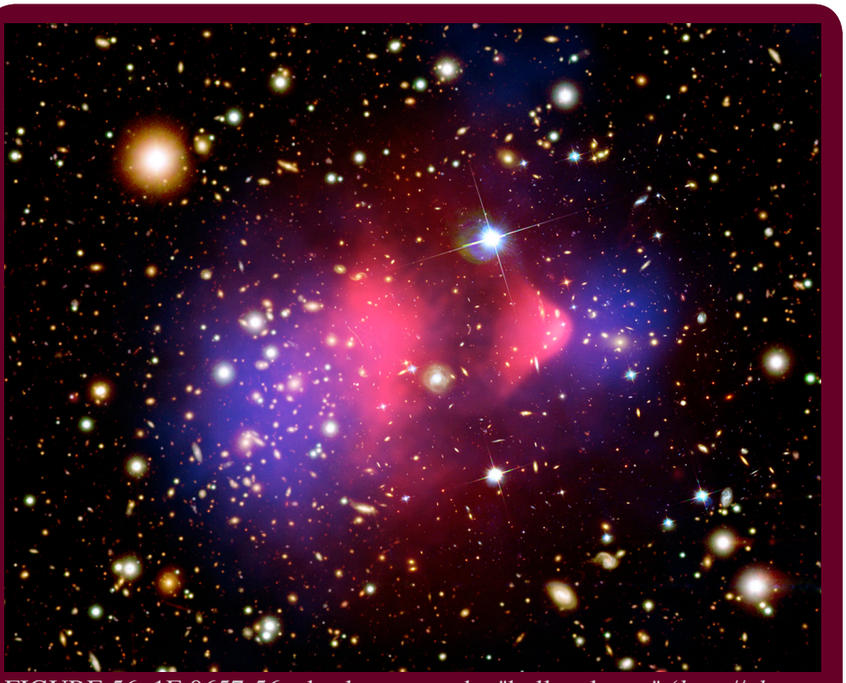

FIGURE 56: 1E 0657-56, also known as the "bullet cluster" (*http://chandra.harvard.edu/photo/2006/1e0657/*)

FIGURE 57: NGC 4696 (*http://chandra.harvard.edu/photo/2006/bhcen/*)

call "cold dark matter," so this discovery is beyond cool. See Figure 56.

NGC 4696: Black Holes Found to Be Green by NASA's *Chandra*

Black holes are the ultimate alternative energy source. This research on supermassive black holes in the centers of galaxies shows that the process of converting gravitational energy of matter falling toward black holes into light and jets of high-energy particles is much more efficient than nuclear energy or fossil fuels. It has been estimated that if a car was as fuel-efficient as some black holes, it could travel more than a billion miles per gallon! See Figure 57.

FIGURE 58: SN2006gy (*http://chandra.harvard.edu/photo/2007/sn2006gy/)*

SN 2006gy: NASA's *Chandra* Sees Brightest Supernova Ever

This cool story hinged on just four X-rays detected by *Chandra*. In fact, it would have been far less cool if *Chandra* had detected thousands of X-rays, because that would have suggested that the supernova was caused by a white dwarf exploding in a dense environment. As it turned out, the evidence points toward a long-predicted but never observed type of supernova that occurs only in extremely massive that are greater than 150 times the mass of the Sun. Sometimes the absence of evidence can be the most important evidence of all. See Figure 58.

Westerlund 1: Neutron Star Discovered Where a Black Hole Was Expected

The Westerlund 1 star cluster, and its sibling, Westerlund 2, were more or less ignored for years because they are hidden in a dusty part of the Galaxy difficult to observe with optical telescopes. Infrared and X-ray telescopes have shown that they are very cool collections of very massive stars, and at least one puzzling neutron star that according to a simple interpretation of stellar theory, should have been a black hole. What happened? See Figure 59.

Saturn: Saturn's Rings Sparkle with X-rays

Chandra images reveal that the rings of Saturn sparkle in X-rays (blue dots in this X-ray/optical composite). The likely source for this radiation is the fluorescence

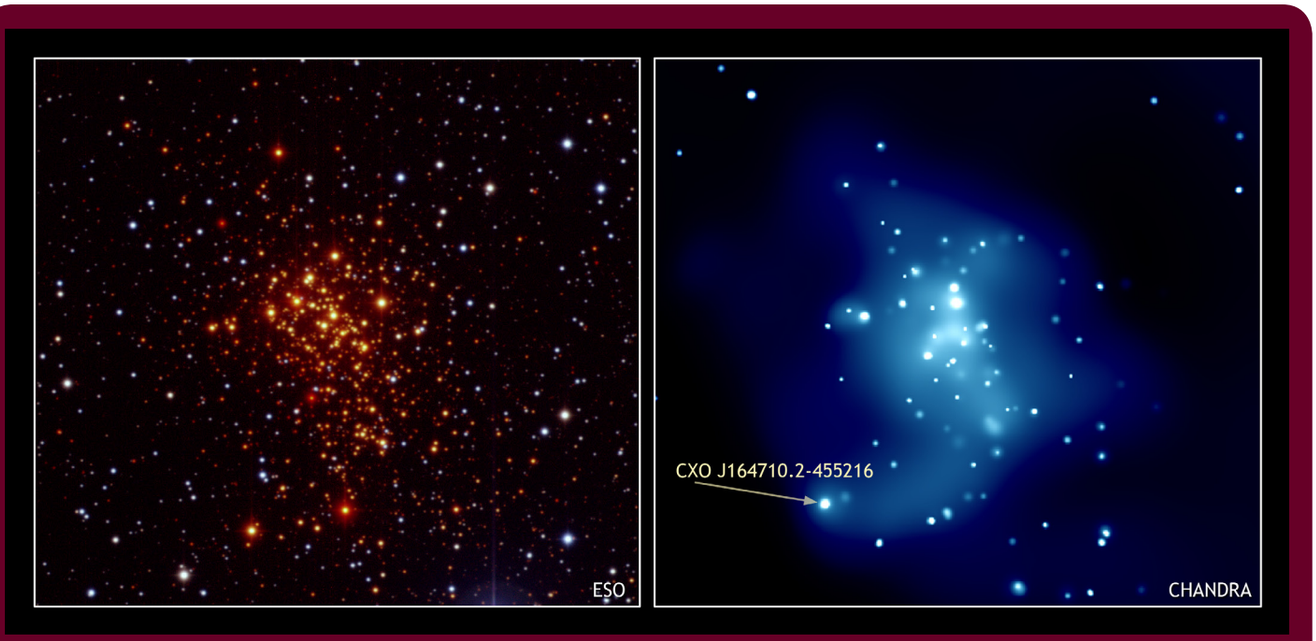

FIGURE 59: Westerlund 1 in optical (left) and x-ray (right) (*http://chandra.harvard.edu/photo/2005/wd1/*)

caused by solar X-rays striking oxygen atoms in the water molecules that comprise most of the icy rings. Nothing very profound, but there's something about this image that's cool. See Figure 60.

Cygnus X-1: "Iron-Clad" Evidence for Spinning Black Hole

No cool images here, just X-ray spectra, which reveal what's going on just a few dozen miles from a black hole, much closer than the distance of Boston from New York City. Not that we're implying that New York City is a black hole! See Figure 61.

"Secrets are the very root of cool." William Gibson

"The most beautiful thing we can experience is the mysterious." Albert Einstein

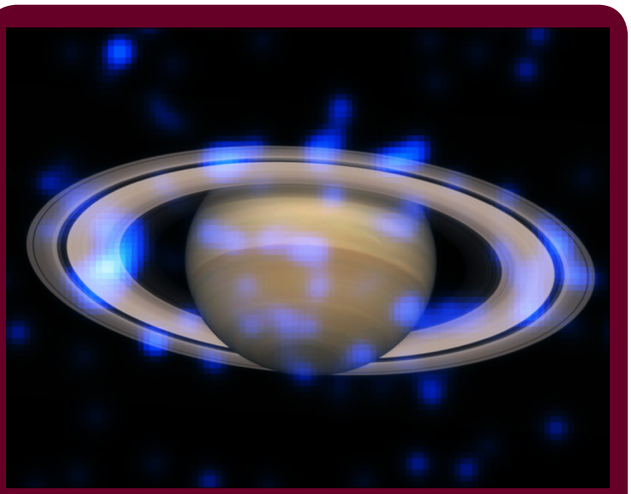

FIGURE 60: Saturn (*http://chandra.harvard.edu/photo/2005/saturn_rngs/*)

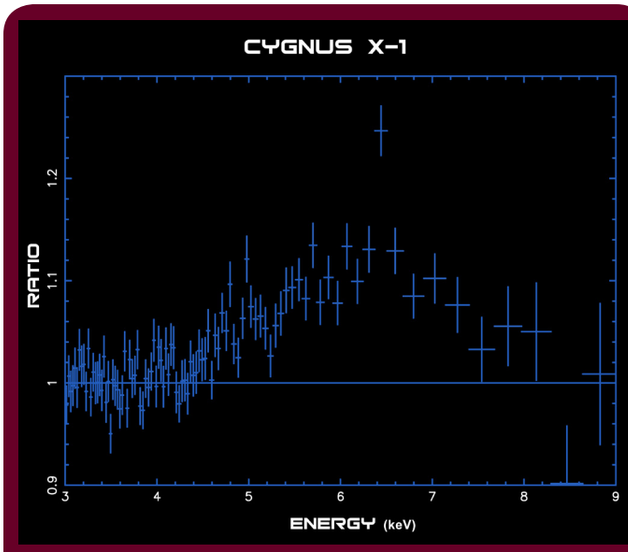

FIGURE 61: Spectrum of Cygnus X-1 (*http://chandra.harvard.edu/photo/2003/bhspin/*)

Other Cool Stories

Perseus A Sound Waves

A supermassive black hole is producing sound waves that correspond to B flat, 57 octaves below middle-C! As a reader wrote, "Imagine playing Bach's Passacaglia & Fugue in C on this celestial organ." See Figure 62.

Cassiopeia A: Elemental Image Of Exploded Star

Not the most beautiful Cas A image, but there's something cool about an image that shows enough calcium atoms to make several nonillion glasses of milk.
See Figure 65.

Brown Dwarf LP 944-20: The Mouse That Roared - Chandra Captures Flare From Brown Dwarf

It's always cool when a mouse roars. See Figure 64.

RX J1856.5-3754 and 3C58: Cosmic X-rays May Reveal New Form of Matter

This result has not been confirmed, but hey, it doesn't have to be right to be cool! See Figure 63. ✯

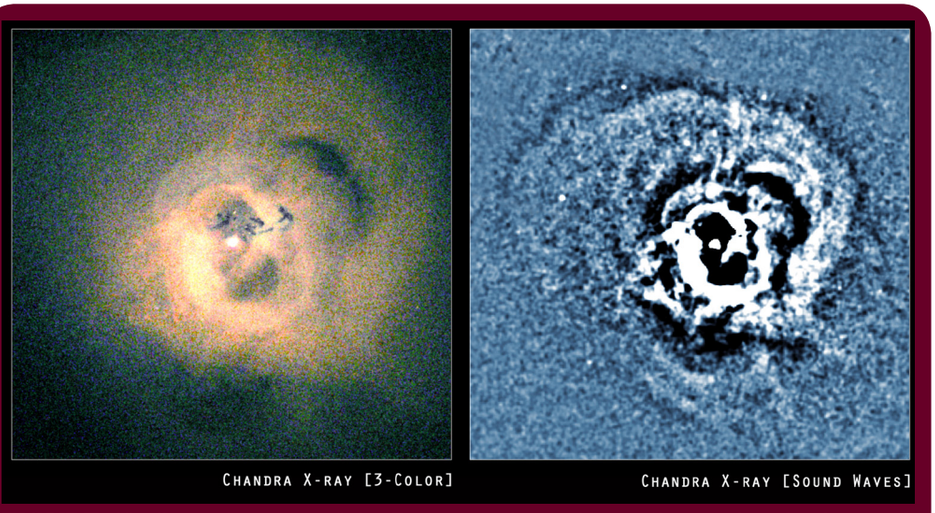

FIGURE 62: Central region of the Perseus galaxy cluster (*http://chandra.harvard.edu/photo/2003/perseus/*)

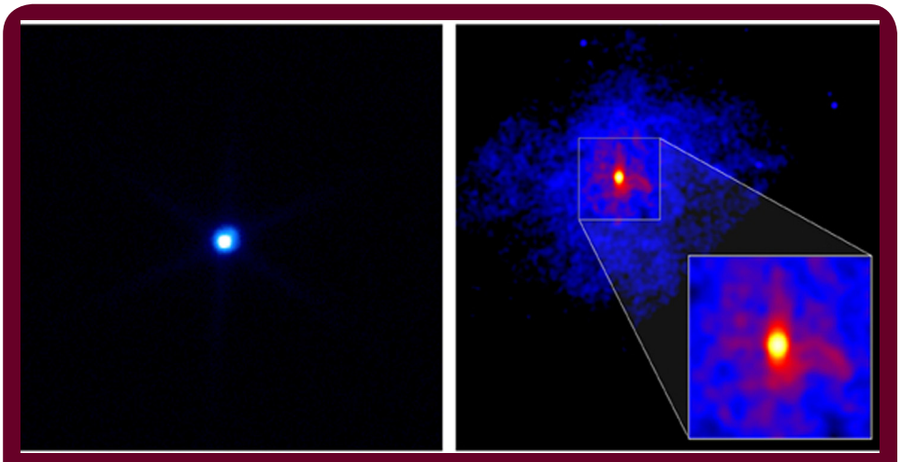

FIGURE 63: RX J1856.5-3754 and the pulsar in 3C58 (*http://chandra.harvard.edu/photo/2002/0211/*)

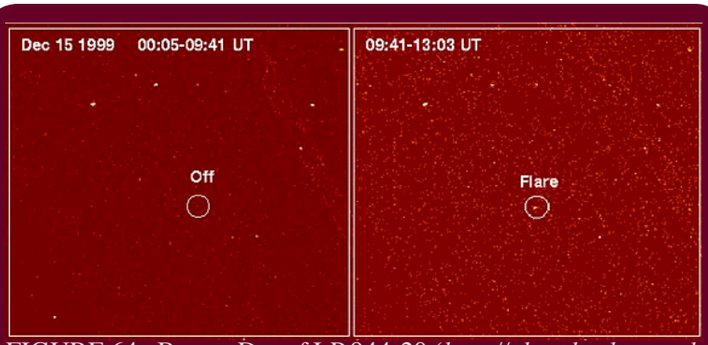

FIGURE 64: Brown Dwarf LP 944-20 (*http://chandra.harvard.edu/photo/2000/1054/*)

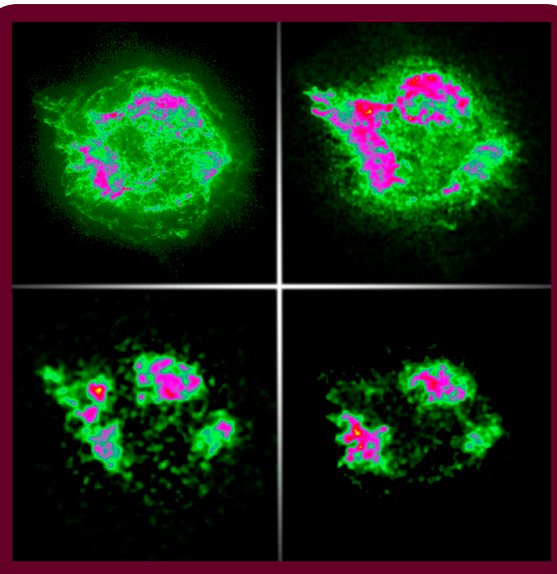

FIGURE 65: Cassiopeia A (*http://chandra.harvard.edu/photo/2000/cas_a062700/*)

Chandra Users' Committee Membership List

The Users' Committee represents the larger astronomical community for the *Chandra X-Ray Center*. If you have concerns about *Chandra*, contact one of the members listed below.

Name	Organization	Email
Steve Allen	Stanford	swa@stanford.edu
Elizabeth Blanton	Boston Univ.	eblanton@bu.edu
Ken Ebisawa	ISAS	ebisawa@isas.jaxa.jp
Matthias Ehle	ESA	Matthias.Ehle@sciops.esa.int
Ann Hornschemeier	GSFC	Ann.Hornschemeier@nasa.gov
Joel Kastner	RIT	jhk@cis.rit.edu
Martin Laming (Chair)	NRL	j.laming@nrl.navy.mil
Jon Miller	U. Michigan	jonmm@umich.edu
Luisa Rebull	*Spitzer* Science Center	rebull@ipac.caltech.edu
Massimo Stiavelli	STScI	mstiavel@stsci.edu
Joan Wrobel	NRAO	jwrobel@nrao.edu
Ex Officio, Non-Voting		
Jaya Bajpayee	NASA HQ	jaya.bajpayee-1@nasa.gov
Wilt Sanders	NASA HQ	wsanders@hq.nasa.gov
Allyn Tennant	NASA/MSFC, Project Science	allyn.tennant@msfc.nasa.gov
Martin Weisskopf	NASA/MSFC	martin@smoker.msfc.nasa.gov
CXC Coordinators		
Belinda Wilkes	CXC Director's Office	belinda@head.cfa.harvard.edu
Paul Green	CXC Director's Office	pgreen@head.cfa.harvard.edu

A few of the people who contributed to *Chandra*, and to the "*Chandra's* First Decade of Discovery" Meeting

Astronauts: Eileen Collins, Jeff Ashby, Michel Tognini, Steve Hawley, and Cady Coleman

Riccardo Giacconi

Steve Murray

Martin Weisskopf

Harvey Tananbaum

Claude Canizares

Gordon Garmire was unable to attend; Mark Bautz discussed ACIS

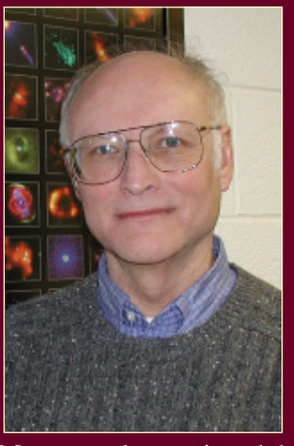

Many people mentioned the contributions of Leon van Speybroeck (1935 - 2002)

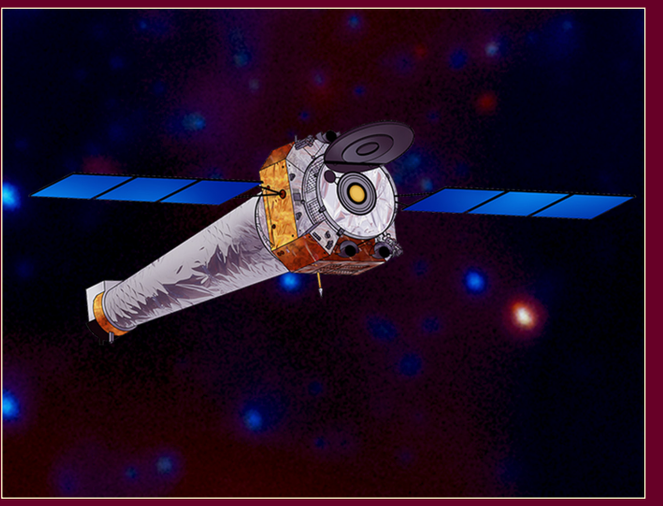

The Chandra Newsletter appears approximately once a year. We welcome contributions from readers. Nancy Remage Evans edits "Chandra News", with editorial assistance and layout by Tara Gokas.

Comments on the newsletter and corrections and additions to the hardcopy mailing list should be sent to: chandranews@head.cfa.harvard.edu.